Gulf General Atomic
Incorporated

AEC RESEARCH AND
DEVELOPMENT REPORT

GA-8468

RESULTS OF HTGR CRITICAL EXPERIMENTS DESIGNED TO MAKE INTEGRAL CHECKS ON THE CROSS SECTIONS IN USE AT GULF GENERAL ATOMIC

by

R. G. Bardes, E. M. Gillette
R. J. Nirschl, R. C. Traylor

Prepared under
Contract AT(04-3)-167
Project Agreement No. 17
for the
San Francisco Operation Office
U.S. Atomic Energy Commission

Gulf General Atomic Project 317.2340

February 12, 1968

Gulf General Atomic
Incorporated
P.O. Box 608, San Diego, California 92112

AEC RESEARCH AND
DEVELOPMENT REPORT

GA-8468

RESULTS OF HTGR CRITICAL EXPERIMENTS DESIGNED TO MAKE INTEGRAL CHECKS ON THE CROSS SECTIONS IN USE AT GULF GENERAL ATOMIC

Work done by:

R. G. Bardes
E. M. Gillette
G. F. Hoover
W. H. Hughes
L. O. Lavigne
R. J. Nirschl
S. E. Nowicki
R. C. Traylor
A. D. Whitney

Report written by:

R. G. Bardes
E. M. Gillette
R. J. Nirschl
R. C. Traylor

Prepared under
Contract AT(04-3)-167
Project Agreement No. 17
for the
San Francisco Operation Office
U.S. Atomic Energy Commission

February 12, 1968

CONTENTS

CONTENTS (continued)

FIGURES

FIGURES (continued)

TABLES

TABLES (continued)

TABLES (continued)

1. INTRODUCTION

During the past year Gulf General Atomic has been engaged in a series of critical experiments designed to provide necessary technical background information for the continued development of large HTGR-type reactor systems. This program receives its financial support from the U.S. Atomic Energy Commission.

This is a summary report of the first phase of this work, in which a series of uranium-graphite cores was constructed to measure the reactivity worths of materials used in the HTGR-type reactors. A detailed comparison was made with calculated results that were based on the differential cross-section sets used in design calculations. In particular, these cores ranged in C/U (carbon-to-uranium) atom ratio from 5000 to 432, giving a wide range of spectral hardness. Each core had a thin radial reflector and no end reflectors. A cylindrical geometry was used so that the results could be analyzed using one-dimensional codes with 30 or more energy groups. The information here is intended to assist other workers in evaluating their cross-section data. For convenience, the core assemblies are referred to throughout the report by the C/U ratios, i.e., C/U-5000, C/U-2500, etc.

2. SUMMARY AND CONCLUSIONS

The HTGR critical experiment program to date has been effective in evaluating cross-section data in current use at Gulf General Atomic. A definition of the data in current use is presented in Section 5.1. By making a detailed comparison of the experimental and calculational results it has been possible not only to reject cross-section data as being inadequate, but also to use the deviations between calculated and experimental results to make allowances for the effect of uncertainties in cross sections on the reactor design calculations.

The materials investigated during the program were U^{233}, U^{235}, U^{236}, U^{238}, Np^{237}, Th^{232}, Pu^{239}, Pu^{240}, and boron, the latter being used as a standard. The neutron spectra in the five critical assemblies discussed in this report can be characterized by their mean fission energy. This ranged from 0.074 eV in the C/U-5000 assembly to 12.7 eV in the C/U-432 assembly. The softer spectra permit the study of cross sections in the thermal energy range while the harder spectra emphasize events in the epithermal range.

The following summary of the comparison between the calculated and measured results for the above materials in the five core assemblies shows the percent deviation of the calculated value for a given material from the measured values. The percent deviation represents the average for the different material loadings of each material investigated and includes an allowance for the estimated experimental uncertainties.

SUMMARY OF REACTIVITY WORTH COMPARISONS
OF SPECIAL MATERIALS

Material	Core Assembly C/U-5000	C/U-2500	C/U-1718	C/U-859	C/U-432
Carbon	< 1%	< 1%	< 1%	< 1%	< 1%
Aluminum		+ 2%	< 1%	+ 3%	- 3%
Boron	+ 9%	- 1%	+ 2%	< 1%	- 3%
U^{235}(a)	+ 7%	- 3%	- 9%	- 20%	
U^{235}(b)	+ 7%	- 1%	- 2%	< 1%	< 1%
U^{233}	+ 8%	+ 3%	+ 4%	+ 7%	+ 7%
Depleted uranium (U^{238})	+ 4%	< 1%	+ 2.5%	+ 4%	- 2%
Thorium	+ 6%	+ 1%	+ 3%	+ 4.5%	- 2%
Np^{237}	+ 2%	- 10%	- 8%	- 6%	- 12%
U^{236}		< 1%	+ 5%	+ 6%	+ 6%
Plutonium (4.5 a/o Pu^{240})		- 2%	< 1%	< 1%	
Plutonium (22 a/o Pu^{240})		+ 10%	+ 10%	+ 4%	

(a) GA Cross-Section Data 92.2350 (see Table 20)

(b) ENDF/B KAPL Cross-Section Data 92.2352 (see Table 20)

From the comparison shown in the summary as well as the detailed comparison shown later in this report, the following conclusions can be made about this phase of the Base Program:

1. The results obtained in the C/U-5000 assembly contain a systematic bias believed to be experimental in nature, and further analysis will have to await the reconstruction of that or a similar core.

2. The good agreement obtained in calculating the absolute worth of the boron special elements is indicative of the adequacy of the calculational model (including the method of evaluating β_{eff}) and the excellent experimental procedures and data.

3. The ENDF/B U^{235} data give much better agreement than the U^{235} data used during the first part of the program, both in calculating the various core eigenvalues and in the central reactivity worth of the U^{235} special elements. The status of U^{235} cross section for HTGR analysis is believed to be excellent.

4. The recent U^{233} cross-section data obtained by ORNL and RPI scientists gives agreement with experiment that is considerably better than that obtained with several of the older cross section sets; however, a discrepancy of about 5% still exists, with the calculated reactivity worths being too high. The HTGR nuclear design will have to take this discrepancy into account. A continuing review of the basic differential data would also be very desirable.

5. While the model used to calculate reactivity worths of the predominantly-resonance energy absorbers is not completely rigorous, it is sufficient to establish the general trends and magnitude of any discrepancies. In addition, a perturbation theory analysis has been used in a number of cases to establish an upper limit to the error introduced by the inadequacies of the calculational model.

For U^{236}, the comparison between calculation and experiment is complicated by the presence of other uranium isotopes, U^{235}, and U^{238}, in the "U^{236}" special elements. U^{236} is only 15 atom-% of the total uranium loadings, and the worth of any single special element in any one of the cores is below \$0.08 in reactivity. It appears, however, that a review of the cross sections is in order because the calculated worth is generally 5% too high.

For U^{238}, the agreement is generally good. The calculated values are high by perhaps 3 or 4%.

The results for thorium are similar to those for U^{238}. It appears that the calculated effective resonance integrals for both U^{238}, and Th^{232} are slightly high, a fact which will affect the Th^{232} loadings in the HTGR.

6. In all cases, the calculated worth of neptunium 237 is approximately 10% too low. This cross section set should be revised. The infinitely dilute resonance integral of 743.8 barns should probably be higher.

7. The analysis for plutonium is not complete enough to draw conclusions about the cross-section data. Agreement is generally within 5% of measured worth if enough detail is used in the calculations.

8. The gold elements had been loaded as a standard for the resonance materials. Due to uncertainties present in the element loading, both particle size and uniformity, and difficulties with the nuclear model, these elements could not be used as a standard for these reactivity measurements.

3. FACILITY DESCRIPTION

3.1 GENERAL

A detailed physical description of the Modified Critical Facility is contained in the Hazards Report for the facility.[1] The critical assembly proper consists of an array of 1.66-in. thick-walled aluminum tubes welded into a honeycomb structure and mounted on a split bed assembly machine. Each section of the honeycomb is approximately 7 ft by 3 ft; thus, when the bed is fully closed, a honeycomb 7 ft by 6 ft by 6 ft is obtained. The fuel elements consist of highly enriched uranium-graphite compacts contained in thin-walled aluminum tubes. Fuel elements with carbon-to-U^{235} (C/U) ratios of 432, 859, 1718, 2500, and 5000 are used for the different core assemblies. Cylindrical graphite extrusions are used as reflector elements and also in combination with the C/U-859 elements to obtain regions of effectively higher C/U ratios. Eight horizontal safety rods and four horizontal control rods are employed. Figures 1 through 3 show the front, top, and end views of a typical critical assembly.

3.2. CORE CONFIGURATION

Five cores were constructed, each with three distinct regions: (1) the center or exact region made up of fuel elements containing the desired C/U ratio: (2) the heterogeneous or driver region containing a combination of fuel elements and graphite elements giving approximately the same C/U ratio as in the exact region; and (3) the reflector region. Figures 4(a) through 4(e) show an end view of the final core configuration for each of the five cores.

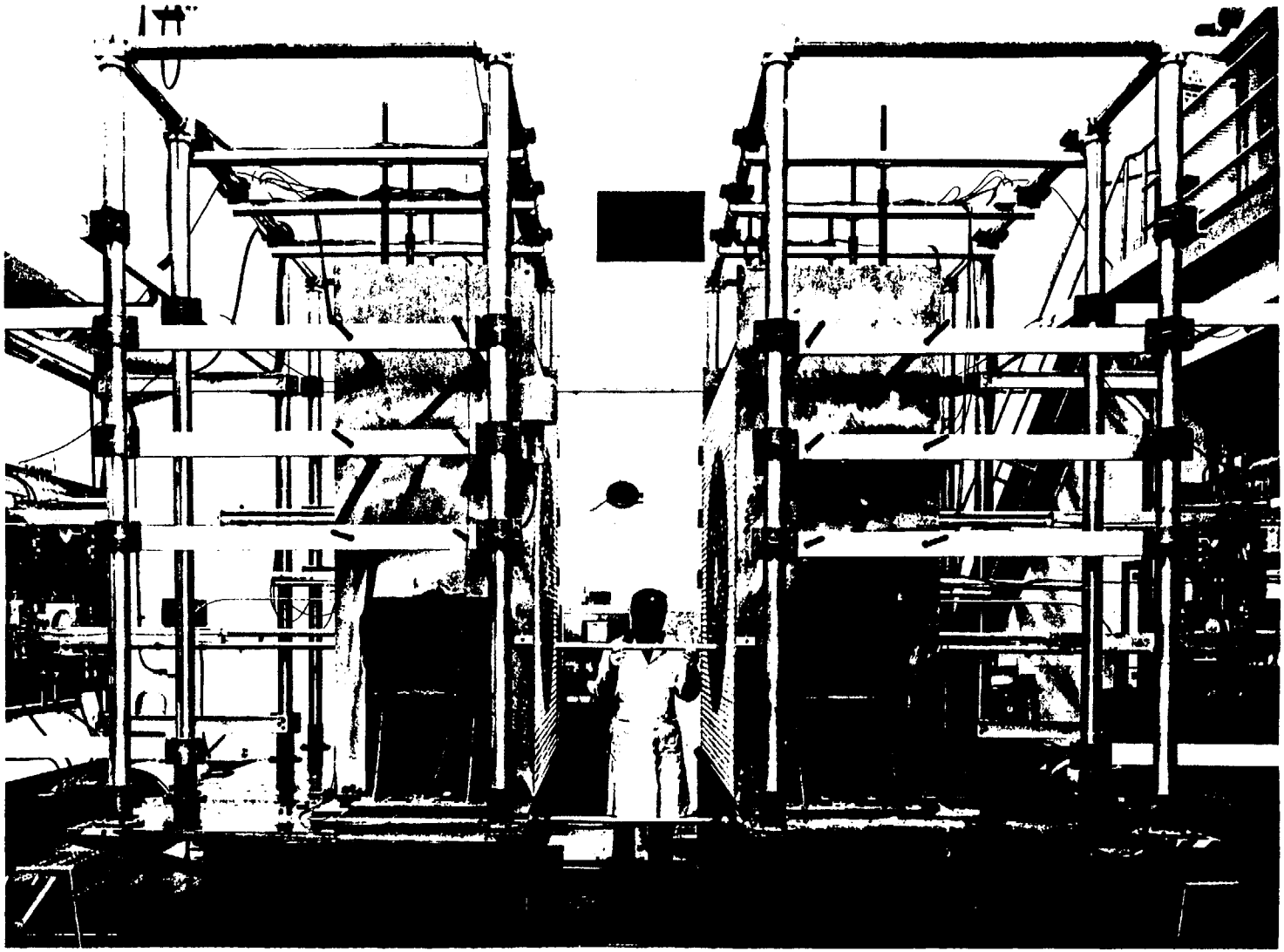

Fig.1. Front view of critical assembly

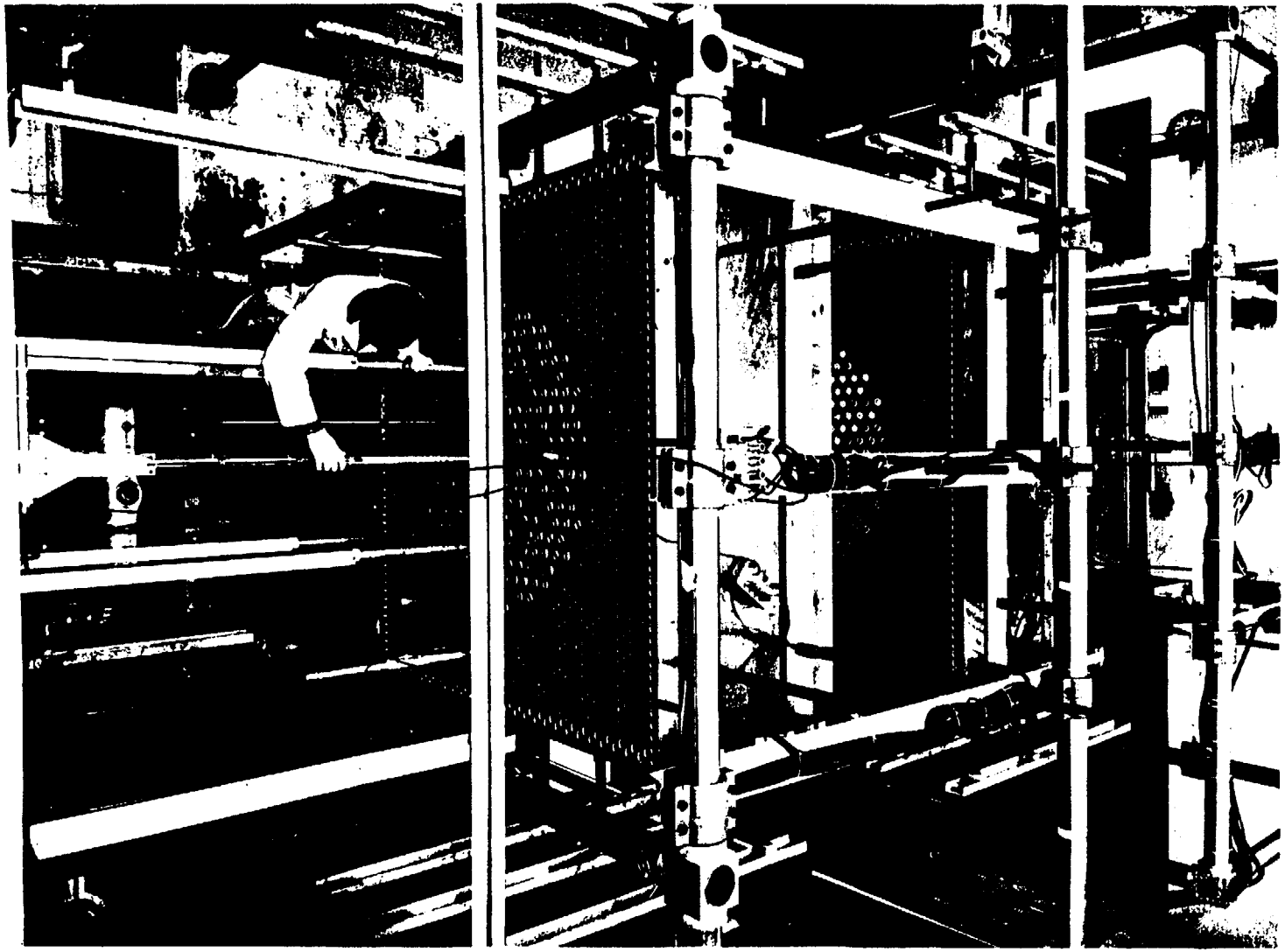

Fig.2. Top View of critical assembly

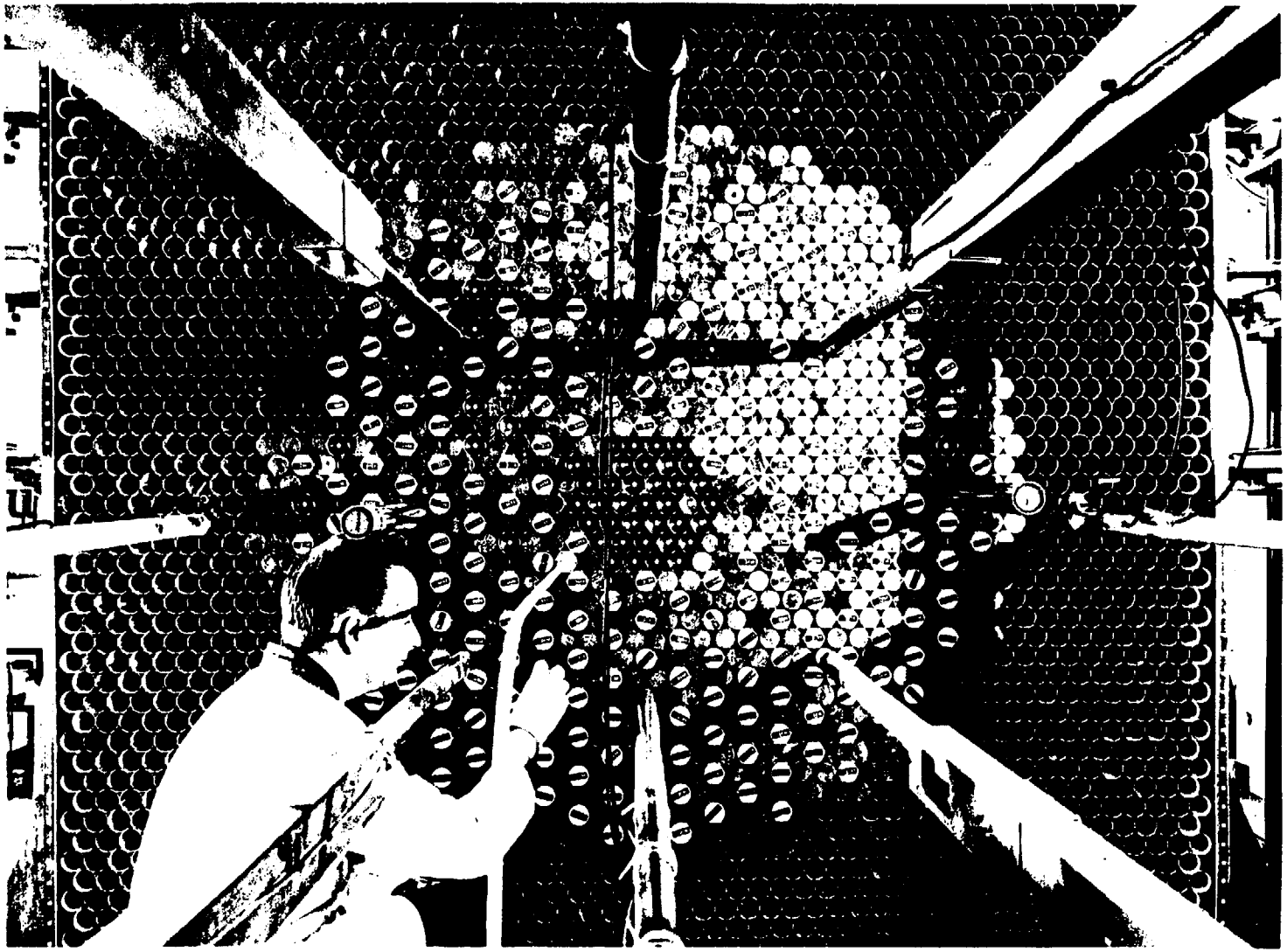

Fig. 3. End view of critical assembly

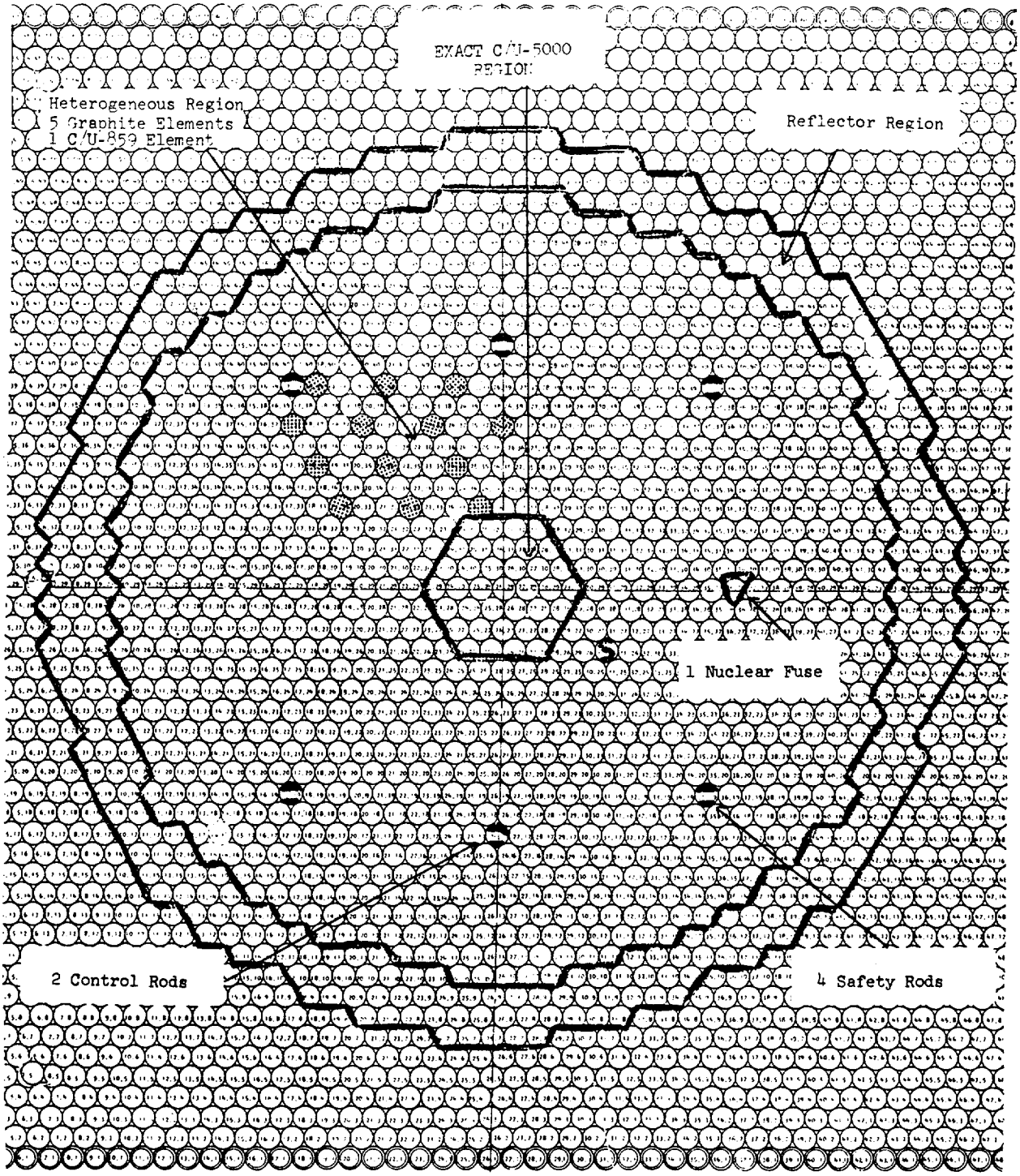

Fig. 4(a). C/U-5000 core configuration

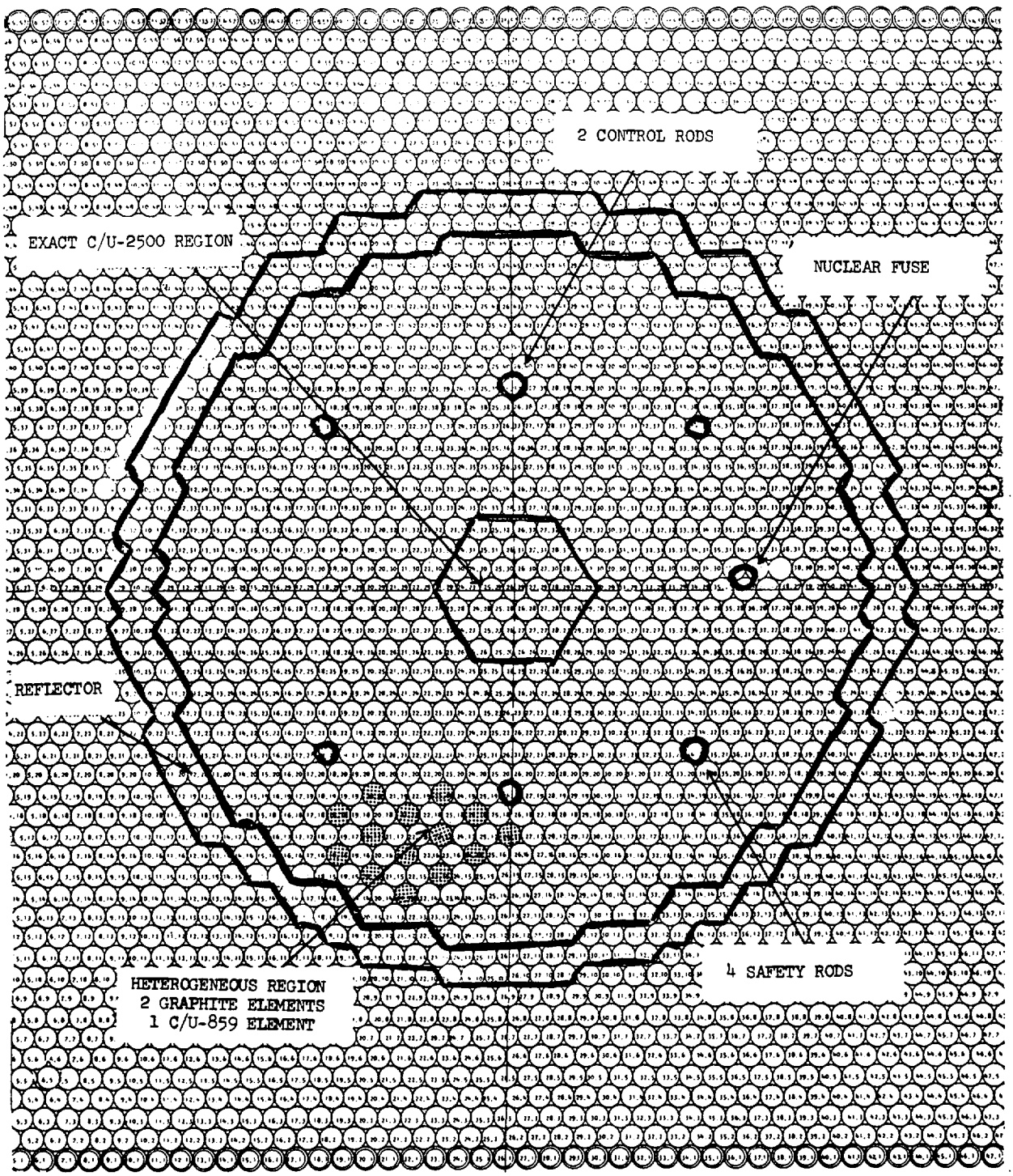

Fig. 4(b). C/U-2500 core configuration

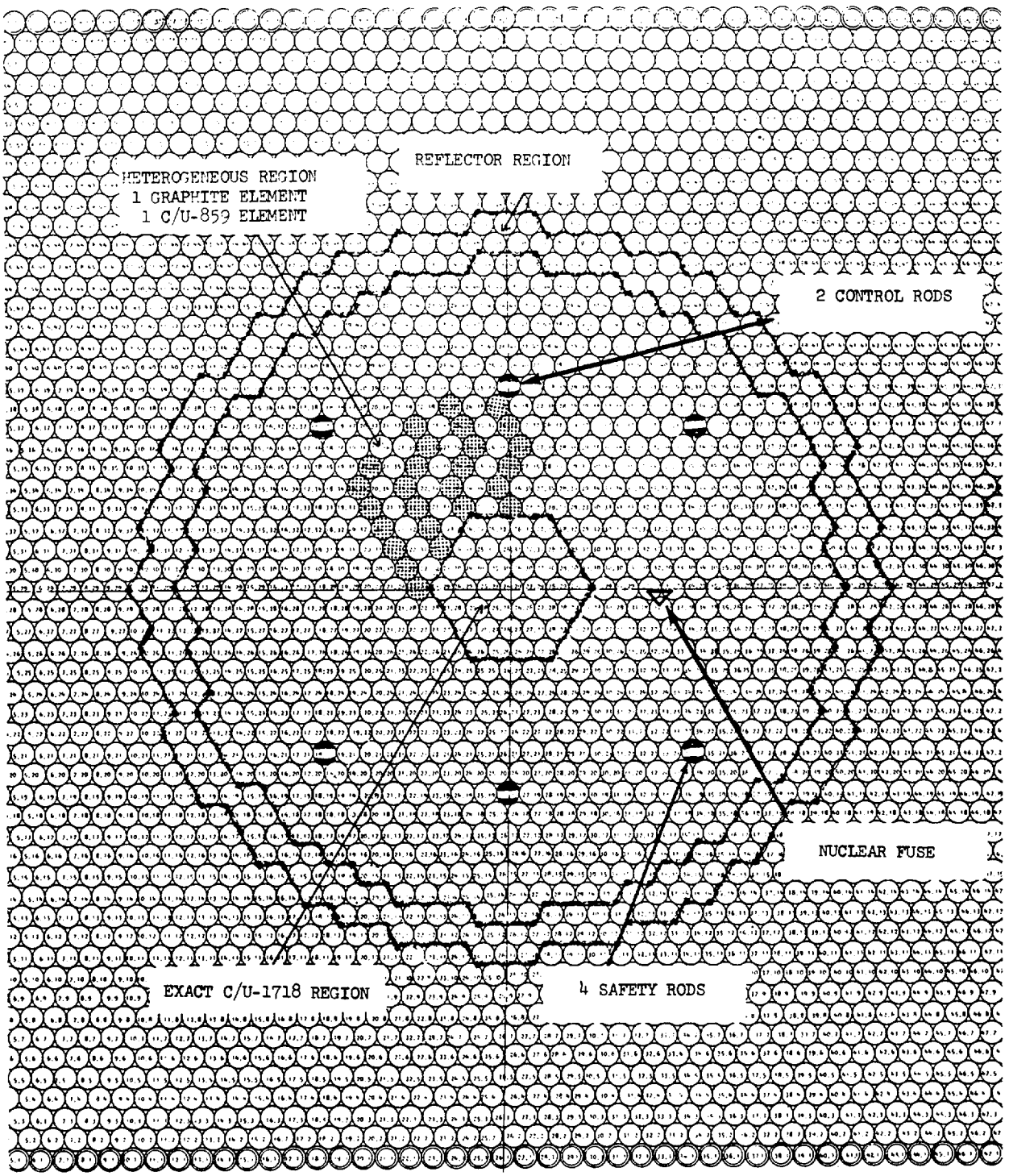

Fig. 4(c). C/U-1718 core configuration

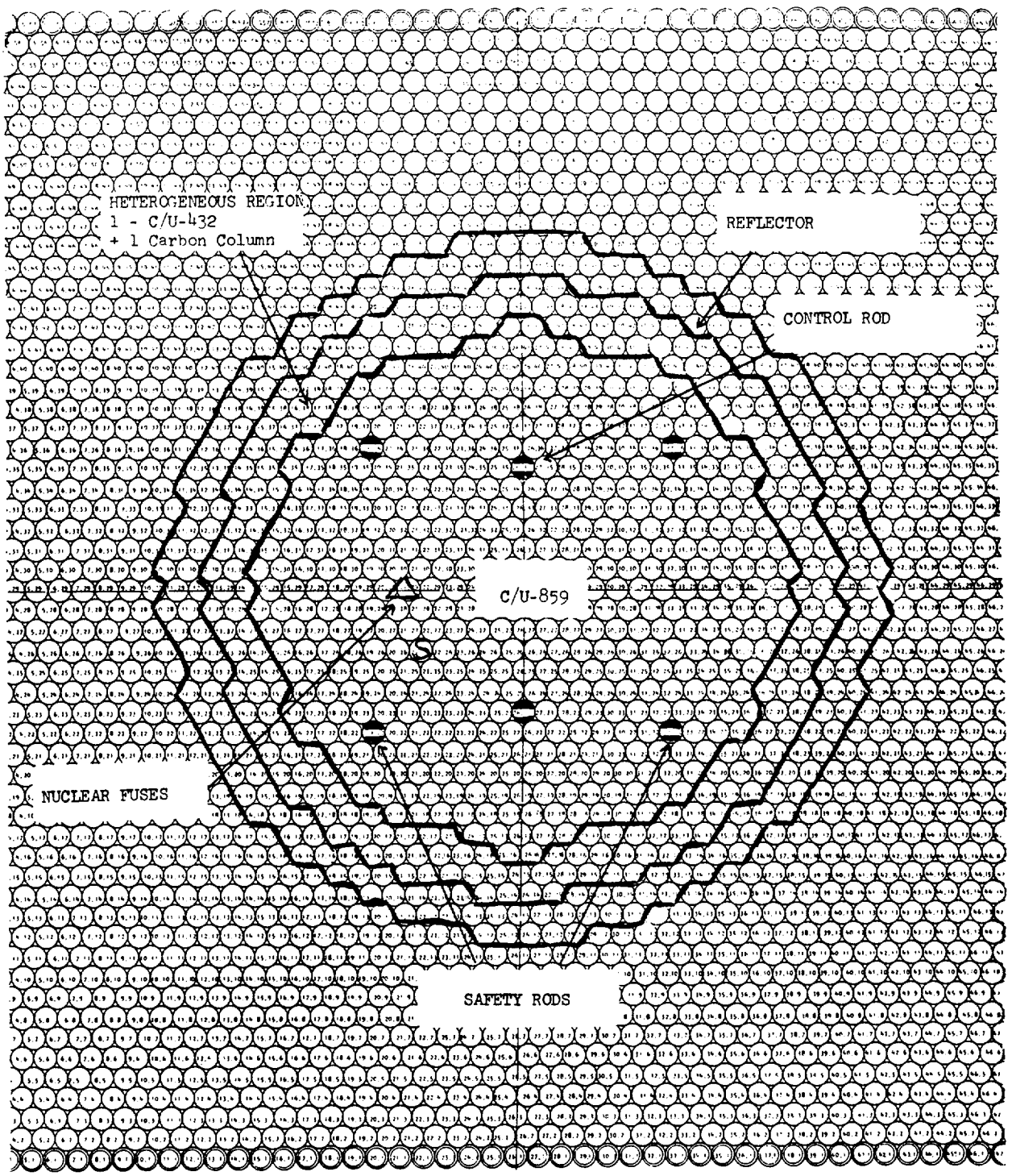

Fig. 4(d). C/U-859 core configuration

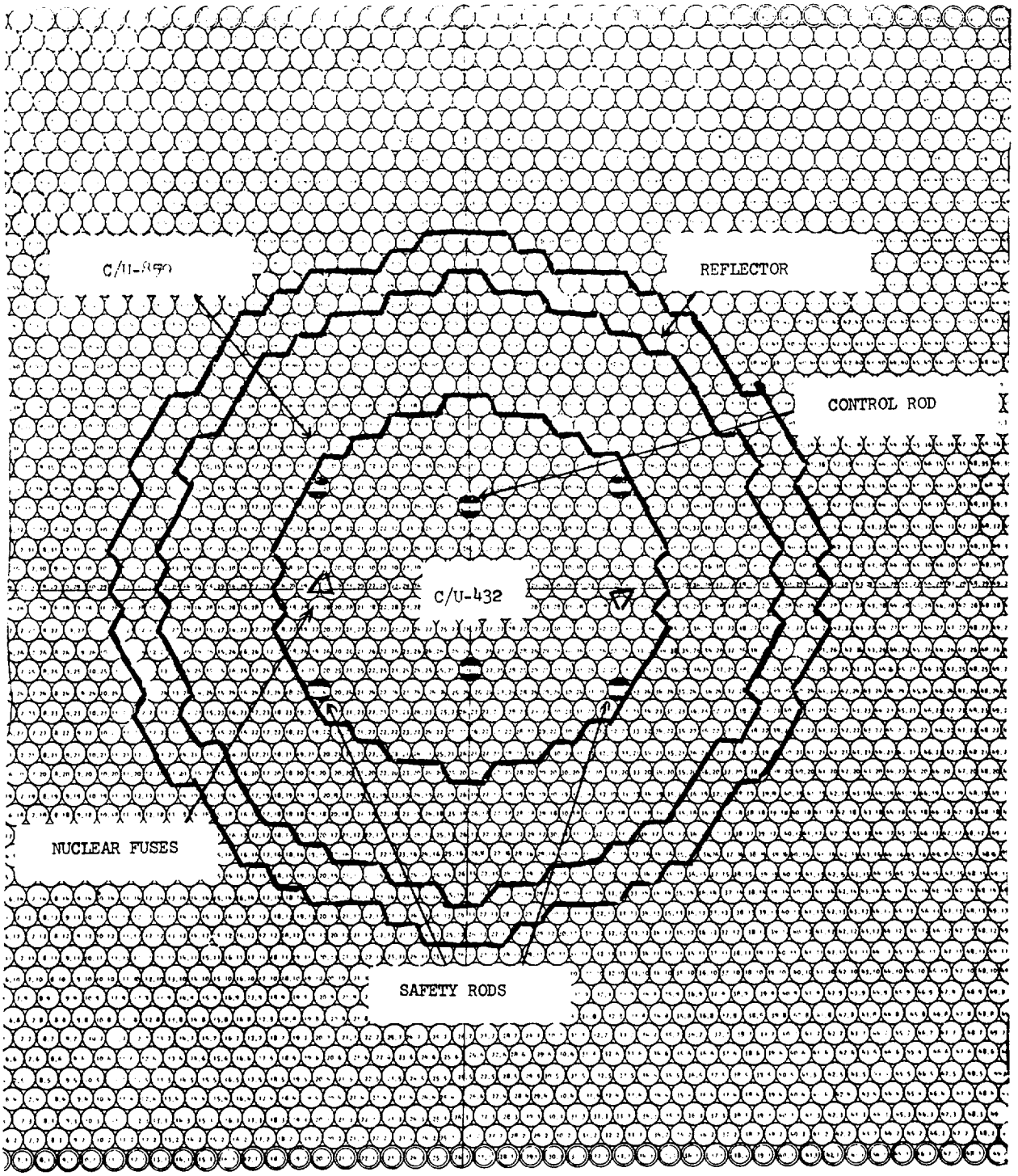

Fig. 4(e). C/U-432 core configuration

3.2.1. Safety Rod, Control Rod, Nuclear Fuse and PoBe Source Locations

The safety rod locations in the five cores shown in Figs. 4(a) through 4(e) are listed in Table 1. Safety rods 1 through 4 are in the fixed half of the assembly, and 5 through 8 are in the moving half.

TABLE 1

SAFETY ROD LOCATIONS

Safety Rod	C/U-5000	C/U-2500	C/U-1718	C/U-859	C/U-432
1	17,19	18,21	18,21	19,22	19,24
2	35,19	34,21	34,21	32,22	32,24
3	17,39	18,37	18,37	19,36	19,34
4	35,39	34,37	34,37	32,36	32,34
5	17,19	18,21	18,21	19,22	19,24
6	35,19	34,21	34,21	32,22	32,24
7	17,39	18,37	18,37	19,36	19,34
8	35,39	34,37	34,37	32,36	32,34

The control rods are located in the cores as indicated in Table 2. Control rods 1 and 2 are in the fixed half of the assembly, and control rods 3 and 4 are in the moving half.

TABLE 2

CONTROL ROD LOCATIONS

Control Rod	C/U-5000	C/U-2500	C/U-1718	C/U-859	C/U-432
1	26,17	26,19	26,19	26,23	26,25
2	26,41	26,39	26,39	26,35	26,33
3	26,17	26,19	26,19	26,23	26,25
4	26,41	26,39	26,39	26,35	26,33

Two nuclear fuses are used in each of the core assemblies except the C/U-432, which has four fuses. The fuses are located in the core assemblies as shown in Table 3.

TABLE 3

NUCLEAR FUSE LOCATIONS

	C/U-5000	C/U-2500	C/U-1718	C/U-859	C/U-432
Fixed	(15,28)	(15,28)	(19,30)	(19,20)	(19,30)
	(16,28)	(I6,28)	(20,29)	(20,29)	(20,29)
	(16,29)	(16,29)	(19,29)	(19,29)	(19,29)
Moving	(34,30)	(35,30)	(32,28)	(32,28)	(32,28)
	(36,30)	(36,30)	(32,29)	(32,29)	(32,29)
	(36,29)	(36,29)	(33,29)	(33,29)	(33,29)

A PoBe neutron source (10-curie initial strength) is used in each half of the assembly and is located as indicated in Table 4.

TABLE 4

SOURCE POSITIONS

	C/U-5000	C/U-2500	C/U-1718	C/U-859	C/U-432
Fixed	(21,26)	(22,26)	(21,26)	(21,26)	(21,26)
Moving	(30,26)	(29,26)	(30,26)	(30,26)	(30,26)

3.2.2. Honeycomb Dimensions

The overall dimensions of each half of the honeycomb assembly are 84.81 in. by 73.44 in. by 35.50 in. The average weight of the aluminum honeycomb tubing is 276 g per 3-ft section with nominal dimensions of 1.590 in. and 1.660 in. Table 5 is a listing of measured dimensions of the honeycomb assembly. All measurements are center to center. These measurements indicate an average actual center to center spacing of the honeycomb tubes of 1.663 in.

TABLE 5

HONEYCOMB ASSEMBLY DIMENSIONS MEASURED

	Position		Measured Dimension
	From	To	(in.)
Fixed	(26,29)	(11,29)	24.94
	(26,29)	(41,29)	24.94
	(26,29)	(26,11)	25.87
	(26,29)	(26,47)	25.90
Moving	(26,29)	(11,29)	24.90
	(26,29)	(41,29)	25.87
	(26,29)	(26,11)	25.90
	(26,29)	(26,47)	25.90

3.2.3. Radial Core and Reflector Dimensions

The dimensions of the effective radii of the core and reflector regions, as determined by the number of unit cells in each region and an equal volume bases, are shown in Table 6.

TABLE 6

EFFECTIVE RADII(cm)

Region/Core	C/U-5000	C/U-2500	C/U-1718	C/U-859	C/U-432
Central exact	13.5	13.5	13.5	47.5	34.2
Heterogeneous	71.5	64.0	59.0	56.5	54.7
Reflector	86.6	71.5	67.4	63.0	61.5

3.2.4. Core Configuration and U^{235} Mass Loading

Table 7 shows the number of fuel elements and the C/U ratio, the number of graphite elements, and the number of reflector columns in each core region. Table 8 presents the U^{235} mass loadings in each core.

TABLE 7

CORE COMPONENTS FOR THE STANDARD CORES

	Exact Region		Heterogeneous Region			
Core	No.3-Ft Fuel Elem.	C/U Ratio	No.3-Ft Fuel Elem.	C/U Ratio	No.3-Ft Graphite Elem.	Reflector Columns
C/U-5000	74	5000	332	859	1672	970
C/U-2500	74	2500	526	859	1042	412
C/U-1718	74	1718	656	859	668	430
C/U-859	898	859	192	432	188	316
C/U-432	440	432	744	859	0	318

TABLE 8

U^{235} MASS LOADINGS

Core	Mass of U^{235} (kg)
C/U-5000	14.6
C/U-2500	23.2
C/U-1718	29.2
C/U-859	54.2
C/U-432	69.4

3.3. FUEL ELEMENTS, SPECIAL ELEMENTS, AND REFLECTOR ELEMENTS

3.3.1. Description

The basic fuel elements for the facility consist of uranium-graphite compacts contained in aluminum tubes sealed on one end by a welded end closure and on the other end by a dust-tight O-ring closure or a swaged-in 1/2-in. teflon plug.

The uranium-graphite compacts are generally made with 93.2 atom-% enriched uranium in the form of U_3O_8, although the exact region elements contain UO_2. The compacts that are cold pressed from a uranium-graphite mixture are approximately 1 in. long with a 1.49-in. diameter. Fuel elements with five different uranium loadings giving five different C/U^{235} ratios are used. The aluminum tubes in which these compacts are contained have an inside diameter of 1.515 in. and an outside diameter of 1.555 in. Each tube is closed by a 0.060-in. aluminum disc welded on the core midplane end and a 0.75-in. aluminum plug on the outer end. The basic fuel element compact stacks are 33.90 ± 0.15 in. long. Approximately 50% of the C/U-859 and C/U-432 fuel elements have been modified by removing the 0.75-in. aluminum plug and adding a 1-in. graphite compact and a 1/2-in. telfon end plug for use as explusion type fuel element.[1] Whenever fuel elements of these C/U ratios are used in any of the five cores, approximately 65% are of the expulsion type.

The special elements are similar to those described above, with the following exceptions: (1) A special material such as neptunium or plutonium is added to the graphite instead of the U_3O_8. (2) The aluminum tube in which the elements are contained has a 0.060-in. aluminum disc welded on each ends and has a nominal wall thickness of 0.035 in. (3) The outer diameter of the compacts is 1.47 in. (4) The special element compact stacks are 34.50 ± 0.15 in. long with a diameter of 1.575 in.; they are not contained in aluminum tubes.

Table 9 lists the core and reflector material densities in the various core regions. For convenience, the densities of the aluminum honeycomb region are included. These densities have been derived from the average element weights using a unit cell area of 15.452 cm^2 and the specified above to compute the volume.

TABLE 9

MATERIAL DENSITIES

Core	Isotopic Mass Loadings (g/cm^3)					
	C	Al	U^{235}	U^{238}	O	H_2O
			Exact Region			
C/U-5000	1.302	0.3073	0.5081-2	0.371-3	0.065-2	1.05-3
C/U-2500	1.299	0.3073	1.0175-2	0.743-3	0.131-2	1.05-3
C/U-1718	1.296	0.3073	1.4765-2	1.078-3	0.190-2	1.05-3
C/U-859	1.393	0.3073	3.1706-2	2.314-3	0.523-2	2.25-3
C/U-432	1.395	0.3073	6.3590-2	4.641-3	1.049-2	3.68-3
			Heterogeneous Region			
C/U-5000	1.476	0.2162	0.5284-2	0.386-3	0.089-2	0.44-3
C/U-2500	1.460	0.2344	1.0569-2	0.771-3	0.179-2	0.80-3
C/U-1718	1.443	0.2526	1.5853-2	1.157-3	0.268-2	1.16-3
C/U-859	1.444	0.2526	3.1795-2	2.320-3	0.525-2	2.50-3
C/U-432[(a)]	1.393	0.3073	3.1706-2	2.314-3	0.523-2	2.25-3
			Reflector Region			
C/U-5000	1.493	0.1980				0.075-3
C/U-2500	1.493	0.1980				0.075-3
C/U-1718	1.493	0.1980				0.075-3
C/U-859	1.493	0.1980				0.075-3
C/U-432	1.493	0.1980				0.075-3
			Aluminum Honeycomb Region			
C/U-5000		0.1980				
C/U-2500		0.1980				
C/U-1718		0.1980				
C/U-859		0.1980				
C/U-432		0.1980				

(a) The "heterogeneous" region of the C/U-432 core consists of exact C/U-859 elements.

Material densities for all of the special elements for which substitution experiments were performed are shown in Table 10. This table gives the material densities for the special material compacts only since all of their aluminum containers were essentially identical and their worths cancel in the measurements.

TABLE 10

SPECIAL ELEMENT ISOTOPIC LOADINGS

Special Element Description	Isotopic Mass Loading (g/cm^3)[a]				
	C	U^{233}	U^{235}	U^{236}	U^{238}
Exact 5000[b]	1.789		0.6982-2		0.510-3
Exact 2500[b]	1.785		1.3982-2		1.021-3
Exact 1718[b]	1.781		2.0290-2		1.481-3
Exact 859[b]	1.914		4.3570-2		3.181-3
Exact 432[b]	1.917		8.7385-2		6.379-3
Special 5000	1.788		0.7586-2		0.558-3
Special 2500	1.784		1.5433-2		1.131-3
Special 1718	1.781		2.2590-2		1.646-3
Special 859	1.766		4.4117-2		3.221-3
Special 432	1.752		8.7417-2		6.384-3
Depleted uranium 50	1.781		1.0910-4		0.0515
Depleted uranium 100	1.755		2.1816-4		0.1030
Depleted uranium 200	1.716		4.3126-4		0.2036
Depleted uranium 300	1.673		6.4118-4		0.3027
Depleted uranium 500	1.599		10.2762-4		0.4851
U^{233} 5000	1.799	0.6254-2	0.200-5		0.258-3
U^{233} 2500	1.775	1.6882-2	0.530-5		0.701-3
U^{233} 432	1.751	5.9007-2	1.832-5		2.462-3
U^{236} 5000	1.761		0.7586-2	0.1552-2	0.096-2
U^{236} 1718	1.761		2.1879-2	0.4476-2	0.275-2
U^{236} 432	1.723		8.7914-2	1.7987-2	1.106-2

(a) Value shown is total mass per element/total volume per element where element does not include aluminum container.

(b) These compacts are 1.49 in. o.d. All others are 1.460 in. o.d.

TABLE 10 (continued)

Special Element Description	Isotopic Mass Loading(g/cm^3)[a] C	Th	Al	Np^{237}	Au	B
Carbon reference density	1.769					
Carbon 90% density	1.649					
Carbon reflector[b]	1.848					
Aluminum rod[b]			2.70			
Boron 0.10	1.805					1.082-4
Boron 0.20	1.821					2.181-4
Boron 0.45	1.804					4.778-4
Boron 0.55	1.809					5.882-4
Boron 1.00	1.794					1.059-3
Boron 1.50	1.804					1.587-3
Boron 1.90	1.782					1.999-3
Thorium 50	1.782	0.0540				
Thorium 100	1.761	0.1049				
Thorium 200	1.725	0.2066				
Thorium 300	1.673	0.3063				
Thorium 500	1.622	0.5044				
Np^{237} 5	1.758			0.518-2		
Np^{237} 15	1.753			1.552-2		
Np^{237} 55	1.738			5.661-2		
Au 5	1.802				0.524-2	
Au 15	1.747				1.549-2	
Au Cn (45)	1.798				4.777-2	

(a) Value shown is total mass per element/total volume per element where element does not include aluminum container.

(b) Reflector carbon column is 1.570 in. o.d. The aluminum rod is 1.50 in. o.d. All other elements are 1.460 in. o.d.

TABLE 10 (continued)

Special Element Description	Isotopic Mass Loading(g/cm^3)(a)				
	C	Pu^{239}	Pu^{240}	Pu^{241}	Pu^{242}
PuH 240 A	1.800	1.9118-2	5.8630-3	1.240-3	2.262-4
PuH 240 B	1.818	0.7111-2	2.1815-3	0.461-3	0.845-4
PuH 240 C	1.794	0.2691-2	0.8259-3	0.175-3	0.315-4
PuL 240 A	1.792	1.9124-2	8.202.4	2.22-5	
PuL 240 B	1.792	0.7117-2	3.049-4	0.83-5	
PuL 240 C	1.783	0.2698-2	1.159-4	0.32-5	

(a) The value shown is total mass per element/total volume per element where element does not include aluminum container.

All compacts are 1.460 in. diameter.

3.3.2. Water Content and Other Impurities

Because of the relatively high reactivity worth of water in several of the core assemblies, measurements were made to determine the water content of the fuel and reflector elements. This was done by heating an element in a stainless steel container using a vacuum pump-cold trap system to collect the moisture. Results for all five types of fuel elements, as well as for the reflector elements, are shown in Table 11.

TABLE 11

AVERAGE WATER CONTENT OF FUEL AND REFLECTOR ELEMENTS

Element Type	Water Content (g/element)	Water Content (g/cm^3)
C/U-5000	1.4	1.3-3
C/U-2500	1.4	1.3-3
C/U-1718	1.4	1.3-3
C/U-859	3.0	2.8-3
C/U-432	4.9	4.6-3
Reflector graphite	0.1	0.9-4

The material used for the honeycomb assembly and the fuel containers is 6061 aluminum. Nuclear grade graphite is used in the fuel and special element compacts and the reflector columns. Nominal impurities (in ppm by weight) in the aluminum and carbon in the assembly are shown in Table 12.

TABLE 12

NOMINAL IMPURITIES FOR CORE MATERIALS

Impurity Element	Al 6061 (ppm)	Reflector Carbon(ppm)	Fuel Element Carbon (ppm)
Al	Remainder	8	100
As		< 40	< 100
B		4	0.5
Cd		< 20	< 10
Co		< 40	< 6
Cr	2,000	< 40	< 40
Cu	2,000	80	< 10
Fe	7,000	800	220
Hg		< 20	< 8
K		< 10	40
Mg	10,000	0.5	10
Mn	1,500	40	5
Mo		1	1
Na		< 50	140
Ni		40	6
P		100	100
Sb		< 20	< 10
Si	6,000	100	210
Sr		< 80	< 40
Ti	1,500	20	< 1
W		< 40	< 40
Zn	2,500	< 10	< 100

3.3.3. Particle Size of Special Materials

All of the special materials except gold and boron are in the chemical form of oxides. The oxide materials generally consist of particles ranging in size from submicron to 5 microns. The gold cyanide and the neptunium and plutonium oxides have particle sizes ranging from submicron to 37 microns, and the distribution within that range is not known. The boron is in the form of B_4C and has a particle size of about 5 microns. Several of the elements containing gold were fabricated using a gold chloride solution. After the solution was mixed with graphite flour, the mixture was dehyrated and the gold chloride was decomposed by heating to 600°F. Analysis has indicated a submicron gold particle size nearly uniformly distributed.

4. EXPERIMENTAL METHODS

4.1. SHUTDOWN MECHANISMS

4.1.1. Control Rods

The differential control rod worth was measured by the period technique. The total intergral worths are listed in Table 13.

TABLE 13

CONTROL ROD WORTH

	Integral Worth ($)				
Control Rod	C/U-5000	C/U-2500	C/U-1718	C/U-859	C/U-432
1	0.3877	0.35	0.25	0.25	0.1608
2	0.38	0.3596	0.2581	0.2478	0.16
3	0.38	0.35	0.2552	0.25	0.16
4	0.3770	0.35	0.25	0.2485	0.1562

4.1.2. Safety Rods

The total worth of a single safety rod was obtained by the subcritical source multiplication technique using a previously calibrated regulating rod to generate the necessary inverse source multiplication curve. The results of these measurements are shown in Table 14.

TABLE 14

SAFETY ROD WORTH

Core	Averaged Worth Per Rod($)
C/U-5000	0.84
C/U-2500	0.85
C/U-1718	0.79
C/U-859	0.87
C/U-432	0.86

4.1.3. Nuclear Fuses

The worth of a nuclear fuse was determined by the inverse source multiplication technique. A fired fuse was inserted in place of a charged fuse and the reactivity loss measured. Results of these measurements are shown in Table 15.

TABLE 15

NUCLEAR FUSE WORTH

Core	Number of Fuses in Core	Worth Per Fuse($)
C/U-5000	2	1.25
C/U-2500	2	0.57
C/U-1718	2	0.86
C/U-859	2	0.54
C/U-432	4	0.31

4.2. EFFECTIVE MULTIPLICATION

To facilitate calculations, experimental corrections were made to the core excess reactivity for the locations taken up by control rods, safety rods, nuclear fuses, etc. These corrections were made by removing graphite columns or fuel elements at the same radial distance as the component under investigation and substituting a stainless sleeve (in the case of the rods) similar to the control and safety rod sleeve. The resultant reactivity loss was then measured with a calibrated control rod. The reflective effect of the honeycomb in the region beyond the radial graphite reflector was measured by measuring the worth of aluminum tubes that were inserted uniformly throughout this region and then applying a straight linear mass extrapolation. These results are shown in Table 16.

TABLE 16

CORRECTED CORE EXCESS REACTIVITY($)

	C/U-5000	C/U-2500	C/U-1718	C/U-859	C/U-432
Measured core excess reactivity	0.445	0.474	0.458	0.475	0.432
Correction for eight safety rod locations	0.928	0.914	1.050	1.029	1.180
Correction for four control rod locations	0.641	0.980	0.689	0.835	0.809
Correction for two nuclear fuses	0.204	0.235	0.535	0.445	0.874
Correction for source tube at two locations	0.026	0.020	0.040	0.051	0.042
Honeycomb correction	-0.354	-0.550	-0.866	-1.074	-1.062
Corrected core excess reactivity	1.890	2.073	1.906	1.761	2.275

4.3. MEASUREMENTS OF THE REACTIVITY COEFFICIENTS OF THE SPECIAL ELEMENTS

The reactivity coefficients of the special elements were measured in the central honeycomb locations, (26,29). The measurements were performed by first determining the control rod positions required to make the assembly slightly supercritical by about $0.002 with the central location occupied by an element containing pure graphite compacts of the same density as the special elements. The actual amount supercritical was determined by the drift technique, which determined the linear component of the expoential increase for periods greater than several thousand seconds. A linear strip chart recorder with a high gain differential input was used for this purpose. The special reference density graphite element was then replaced by the special element under investigation, and the new control rod position required to make the core just slightly supercritical was again determined by the drift technique. In cases where this difference in worth was more than $0.50 (the maximum allowable excess reactivity), the intermediate steps were taken in which reflector graphite elements were added or removed to

adjust the total excess reactivity. The reactivity worth of these reflector changes was again measured on the control rods. Several of the control rod calibration points were checked with the added reflector material present, and these checks indicated that the calibration was not changed. The results of these measurements are shown in Table 17. The estimated experimental uncertainty is ±$0.001.

4.4. PULSE NEUTRON MEASUREMENTS OF β_{eff}/Λ

All five core assemblies were pulsed, and a prompt decay constant was determined for each core. Using the expression

$$\frac{\beta_{eff}}{\Lambda} = \frac{\alpha}{\rho - 1} \quad ,$$

where ρ represents the reactivity in dollars that the core is subdelayed critical, Λ represents the prompt generation time, and α is the prompt decay constant, a value of $\beta_{eff}/$ was obtained for each core. Results of these measurements are shown in Table 18.

TABLE 17

REACTIVITY WORTH OF SPECIAL ELEMENTS($)
(RELATIVE TO REFERENCE DENSITY GRAPHITE)

Special Element Description	Core Assembly C/U-5000	C/U-2500	C/U-1718	C/U-859	C/U-432
U^{235} 5000	0.082	0.047	0.024	0.010	
U^{235} 2500	0.156	0.080	0.043	0.015	
U^{235} 1718	0.216	0.111	0.060	0.019	
U^{235} 859	0.387	0.196	0.104	0.029	0.011
U^{235} 432	0.656	0.332	0.185	0.053	0.022
Depleted uranium 50	-0.074	-0.093	-0.099	-0.096	-0.078
Depleted uranium 100	-0.119	-0.150	-0.152	-0.143	-0.128
Depleted uranium 200	-0.182	-0.225	-0.238	-0.228	-0.190
Depleted uranium 300	-0.233	-0.285	-0.300	-0.288	-0.244
Depleted uranium 500	-0.308	-0.370	-0.389	-0.369	-0.318
U^{233} 5000	0.110	0.076	0.059	0.025	
U^{233} 2500	0.284	0.186	0.135	0.079	0.052
U^{233} 1718	0.854	0.565	0.415	0.243	0.164
U^{236} 5000	0.071	0.029	0.010	-0.004	-0.005
U^{236} 2500	0.191	0.082	0.033	-0.005	-0.010
U^{236} 432	0.596	0.263	0.115	-0.010	-0.026
PuH 240 A	0.070	-0.145	-0.222	-0.251	-0.183
PuH 240 B	0.016	-0.083	-0.121	-0.131	-0.093
PuH 240 C	0.003	-0.038	-0.052	-0.058	-0.040
PuL 240 A	0.264	0.079	-0.003	-0.061	-0.046
PuL 240 B	0.116	0.035	+0.001	-0.025	-0.019
PuL 240 C	0.050	0.016	+0.002	-0.009	-0.006
Carbon 90% density	-0.008	-0.009	-0.015	-0.018	-0.017
Void	-0.171	-0.248		-0.318	-0.343
Aluminum rod	-0.360	-0.360	-0.361	-0.301	-0.256

TABLE 17 (continued)

Special Element Description	Core Assembly C/U-5000	C/U-2500	C/U-1718	C/U-859	C/U-432
Boron 0.10	-0.080	-0.061	-0.048	-0.026	
Boron 0.20	-0.162	-0.116	-0.096	-0.054	
Boron 0.45	-0.341	-0.271	-0.212	-0.120	-0.061
Boron 0.55	-0.430	-0.346	-0.268	-0.156	-0.078
Boron 1.00	-0.725	-0.593	-0.461	-0.273	-0.141
Boron 1.50	-1.025	-0.853	-0.668	-0.399	-0.211
Boron 1.90	-1.231	-1.031	-0.817	-0.494	-0.266
Thorium 50	-0.046	-0.053	-0.055	-0.056	-0.048
Thorium 100	-0.085	-0.094	-0.093	-0.092	-0.080
Thorium 200	-0.157	-0.171	-0.170	-0.159	-0.139
Thorium 300	-0.218	-0.232	-0.230	-0.211	-0.185
Thorium 500	-0.330	-0.342	-0.331	-0.296	-0.258
Np^{237} 5	-0.084	-0.084	-0.077	-0.064	-0.045
Np^{237} 15	-0.242	-0.243	-0.227	-0.185	-0.136
Np^{237} 55	-0.790	-0.791	-0.736	-0.589	-0.427
Au 5	-0.097	-0.104	-0.103	-0.088	-0.063
Au 15	-0.246	-0.266	-0.256	-0.219	-0.165
Au Cn (45)	-0.533	-0.558	-0.526	-0.437	-0.323

TABLE 18

PULSE NEUTRON MEASUREMENTS

Core	ρ ($)	α	β_{eff}/Λ
C/U-5000	-0.20	22.33	18.6
C/U-2500	-0.15	37.49	32.6
C/U-1718	-0.20	55.54	46.3
C/U-859	-0.199	113.28	94.4
C/U-432	-0.161	175.07	150.8

4.5. REPRODUCIBILITY AND EXPERIMENTAL UNCERTAINTY

All reactivity measurements were performed using calibrated control rods. The control rod drive is provided with a stepping system which allows the rod to be moved in steps of 0.003 in. The maximum worth of a calibrated control rod is $0.03 per in. which is < $0.001 per step.

Table 19; lists measurements made in the C/U-1718 core over a one-month period; it represents the typical reproducibility obtained in making substitution measurements. Similar results were obtained for the other cores.

TABLE 19

TYPICAL REPRODUCIBILITY OF
SUBSTITITUION MEASUREMENTS

Basic Core Excess Reactivity($)	Excess Reactivity With Boron 0.55 Special Element in Center of Core($)	Worth of Boron 0.55 Special Element($)	Deviation($) From Mean
0.4294	0.1013	0.3281	0.0004
0.4296	0.1012	0.3284	0.0001
0.4301	0.1014	0.3287	0.0002
0.4301	0.1015	0.3286	0.0001
0.4316	0.1029	0.3287	0.0002
0.4436	0.1152	0.3284	0.0001

Although it is impossible to condense the evaluation of experimental uncertainties into a simple sentence or expression encompassing all the cores and special elements the following should serve as a guide. It is believed that aside from loading errors the experimental results should not be relied upon to better than ±1% with a minimum uncertainty of ±$0.001.

5. ANALYTICAL METHODS

5.1. CROSS-SECTION DATA

The analysis reported here has used the cross-section data existing on the GAM[2] and GATHER[3] data tapes at Gulf General Atomic. The sources of the data for the important nuclides are listed in Table 20. For several nuclides, more than one cross-section set available; in many cases, the reactivity coefficient analysis was made using the several sets. In the GAM energy range the basic differential cross-section data was averaged over a 1/E spectrum using the GAVER[4] code.

The initial analysis for the C/U-2500,-1718 and -859 core assemblies was made utilizing the U^{235} cross-section data listed as nuclide number 92.2350 (Table 20). From the comparison between experiment and analysis of the core effective multiplication constants and the reactivity coefficients for U^{235}, it was evident that the value of α^{235}_{epi} was to high. When the cross-section data for nuclide number 92.2352 became available and was used in the calculations for these cores, the difference mentioned above was essentially eliminated. The major differences between the two sets of cross-section data are summarized in Table 21. The resonance integrals calculated from the new set of data are in good agreement with experimentally measured values.[5]

A revised set of neutron cross sections for U^{233} (92.2334) has been obtained from the Oak Ridge National Laboratory. This set is similar to the "GA Best Fit" 92.2333 set described by Drake except for the neutron energy range between 0.5 eV and 10 keV. In this energy range, new fission and capture cross-section data has been obtained in differential measurements made at Rensselaer Polytechnic Institute by Oak Ridge National Laboratory and Rensselaer Polytechnic Institute scientists. A comparison between the new and old data is shown in Table 22.

TABLE 20

SOURCE DATA REFERENCES FOR
GAM AND GATHER CROSS SECTIONS

Nuclide	References
Natural Boron	BNL-235, 2nd Ed., Supplement 2, 1964.
Carbon, 300° K	(1) Bell, J., "SUMMIT, An IBM-7090 Program for the Computation of Crystalline Scattering Kernels", GA-2492, February 1962. (2) Young, J.A., et al., "Neutron Thermalization in Graphite", GA-6075, February 1965. (3) 6.003021 Gasket to 2.38 eV.
Al	Joanou, G. D. and C. A. Stevens,"Neutron Cross Sections for Aluminum". GA-5884, November 1964.
Au	BNL-325 3rd Ed. and ENDF/B File from Battelle Northwest, documnent to be published.
Th (90.2320 and 90.2321)	Drake, M.K. and P. F. Nichols, "Neutron Cross Sections for Thorium", GA-6404,September 1966.
U^{233} (92.233)	(1) Hughes, D. J., B. A. Magurno, and M. K. Brussel, "Neutron Cross Sections,", BNL-235 Supplement 1, Brookhaven National Laboratory, January 1960. (2) Howerton, R.J., "Semi-Empirical Neutron Cross Sections", UCRL-5351 Lawrence Radiation Laboratory, November 1956. (3) Hopkins, J.C. and B.C. Diven, "Neutron Capture to Fission Ratios in U^{233}, U^{235}, Pu^{239}", NSE, Vol. 12, No. 2, Page 169, February 1962. (4) Pattenden, N.J. and J. A. Harvey, "Measurement of the Neutron Total Cross Section of U^{233} from 0.07 to 10,000 eV", NSE, Vol. 17, Page 404, November 1963. (5) Morre, M.S., L.G. Millter, and O. D. Simpson, "Slow Neutron Total and Fission Cross Section of U^{233}", Phys. Rev. Vol. 118, No. 3, Page 714, May 1960.
U^{233} (92.2333)	Drake, M.K., "Neutron Cross Sections for U^{233}", GA-7076, September 1966.

TABLE 20 (continued)

Nuclide	References
U^{233} (92.2334)	RPI Preliminary ENDF/B Data March 1967, Weston, L. W., (ORNL-TM) to be released.
U^{235} (92.2350)	Joanou, G.D. and M. K. Drake, "Neutron Cross Sections for U^{235}", GA-6087, February 1965.
U^{235} (92.2352)	Lubitz, C. R., and M. K. Drake, "U^{235} Cross Sections for ENDF/B" unpublished memo KAPL, December 1966.
U^{236} (92.2360 and 92.2361)	BNL-325, 2nd Edition, Supplement 2.
U^{238} (92.2380 and 92.2381)	Joanou, G.D. and C. A. Stevens, "Neutron Cross Sections for U^{238}", GA-6087, February 1965.
Np^{237} (92.2372 and 93.2372)	Drake, M. K., "Np^{237} Cross Section set as re-evaluated December 1966", GAMD to be published.
Pu^{239}	Drake, M.K. and M. W. Dyos, "A Compilation Evaluation of the Nuclear Data Available for the Major Plutonium Isotopes", GA-6576, July 1955.
Pu^{240}	Same reference as Pu^{239}.
Pu^{241}	Same reference as Pu^{239}.
Pu^{242}	Same reference as Pu^{239}.

TABLE 21

U^{235} CROSS SECTION DATA

	92.2352	92.2350
	2200 m/sec Values	
$\sigma_{n,\gamma}$	100.5 barns	101.0 barns
$\sigma_{n,f}$	579.5 barns	581.0 barns
α	0.1734	0.1738
η	2.071	2.070
ν	2.430	2.430
	Epithermal Values (0.5 eV cutoff)	
Capture integral	142.5 barns	147.8 barns
Fission integral	280.0 barns	263.2 barns
α_{epi}	0.509	0.562

TABLE 22

U^{233} CROSS SECTION DATA

	92.2334	92.2333
	2200 m/sec Values	
$\sigma_{n,\gamma}$	48.2	48.2
$\sigma_{n,f}$	525	525
α	0.0918	0.0918
η	2.293	2.293
ν	2.503	2.503
	Epithermal Values (0.5 eV cutoff)	
Capture integral	140 barns	135 barns
Fission integral	770 barns	775 barns
α_{epi}	0.182	0.175

The GAM and GATHER spectrum calculations were run in the B_1 approximation to the static Boltzmann transport equation. The as-built isotopic atom densities and dimensions were used for the five assemblies and are tabulated in Table 23. The calculated GAM and GATHER spectra are plotted in Figs. 5(a) through 5(e) as a function of lethargy for the five assemblies.

TABLE 23

ISOTOPIC ATOM DENSITIES FOR
SPECTRUM CALCULATIONS

Isotopes	Atom Density for each core assembly (atoms/barn-cm) C/U-5000	C/U-2500	C/U-1718	C/U-859	C/U-432
Base Core Constituents					
C	7.372-2	7.294-2	7.201-2	7.044-2	6.994-2
O	3.831-5	1.475-4	1.146-4	2.642-4	5.780-4
Al	4.895-3	5.230-3	5.690-3	6.856-3	6.856-3
U^{235}	1.3527-5	2.7220-5	4.0498-5	8.1633-5	1.6308-4
U^{238}	9.750-7	1.990-6	2.951-6	5.958-6	1.189-5
Impurities of C and Al					
H (in H_2O)	0.302-4	0.555-4	0.804-4	1.484-4	2.420-4
B	3.5-7	3.5-7	3.5-7	3.5-7	3.5-7
Na	8.2-6	8.2-6	8.2-6	8.2-6	8.2-6
Cr	9.0-6	8.9-6	8.9-6	8.9-6	8.9-6
Mn	5.1-6	5.1-6	5.1-6	5.1-6	5.1-6
Fe	4.2-6	4.2-6	4.2-6	4.2-6	4.2-6
Cu	7.3-6	7.3-6	7.3-6	7.3-6	7.3-6
Buckling B^2	1.02-3	1.2-3	1.5-3	1.6-3	1.6-3

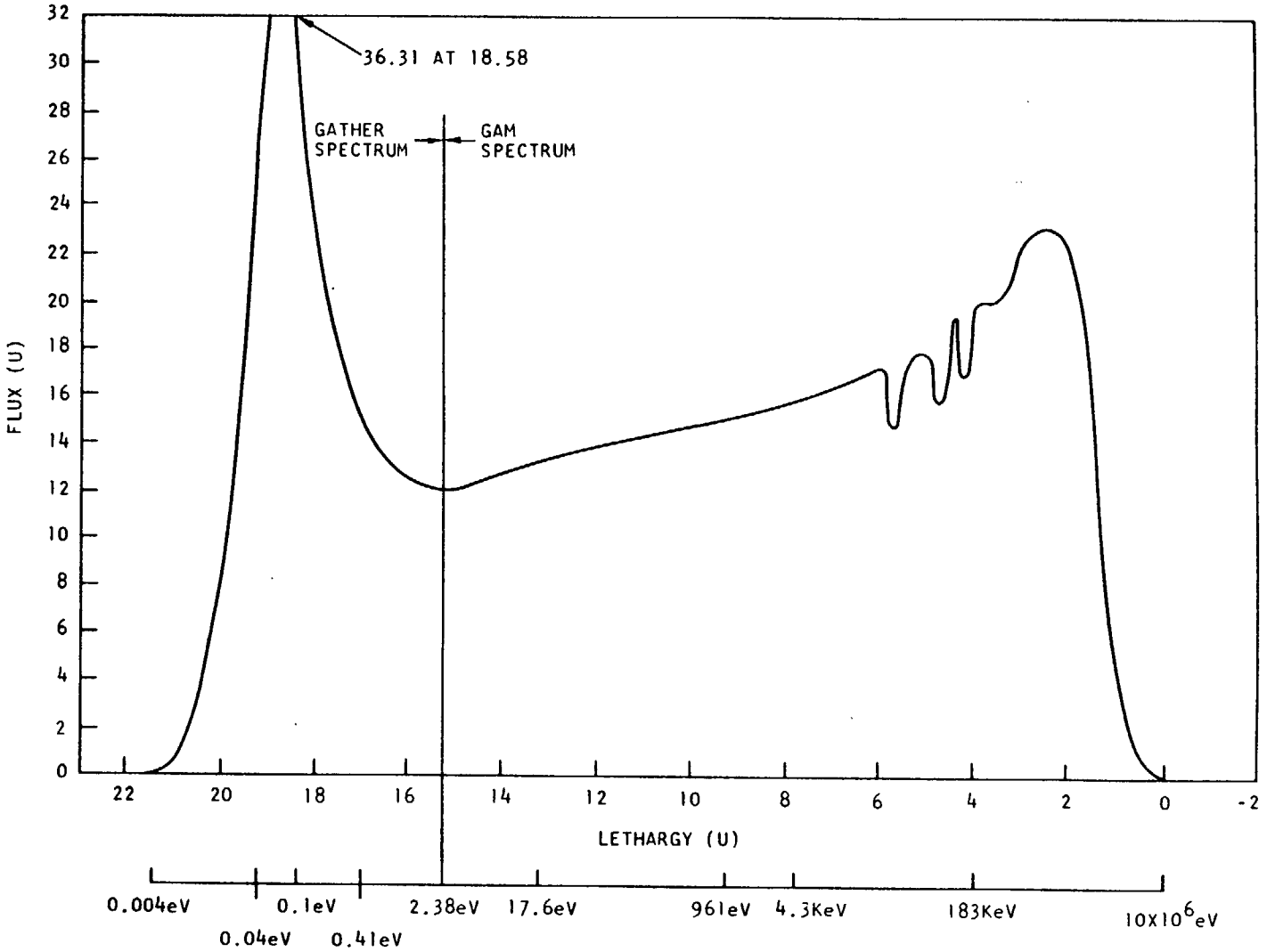

Fig. 5(a). C/U-5000 critical assembly flux spectrum

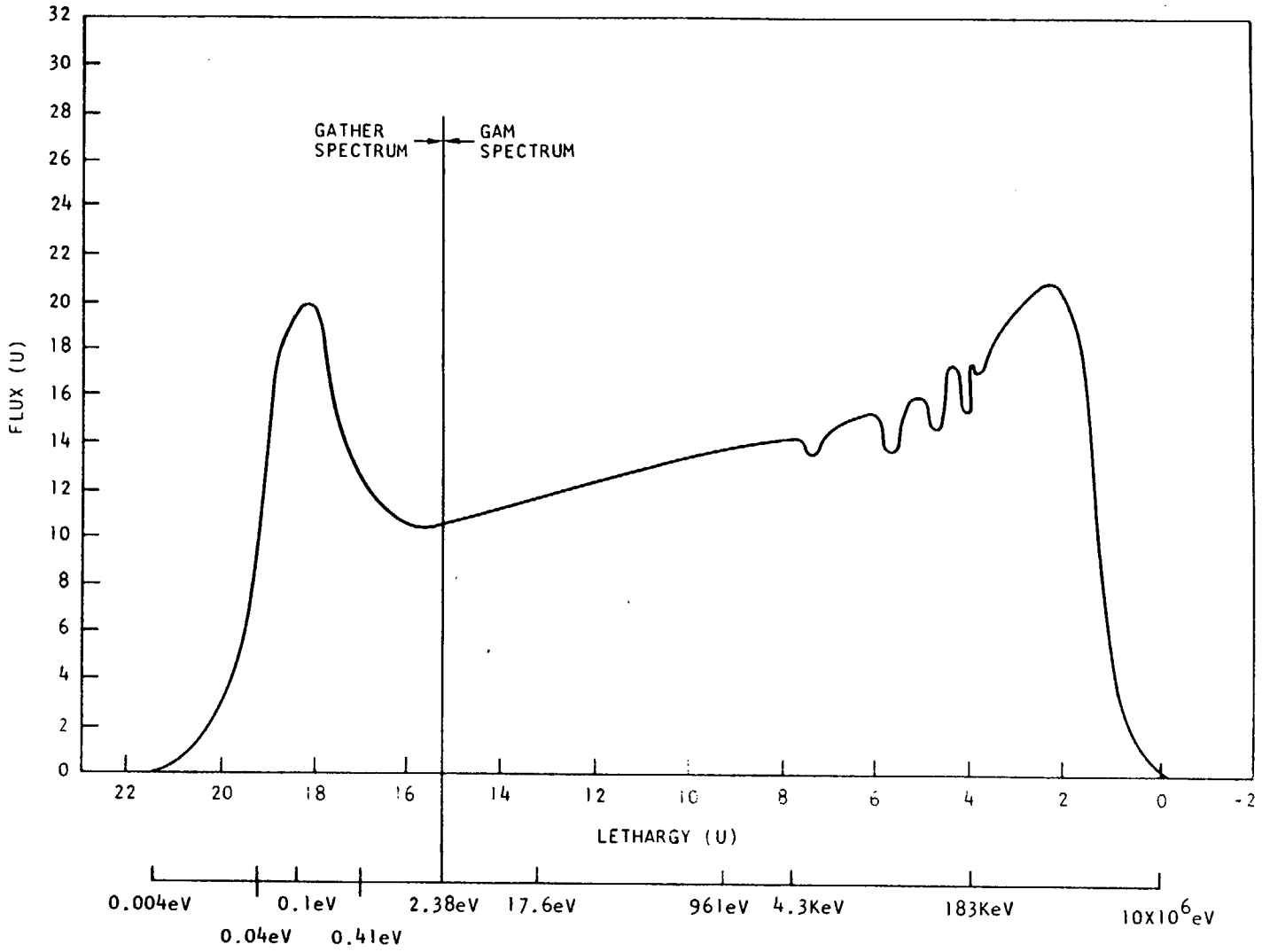

Fig. 5(b). C/U-2500 critical assembly flux spectrum

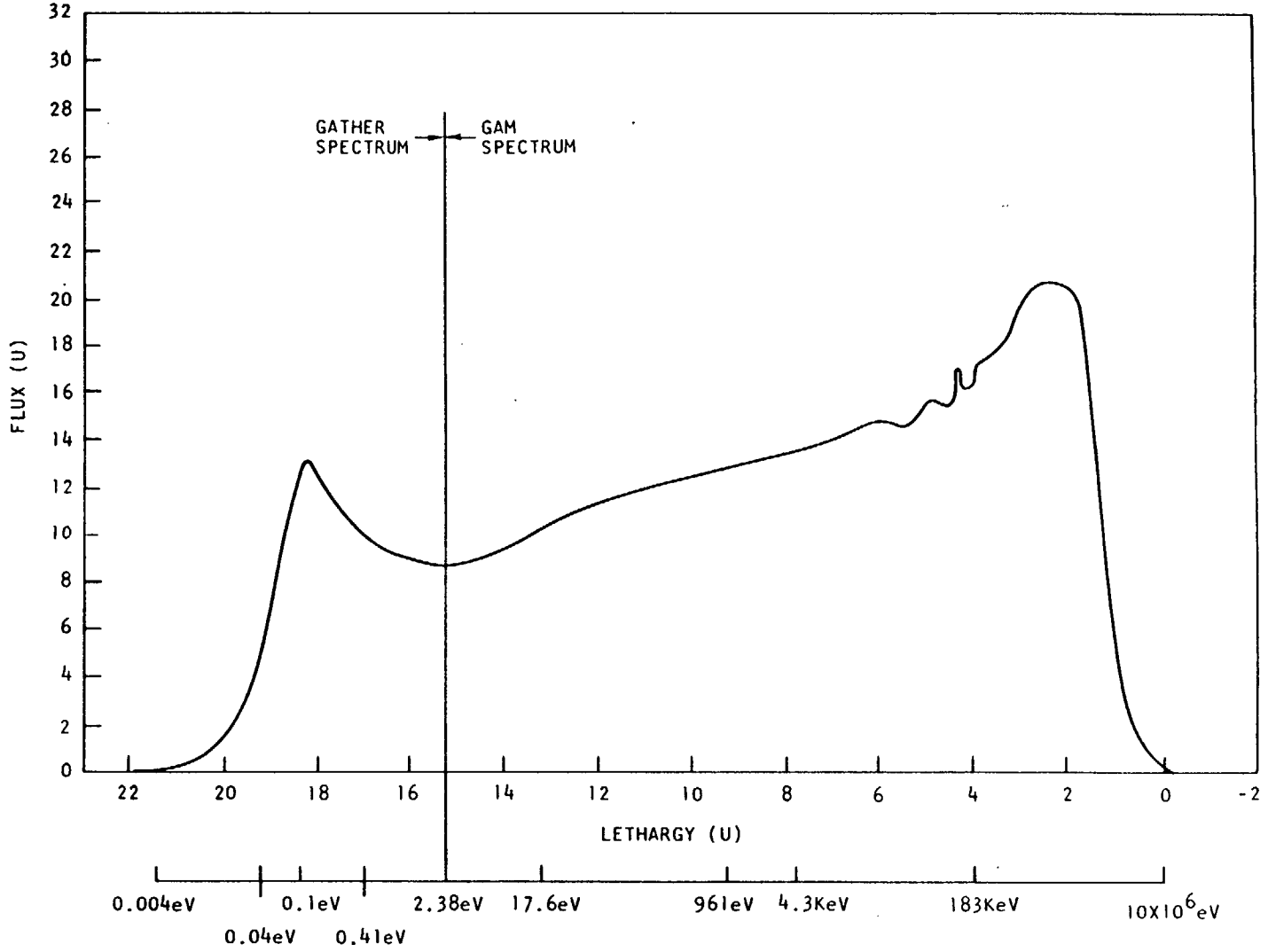

Fig. 5(c). C/U-1718 critical assembly flux spectrum

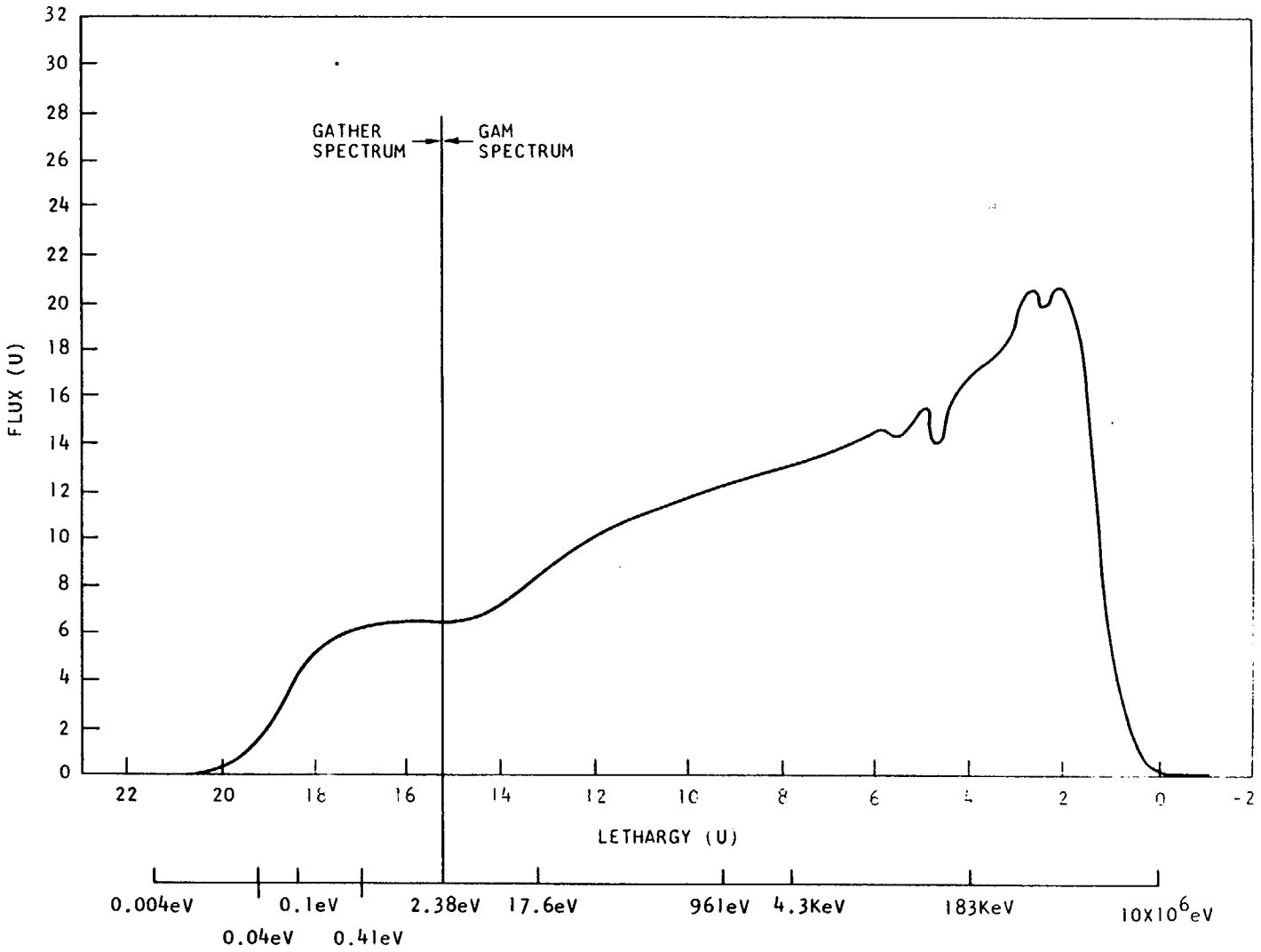

Fig. 5(d). C/U-859 critical assembly flux spectrum

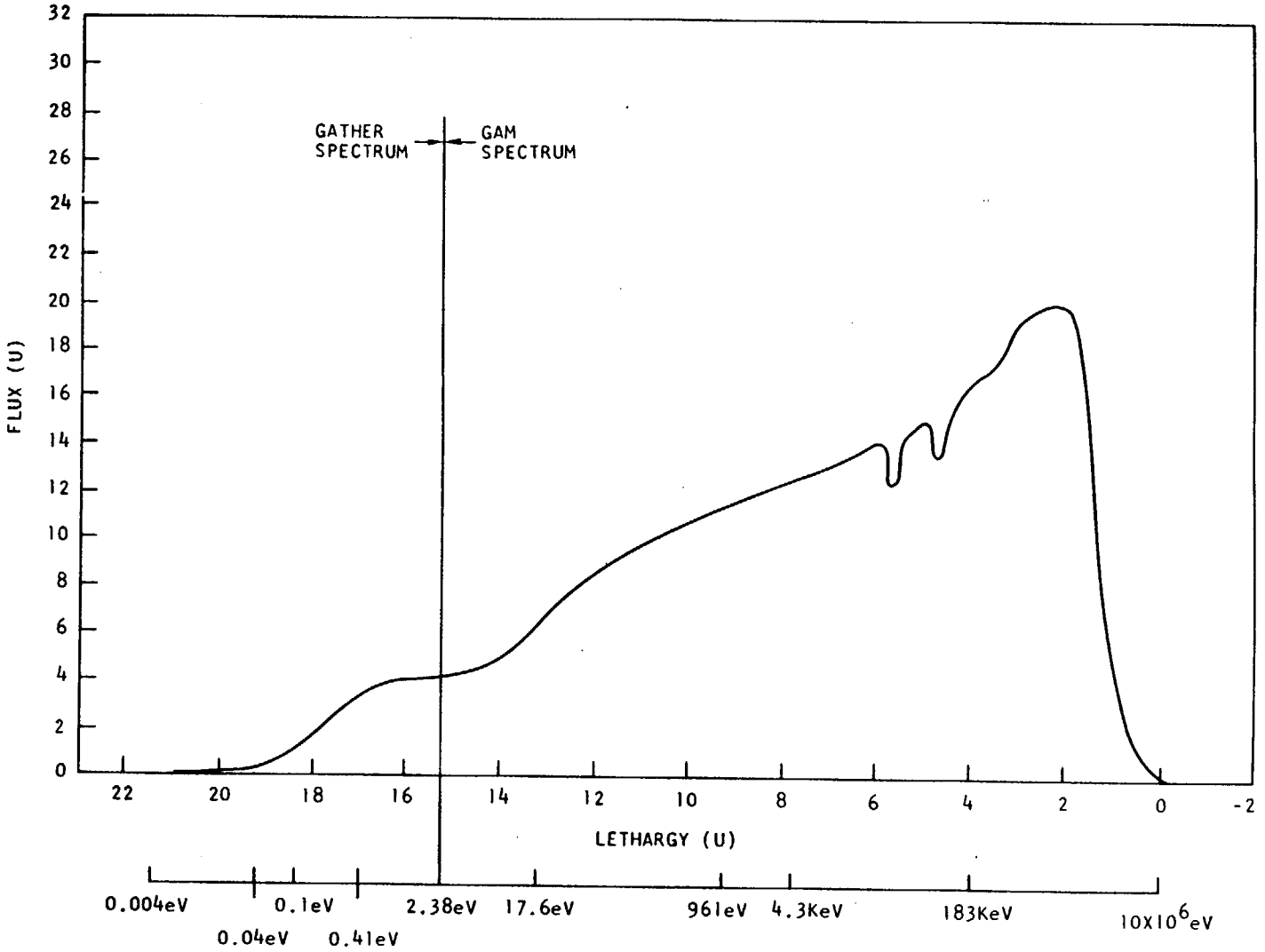

Fig. 5(e). C/U-432 critical assembly flux spectrum

In the original analysis on the C/U-2500, C/U-1718, and C/U-859 core assemblies, the SUMMIT crystal kernel[6] was used to describe the graphite scattering properties below 1.0 eV where the detailed structure of the graphite crystalline lattice is important. A free gas kernel was used to describe the graphite scattering properties between the energies of 1.0 and 2.38 eV. The "effective" temperature at which the free gas kernel was generated was adjusted to provide for a continuous transitition in flux between the two kernels. However, on close examination, a discontinuity was observed at just above 1.0 eV. A continuous carbon scattering kernel from 0.0 to 2.38 eV was generated using the GASKET[7] code. Using this kernel in GATHER, a new spectrum was generated, and the thermal broad group cross sections were reaveraged. This resulted in very little change in the calculated results for the three core assemblies. The changes were less than 0.002 Δk in the calculated effective multiplication and less than \$0.001 in any of the calculated reactivity coefficients for the special materials. The entire analysis for the C/U-432 and C/U-5000 core assemblies was done with the new carbon kernel.

The effective broad group cross sections used in the analysis of the five cores were obtained by averaging over the flux spectrum as computed with GAM and GATHER. The boundaries of the broad group structure used in the analysis were selected on the bases of (a) nuclide properties (resonance energies), (b) compatibility with usual HTGR analysis practices, and (c) considerations of the size of the critical facility. The primary resonance energy levels of the nuclides of interest are depicted in Fig. 6. Group boundaries in the energy range 2.38 eV to 183 eV were selected to provide detail around the major resonances of the most important nuclides. Above 183 eV, the fission spectrum was divided into four segments to more accurately describe the fast leakage. Below 2.38 eV, group boundaries were selected to be consistent with usual HTGR nuclear analysis practice and to provide detail around the low energy Pu^{239} and Pu^{240} resonances.

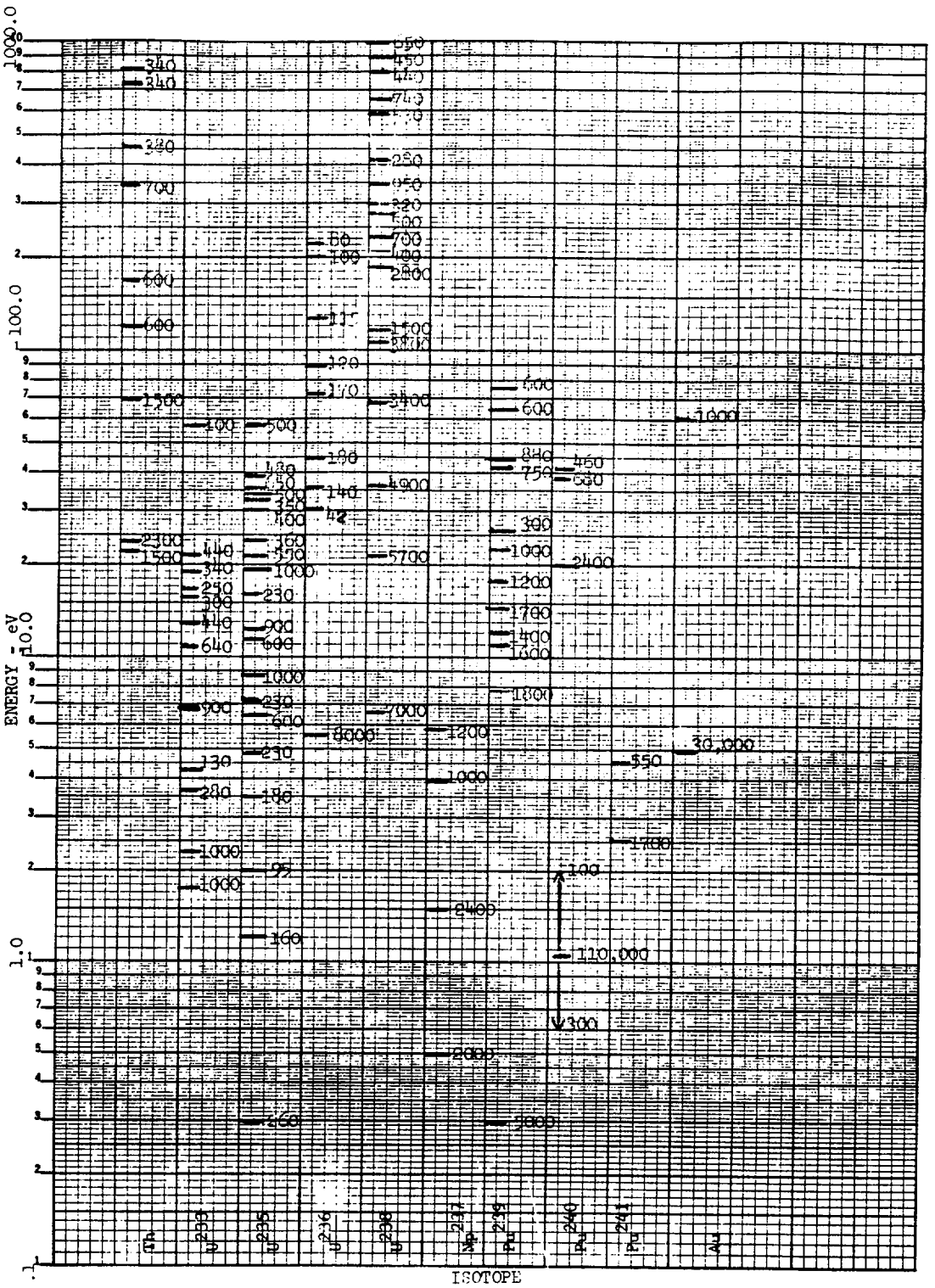

Fig. 6. Resonance location and approximate peak magnitude(barns) of special element nuclide

The considerations discussed above led to the broad group boundaries listed in Table 24. Three group structures were selected for use. The 12-group set was chosen for its compatability with the engineering design analysis structure. For the analysis of the reactivity coefficient experiments, where detailed knowledge of the cross sections is necessary to resolve experimental-analytical discrepancies, the 30-group set was used exclusively for all of the elements except plutonium. The 30-group set was also used in the computation of core eigenvalues, the effective delayed neutron fraction, and the neutron lifetime for all five assemblies. In the case of the plutonium reactivity coefficient calculations, a finer thermal group structure was selected (the 38-group set) because of low-lying resonance at 1.05 eV for Pu^{240} and 0.3 eV for Pu^{239}. This will be discussed later.

Transport cross sections, σ_{tr}, were averaged over the current, J(E) according to the equation

$$\bar{\sigma}_{tr} = \bar{\sigma}_{total} - \frac{1}{3} \frac{\int_E^{\infty} J(E') \, \sigma^1(E'-E) \, dE}{J(E)}$$

where $\sigma^1(E'-E)$ is the P1 scattering cross section from E' to E. This definition is used since the various cores have only "thin" reflectors; hence the average currents closely approximate those of a bare core.

The reflector broad group cross sections were obtained by averaging over the core spectrum. This was done since the "thin" reflectors resulted in very little peaking of the thermal flux. The buckling used in the GAM and GATHER spectrum calculations accounts for the "average" effect of the reflector.

The broad group cross sections for the nuclides in the special reactivity coefficient elements were obtained by averaging over the core spectrum. This calculation assumes that the presence of the element does not perturb the spectrum appreciably. The validity of this approximation is discussed later.

TABLE 24

BROAD GROUP UPPER ENERGY(eV)

	12-Group Set		30-Group Set		38-Group Set
1	14.92×10^6	1	14.92×10^6	1 through 22	identical with the 30 group
2	3.329×10^6	2	3.329×10^6		
3	1.353×10^6	3	1.353×10^6		
4	4.978×10^5	4	4.978×10^5	23	2.38
5	1.832×10^5	5	1.832×10^5	24	2.20
6	9.611×10^2	6	3.183×10^4	25	1.90
7	1.760×10^1 GAM	7	4.307×10^3	26	1.60
8	3.928	8	9.311×10^2	27	1.30
9	2.38	9	5.828×10^2	28	1.11
10	0.414 GATHER	10	2.144×10^2	29	1.07
11	0.10	11	1.301×10^2	30	1.025
12	0.04	12	7.889×10^1	31	0.95
		13	4.785×10^1	32	0.75
		14	2.902×10^1	33	0.625
		15	1.760×10^1	34	0.414
		16	1.371×10^1	35	0.350
		17	1.068×10^1	36	0.250
		18	8.315	37	0.10
		19	6.476	38	0.04
		20	5.043 GAM		
		21	3.928		
		22	3.059		
		23	2.38		
		24	1.60 GATHER		
		25	1.30		
		26	0.95		
		27	0.625		
		28	0.414		
		29	0.10		
		30	0.04		

For nuclides in which resonance self-shielding is important, such as gold, thorium, U^{238}, U^{236}, and Np^{237}, resonance calculations were performed using the Nordheim integral method as incorporated in the GAM section of GGC II.[8] The resultant self-shielding cross sections were then averaged over the core flux spectrum. A tabulation of the significant input data for the resonance calculations is presented in Table 25. All of the resonance calculations were done for a cylindrical cell having the radius of a fuel compact, 1.8542 cm. Initially the resonance calculations were performed using the integral method of computing the absorber contribution to the collision density and using the asymptotic (1/E) approximation for the first and second moderator contributions to the collision density. This was done because of convergence difficulties with GGC II when the integral method was used for the moderators. After analysis of the first three core assemblies indicated that the calculated resonance integrals were too high, a program was initiated to correct GGC II so that the integral method of computing the moderator contribution to the collision density could be used. This resulted in a slight reduction in the calculated values of the resonance integrals. The corrected results are presented later in this report.

Table 26 gives a summary of the neutron cross sections for those nuclides containing resonances which were used in the reactivity coefficient measurements. These dilute resonance integrals have been calculated using a 1/E flux with a cutoff energy of 0.5 eV, except for Np^{237}, for which the cutoff energy is 0.414 eV, to allow for the inclusion of the large resonance at 0.489 eV for neptunium.

TABLE 25

RESONANCE CALCULATION INPUT DATA

Loading (g/elem.)	Lump Absorber Atom Density (barn-cm)	Lump Carbon Atom Density (barn-cm)	$\sigma_m^{(C)}$ (a)	$\sigma_m^{(0)}$ (a)	$\sigma_{m\ eff}$ (b)
		Thorium Dioxide With Graphite			
50	1.4028-4	8.8761-2	2974	7.4	4153
100	2.7251-4	8.7715-2	1513	7.4	2131
200	5.3671-4	8.5922-2	752	7.4	1073
300	7.9572-4	8.3331-2	492	7.4	713
500	1.3104-3	8.0791-2	290	7.4	429
		Depleted Uranium Dioxide With Graphite			
50	1.3168-4	8.8711-2	3173	7.4	4434
100	2.6134-4	8.7416-2	1575	7.4	2215
200	5.1660-4	8.5473-2	779	7.4	1108
300	7.6806-4	8.3331-2	511	7.4	736
500	1.2310-3	7.9646-2	305	7.4	449
		Gold With Graphite			
5	1.6031-5	8.9757-2	26,370	0	36,650
15	4.7390-5	8.7017-2	8,648	0	12,090
45	1.4615-4	8.9558-2	2,886	0	4,022
		Np^{237} With Graphite			
55	1.4396-4	8.6569-2	2832	7.4	3978
		15 a/o U^{236} With Graphite			
17.4	4.5935-5	8.5822-2	8800	42.0	12,379

(a) $\sigma_m = \frac{N(mod.)}{N(resonance \cdot abs.)} \times \sigma_s\ (mod.)$

(b) $\sigma_m^{eff} = \sigma_{p_{res}} + \sigma_m + \sigma_e \left(\frac{\sigma_m}{\sigma_m+\sigma_e}\right)$

$\sigma_e = \frac{1}{\ell N(res.abs.)} \qquad \ell = 2r$

TABLE 26

SUMMARY OF NEUTRON CROSS SECTIONS
FOR RESONANCE MATERIALS

Material	2200 m/sec(barns)		Resonance Integrals(barns)		
	Capture	Fission	Capture	Fission	Absorption
Au	98.8		1618.4		1618.4
Th^{232}	7.45		85.7	0.46	86.3
U^{236}	6.97		321.0	2.81	323.8
U^{238}	2.70		275.5	1.64	277.2
Np^{237}	170.0		738.2	5.65	743.8
Pu^{239}	274.1	740.9	178.1	278.2	456.4
Pu^{240}	279.7	0.05	8498.6	7.16	8505.8
Pu^{241}	395.4	962.0	140.0	573.0	712.7
Pu^{242}	17.76		1099.6	5.75	1105.3

The treatment of the self-shielding within a lumped resonance absorber embedded in another material is best handled by the above methods. However, large resonances of Pu^{239} (at 0.296 eV), Pu^{240} (at 1.057 eV), and Np^{237} (at 0.489 eV) lie in an energy range in which there is substantial up-scattering in carbon-moderated systems. These methods therefore cannot be used since the mathematical procedures for treating a lumped resonance absorber with up-scatter have not been developed. The method used to obtain broad group cross sections for plutonium and neptunium in the energy range below 2.38 eV, by averaging the "dilute" pointwise cross-section data over the adjoining core spectrum, is therefore questionable. To account for the self-shielding in these low energy resonances, several "exact" calculations for plutonium were done using an increased number of thermal broad groups (38-group set) and a multigroup transport calculation using the S_n approximation of Carlson[9].

5.2. HETEROGENEOUS REGION DISADVANTAGE FACTORS

The heterogeneous region of the C/U-859, C/U-1718, C/U-2500, and C/U-5000 core assemblies was composed of an array of fuel elements with either the C/U-432 or C/U-859 atom ratios and graphite columns. The number of graphite columns used was selected so that the C/U-ratios in the heterogeneous region gave the best approximation possible to the exact region C/U-ratios using existing materials. Table 7 in Section 3.2.4. lists the number of fuel and graphite elements in the heterogeneous region of the five critical assemblies. Figures 4(a) through 4(e) show the arrays in which they were loaded. The arrangement results in self-shielding of the heterogeneous region fuel elements. 1DF--a Gulf General Atomic modification of the DTF[10] code, a one-dimensional multigroup transport theory code based on Carlson's discrete S_n method--was employed to compute the required self-shielding factors. The S_n approximation with P1 cross sections was used. For the C/U-5000 and C/U-2500 cores, the hexogonal array of cylinders was approximated by the model shown in Fig. 7[a]. A "white" or isotropic return boundary condition rather than the reflective boundary condition was used at the outer boundary of the cell.

For the C/U-1718 core, a model of repeating slabs was used to represent the heterogeneous array of one fuel element for each graphite element in the cell calculation. The aluminum honeycomb, fuel element, and void within the honeycomb were homogenized into a slab that conserved the volume of the individual elements and had a thickness equal to 0.866 of the aluminum honeycomb center-to-center pitch. A similar slab of equal thickness, containing the graphite element, its honeycomb tube, and the associated void, was located adjacent to it. A reflective boundary condition was located at the centerline of each of the adjacent slabs. This cell is depicted in Fig. 7[b]. While not precise, this description of the explicit heterogeneous array should be more accurate [see Fig. 4(e)] than a cylindrical description.

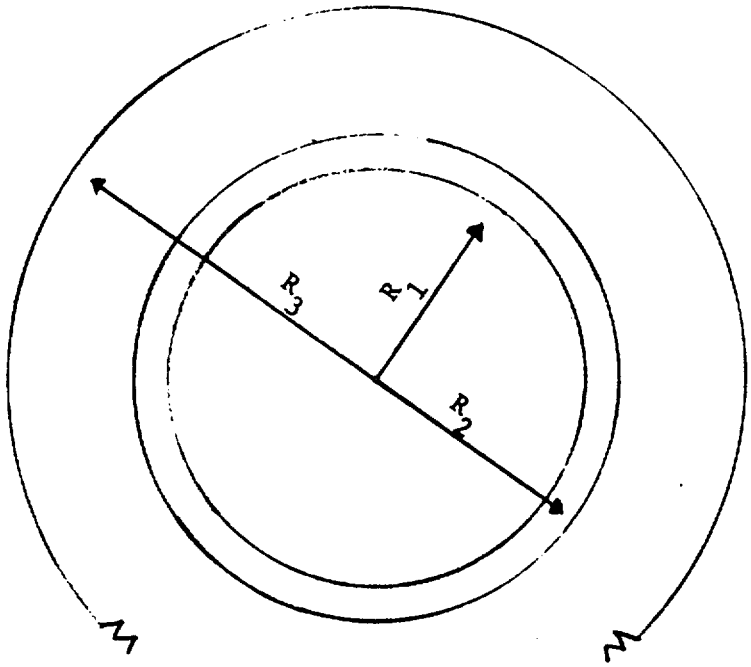

R_1 = Outside radius of fuel slug = 1.8923 cm

R_2 = Outside radius of homogenized fuel can and honeycomb tube = 2.112 cm

R_3 = Outside radius of cell = 3.841 cm C/U-2500
= 5.4325 cm C/U-5000

(a)

Graphite Element and Al Honeycomb t = 3.658 (t = thickness of slab region)	Fuel Element and Al Honeycomb t = 3.658	Graphite Element and Al Honeycomb t = 3.658

(b)

Fig.7. Disadvantage factor cell models:
(a) C/U-5000 and C/U-2500;
(b) C/U-1718

In the C/U-859 core assembly, the heterogeneous region consisted of C/U-432 fuel elements mixed with an equal number of graphite elements in a very thin region at the edge of the core. Because of the small volume of this region, its low nuclear worth, and the difficulty in describing a calculational model, the disadvantage factors for this region were neglected. This is believed to have a negligible effect on the calculated reactivity coefficients and on the estimate of the core reactivity.

A summary of the calculated disadvantage factors for the C/U-5000, -2500, and -1718 core assemblies is given in Table 27. The disadvantage factor, g_i, for each group is defined as follows:

$$g_i = \frac{\Phi_i(\text{fuel})}{\Phi_i(\text{cell})} \quad .$$

5.3 EIGENVALUE CALCULATIONS

Analytical prediction of the eigenvalue k_{eff} of a critical assembly is a complex test of the calculational methods as well as the basic nuclear cross-section data. The cores described in this report were designed such that a good mathematical approximation of the physical geometry could be made, thereby placing the primary emphasis on cross-section values rather than on complicated approximations of physical features.

In view of the physical characteristics of the assembly the GAZE[11] one-dimensional multigroup diffusion theory computer code was selected for analyzing the majority of the measurements. The microscopic structure of the assembly was homogenized by conserving the nuclide mass and lattice volume for each region. The radial dimensions and isotopic atom densities for the five cores are shown in Fig. 8 and Table 28.

Transverse(axial) bucklings by group were derived from an axial-radial GAZE problem iteration. The initial radial calculation was made with the geometric buckling for the core in the axial or transverse direction. An axial calculation was then made homogenizing the core materials and using group-dependent radial core bucklings as obtained from the initial radial calculation. The radial calculation was repeated using the calculated transverse bucklings from the axial calculation. For all five core assemblies, the calculated effective multiplication factor became stationary with just three iterations. This was expected since the assemblies were unreflected on the ends.

TABLE 27

CALCULATED FUEL DISADVANTAGE
FACTORS FOR HETEROGENEOUS REGION

Group	C/U-5000 1 C/U-859 Fuel Elem. 5 Graphite Elem.	C/U-2500 1 C/U-859 Fuel Elem. 2 Graphite Elem.	C/U-1718 1 C/U-859 Fuel Elem. 1 Graphite Elem.
1	1.583	1.180	1.049
2	1.346	1.105	1.031
3	1.193	1.059	1.020
4	1.089	1.025	1.009
5	1.029	1.009	1.002
6	0.996	0.997	0.999
7	0.997	0.998	0.999
8	0.996	0.998	0.998
9	0.994	0.996	0.998
10	0.993	0.996	0.997
11	0.991	0.995	0.997
12	0.988	0.993	0.995
13	0.983	0.990	0.994
14	0.979	0.988	0.992
15	0.984	0.991	0.994
16	0.977	0.987	0.991
17	0.972	0.982	0.988
18	0.978	0.987	0.991
19	0.980	0.989	0.993
20	0.987	0.994	0.996
21	0.988	0.993	0.996
22	0.992	0.996	0.997
23	0.991	0.995	0.998
24	0.993	0.996	0.998
25	0.984	0.990	0.994
26	0.985	0.991	0.994
27	0.979	0.988	0.992
28	0.947	0.969	0.980
29	0.912	0.948	0.965
30	0.844	0.906	0.935

Radial Core and Reflector Regions for GAZE Calculation

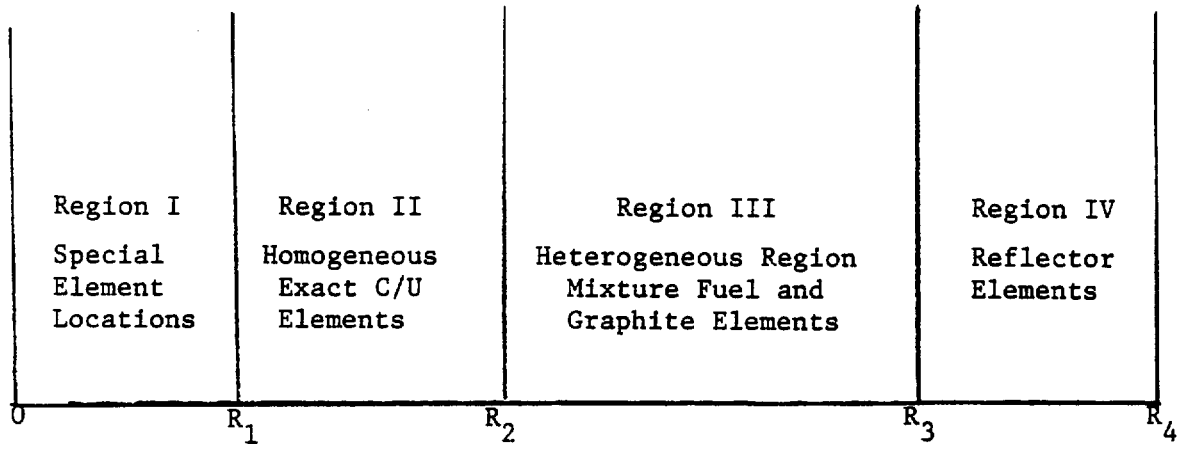

Radius	Radius (in cm)				
	C/U-5000	C/U-2500	C/U-1718	C/U-859	C/U-432
R_1	1.8542	1.8542	1.8542	1.8542	1.8542
R_2	13.490	13.490	13.490	47.530	34.142
R_3	71.487	63.865	59.053	56.510	54.731
R_4	86.578	71.451	67.378	63.030	61.461

Fig.8. GAZE radial calculational model

TABLE 28

ISOTOPIC ATOM DENSITIES (barn-cm) USED
IN CALCULATIONS FOR FIVE CORE ASSEMBLIES

Isotope	C/U-5000	C/U-2500	C/U-1718	C/U-859	C/U-432
			Exact or Homogeneous Region[(a)]		
C	6.531-2	6.536-2	6.455-2	6.939-2	6.948-2
Al	6.856-3	6.856-3	6.856-3	6.856-3	6.856-3
U^{235}	1.3026-5	2.6371-5	3.7868-5	8.1315-5	1.6308-4
U^{238}	9.39-7	1.85-6	2.66-6	5.72-6	1.19-5
H_2O	0.35-4	0.35-4	0.35-4	0.75-4	1.21-4
			Heterogeneous Region[(a)]		
C	7.403-2	7.330-2	7.188-2	7.190-2	
Al	4.823-3	5.230-3	5.650-3	5.650-3	
U^{235}	1.3545-5	2.7106-5	4.066-5	8.2402-5	
U^{238}	9.76-7	1.99-6	2.86-6	5.79-6	
H_2O	0.15-4	0.28-4	0.40-4	0.62-4	
			Reflector Region[(a)]		
C	7.437-2	7.437-2	7.437-2	7.437-2	7.437-2
Al	4.42-3	4.42-3	4.42-3	4.42-3	4.42-3

(a) Impurities for carbon and aluminum are not included in this table but were explicitly included in the calculation.

In all the calculations, the in-core locations occupied by nuclear fuses, safety rods, and control rods were neglected, and experimental corrections were made to the measured eigenvalue. Experimental corrections were also made to account for the reflective effect of the aluminum honeycomb in the region beyond the radial graphite reflectors.

A best estimate of the impurities present in each core assembly was made using the data shown in Tables 10 and 11 and is included in the calculations. The importance of these impurities to the calculated core excess reactivity and reactivity coefficients was determined for several of the cores and is discussed in Section 6.

5.4. EFFECTIVE DELAYED NEUTRON FRACTION AND PROMPT NEUTRON GENERATION TIME

The effective delayed neutron fraction β_{eff} and the prompt neutron generation time Λ were calculated for each of the five cores in the following manner. A perturbation theory derivation of the kinetics equations shows that the effective delayed neutron fraction equals the reactivity change associated with the introduction of the actual delayed neutron fraction into an effective multiplication constant calculation with the delayed neutron spectrum.[12] In order to evaluate this reactivity change, a 30-group GAZE calculation was run using a typical prompt plus delayed neutron spectrum normalized to 1.0. The calculation was then repeated with a delayed neutron spectrum containing an additional 0.0065 neutrons.[13] The value of β_{eff} is defined as

$$\beta_{eff} = \frac{k' - k}{k^2}$$

where k' and k are the effective multiplications obtained from the two GAZE calculations.

Similarly, the prompt neutron generation time has been shown to be identical with the reactivity change which results when the macroscopic absorption cross section is perturbed uniformly throughout the core and reflector by a small change in the concentration of 1/v absorber. This was accomplished using two 30-group GAZE calculations which differed only by the presence of the 1/v perturbation. The 1/v broad group cross sections were

obtained by averaging over GAM and GATHER spectra. The prompt neutron generation time was then defined as

$$\Lambda = \frac{k_2 - k_1}{k_2 k_1} \cdot \frac{1}{N(1/v)\ \sigma_o v_o} ,$$

where k_2 represents the effective multiplication obtained from the GAZE calculations with the 1/v perturbation present and k_1 is the GAZE effective multiplication without the perturbation.

5.5. SPECIAL ELEMENT REACTIVITY CALCULATIONS

The reactivity changes associated with the substitution of the special elements into the central cell location were calculated using the equation

$$\Delta\rho(\$) = \frac{k_2 - k_1}{k_2 k_1} \quad \frac{1}{\beta_{eff}} ,$$

where k_2 is the effective multiplication with the special element in the central location, k_1 is the effective multiplication with the reference density carbon element in that location, and β_{eff} is as defined previously. All of the calculations were made using the radial model shown in Fig.7 and 30-group cross sections. All of the special elements including the reference carbon element had the same compact radius as the central cell shown in Fig.7. The GAZE calculations were converged to 10^{-6} for both flux and source iterations (see page 33-45 of Ref. 11). An even tighter convergence, 10^{-8}, was employed for some of the calculations with no appreciable change in the calculated results. The special element atom densities used in the analysis of the reactivity coefficients are shown in Table 29.

TABLE 29

SPECIAL ELEMENT ISOTOPIC
ATOM DENSITIES[a]

Special Element Description	C	Th	U^{238}	U^{235}	Np^{237}	Au	B
Boron 0.10	8.9906-2						6.0270-6
Boron 0.20	9.0703-2						1.2149-5
Boron 0.45	8.9857-2						2.6615-5
Boron 0.55	9.0106-2						3.2764-5
Boron 1.00	8.9358-2						5.8988-5
Boron 1.50	8.9857-2						8.8399-5
Boron 1.90	8.8761-2						1.1135-4
Thorium 50	8.8761-2	1.4028-4					
Thorium 100	8.7715-2	2.7251-4					
Thorium 200	8.5922-2	5.3671-4					
Thorium 300	8.3331-2	7.9572-4					
Thorium 500	8.0791-2	1.3104-3					
U^{238} 50	8.8711-2		1.3142-4	2.6336-7			
U^{238} 100	8.7416-2		2.6082-4	5.2268-7			
U^{238} 200	8.5473-2		5.1557-4	1.0332-6			
U^{238} 300	8.3331-2		7.6652-4	1.5361-6			
U^{238} 500	7.9646-2		1.2285-3	2.4620-6			
Np^{237} 5	8.7564-2				1.3173-5		
Np^{237} 15	8.7316-2				3.9468-5		
Np^{237} 55	8.6569-2				1.4396-4		
Au 5	8.9757-2					1.6031-5	
Au 15	8.7017-2					4.7390-5	
Au 45	8.8014-2					1.4391-4	
Au CN 45	8.9558-2					1.4615-4	

TABLE 29 (continued)

Special Element Description	C	U^{233}	U^{235}	U^{236}	U^{238}	
Special C/U 5000	8.9060-2		1.9456-5		1.4131-6	
Special C/U 2500	8.8860-2		3.9581-5		2.8641-6	
Special C/U 1718	8.8711-2		5.7936-5		4.1683-6	
Special C/U 859	8.7964-2		1.1315-4		8.1567-6	
Special C/U 432	8.7266-2		2.2420-4		1.6167-5	
U^{233} C/U 5000	8.8611-2	1.6177-5	5.1290-9		6.5530-7	
U^{233} C/U 1718	8.8412-2	4.3669-5	1.3593-8		1.7752-6	
U^{233} C/U 432	8.7220-2	1.5263-4	4.6985-8		6.2350-6	
U^{236} C/U 5000	8.7715-2		1.9456-5	3.9635-6	2.4311-6	
U^{236} C/U 1718	8.7715-2		5.6113-5	1.1431-5	6.9639-6	
U^{236} C/U 432	8.5822-2		2.2547-4	4.5935-5	2.8008-5	
		Pu^{239}	Pu^{240}	Pu^{241}	Pu^{242}	Al
PuH 240 A	8.9657-2	4.8211-5	1.4723-5	3.1010-6	5.6335-7	
PuH 240 B	9.0554-2	1.7932-5	5.4783-6	1.1525-6	2.1045-7	
PuH 240 C	8.9358-2	6.7860-6	2.0740-6	4.3765-7	7.8451-8	
PuL 240 A	8.9259-2	4.8226-5	2.0600-6	5.5500-8		
PuL 240 B	8.9259-2	1.7947-5	7.6568-7	2.0757-8		
PuL 240 C	8.8811-2	6.8037-6	2.9105-7	8.0026-9		
Carbon reference density	8.8113-2					
Carbon 90% density	8.2136-2					
Aluminum rod						6.361-2

(a) All atom densities are for those within the compact, which has a outer diameter of 1.460 in.

6. CALCULATED RESULTS AND COMPARISON WITH MEASUREMENTS

6.1. Effective Multiplication Constant

To provide as clean an analytical model as possible, the calculations were performed on a uniform core. The corrections for the locations occupied by control and safety rods, fuses, and sources were determined experimentally. In addition, the reactivity worth of the unfilled honeycomb was experimentally determined and its effect included in the "measured" total excess reactivity (see Table 16 in Section 3 for the measured excess reactivity in each of the five core assemblies).

Using the analytical model described earlier, the calculated effective multiplication factor for each of the as built critical assemblies is given in Table 30. The calculations were made using both sets of U^{235} cross-section data available. From the comparison with the measured results, it is quite clear that the ENDF/B KAPL data yields considerably better agreement with the measured results. This is particularly true in the assemblies with the harder spectra and higher mean fission energies such as exhibited in the C/U-432 and C/U-859 cores.

Some of the central cell nuclear characteristics for the five different critical assemblies are shown in Table 31. By reducing the C/U atom ratio for the cores a hardening of the thermal spectra is obtained but equally important is the change in fast/thermal flux ratio. As a result of this, the mean fission energy for the cores changes from 0.074 eV in the most thermal system to 12.7 eV in the least thermal. The sharp change in mean fission energy between the C/U-432 and -859 cores is peculiar to the U^{235} fission cross section behavior as a function of energy between 0.4 and 10.0 eV. For a material such as boron with a cross section that varies as 1/v, the change in mean capture energy between the C/U-432 and C/U-859 cores is not as great. The mean capture energy for boron changes from 0.35 eV in the C/U-859 core to 0.80 eV in the C/U-432 core.

TABLE 30

COMPARISON BETWEEN CALCULATED AND MEASURED VALUES OF k_{eff}

Core Assembly	Calculated k_{eff} With U^{235} (92.2350) Cross Sections[a]	Calculated k_{eff} With U^{235} (92.2352) Cross Sections[a]	Measured k_{eff} (Using Calculated β_{eff})[b]
C/U-5000	1.018 ± 0.005	1.023 ± 0.005	1.013 ± 0.003
C/U-2500	1.009 ± 0.005	1.017 ± 0.005	1.014 ± 0.003
C/U-1718	1.003 ± 0.005	1.013 ± 0.005	1.013 ± 0.003
C/U-859	0.995 ± 0.005	1.012 ± 0.005	1.013 ± 0.003
C/U-432	0.997 ± 0.005	1.019 ± 0.005	1.016 ± 0.003

(a) Uncertainty is based on impurity content.

(b) Uncertainty is based on ability to measure the reactivity worth of the unfilled aluminum honeycomb and the core safety devices.

TABLE 31

CHARACTERIZATION OF SPECTRA IN DIFFERENT C/U CORE ASSEMBLIES

Core Assembly	Mean Fission Energy (eV)	Most Probable Thermal Energy (Below 2.38 eV) (eV)	Fast/Thermal Flux Ratio (2.38 eV Cutoff)	Effective Boron Cross Section (Below 2.38 eV) (barns)
C/U-5000	0.074	0.050	2.15	415
C/U-2500	0.12	0.059	3.40	336
C/U-1718	0.20	0.061	4.62	297
C/U-859	0.40	0.085	12.07	232
C/U-432	12.7	0.140	15.33	183

Several interesting features of the cores are shown by the neutron balance in Table 31. Even though the C/U-5000 core is significantly larger than the C/U-432 core (outer radius of 86.6 cm as compared to 61.5 cm) the total leakage from the two cores is almost identical because of the increased water and aluminum content for the C/U-432 core. The amount of water in the C/U-432 and C/U-859 fuel elements is about 40 times greater than in the solid graphite columns (see Section 3.3.2).

The total leakage is about 40% for all of the cores so that any uncertainty in calculation of the leakage, such as treatment of the unfilled honeycomb or other scattering sources in the assembly room, could result in a large uncertainty in the comparison of calculated and measured values of k_{eff}. To minimize this uncertainty, a boral sheet was located at the outer edge of the aluminum honeycomb to prevent the return of thermal neutrons produced outside the core. In addition, an experimental correction to the effective core multiplication factor was made to account for the unfilled aluminum honeycomb (see Table 16).

The effective value of α^{235} for the different cores has been calculated and is shown in Table 32. Note that in the most thermal core it is 0.215, which is near the 2200 m/sec value of 0.173, whereas in the C/U-432 core it is 0.383, which is approaching the value of the epithermal α, 0.509.

Because of the lack of any end reflection on the core assemblies, the sensitivity of the core eigenvalue to the iteration on group-dependent transverse bucklings is small. Approximately 0.003 Δk was obtained in the iteration from the single value of the geometric buckling to the iterated group-dependent transverse bucklings.

Some calculations were made on the first critical assembly, the C/U-2500 core, to study the problems of calculating the reactivity worth of the unfilled honeycomb and the effect of using a reduced number of broad groups.

TABLE 32

NEUTRON BALANCE IN FIVE DIFFERENT CRITICAL ASSEMBLIES

Core Assembly Fractional Losses	C/U-5000	C/U-2500	C/U-1718	C/U-859	C/U-432
U^{235} capture	0.0904	0.1037	0.1141	0.1404	0.1604
U^{235} fission	0.4209	0.4238	0.4173	0.4151	0.4188
U^{238} absorption	0.0034	0.0059	0.0109	0.0131	0.0167
C capture	0.0190	0.0086	0.0045	0.0023	0.0014
Al capture	0.0650	0.0400	0.0225	0.0150	0.0106
Impurities capture	0.0184	0.0127	0.0086	0.0038	0.0017
Total core absorption	0.6171	0.5947	0.5779	0.5897	0.6096
Total reflector capture (Al)	0.0130	0.0031	0.0023	0.0008	0.0009
Radial leakage	0.2570	0.3158	0.3375	0.3374	0.3200
Transverse leakage	0.1129	0.0864	0.0823	0.0721	0.0695
Total leakage	0.3829	0.4053	0.4221	0.4103	0.3904
α_{eff}^{235} (92.2352)	0.215	0.245	0.273	0.338	0.383

Because of the high degree of anisotropy that exists in the diffuse unfilled honeycomb region, calculations to estimate its reactivity worth were made using the 1DF transport code. An upper value for the positive reactivity worth due to the reflective properties of this region was calculated to be $1.15, whereas the measured worth was estimated as $0.55. This upper value was obtained by successive radial transport calculations. In one case, the honeycomb region was removed, and in the other case, the unfilled honeycomb region was added with zero transverse leakage.

Using the 12-group set described earlier, the effective multiplication factor was calculated to be about 0.004 Δk higher than that with the 30-group set for the C/U-2500 core. This calculated difference is due to the more refined treatment of the fast leakage with the 30-group set. The 30-group set was used almost exclusively in the calculations for these core assemblies.

As a result of the experimental corrections mentioned above, the primary uncertainties remaining in the calculation of the core effective multiplication factor are the impurities present, including both water and other parasitic absorption, and the perturbation at the core midplane where the two halves of the bed assembly come together.

In the experimental determination of the amount of water in the fuel and reflector elements (see Section 3.3.2.), only a small sample of each element was tested, from which the nominal water content was determined. In addition, the water content varies for the different elements; i.e., the C/U-5000 core contains about 0.5 g per 3-ft element of the core, wherease the C/U-432 core contains about 3.8 g per 3-ft element. The reactivity worth for this nominal water content was calculated to be 0.003 Δk in the C/U-5000 core and 0.031 Δk in the C/U-432 core. A nominal amount of absorption impurities was determined for each of the cores by using the results of emission spectrographic analysis of the graphite and published nominal impurities for the aluminum. The calculated reactivity worth of these nominal impurities varied from 0.016 Δk in the C/U-5000 core to about 0.002 Δk in the C/U-432 core. The total worth of the impurities, both water and parasitic materials, in the core varies from about 0.02 to 0.03 Δk.

The interface between the fixed and moveable halves of the assembly creates a gap in the fuel compacts because of the welded end of the aluminum tubes containing fuel elements. The effect on the C/U-2500 core reactivity was estimated from an axial GAZE calculation having a 1/4 in.-wide zone at the centerline filled with homogenized aluminum and graphite. The calculation indicated the worth to be about 0.003 Δk, and this value was somewhat substantiated by reactivity measurements in which a void was created by separating the beds slightly. This probably represents an upper limit of the effect on reactivity as only the fuel elements and not the diluting graphite columns are contained in aluminum tubes.

6.2. Effective Delayed Neutron Fraction and Neutron Generation Time

Using the methods described earlier, the effective delayed neutron fraction, β_{eff}, and the neutron lifetime, Λ, for each of the cores was calculated; these are summarized in Table 33. In this table, a comparison of the calculated and measured β_{eff}/Λ is also made.

TABLE 33
COMPARISON OF CALCULATED AND MEASURED VALUES OF β_{eff}/Λ

Core Assembly	Calculated β_{eff}	Calculated Λ ($\times 10^{-6}$ sec)	Calculated β_{eff}/Λ	Measured β_{eff}/Λ
C/U-5000	0.00680	388.6	17.5	18.6 ± 0.2
C/U-2500	0.00689	207.5	33.2	32.6 ± 0.4
C/U-1718	0.00707	145.6	48.6	46.3 ± 0.5
C/U-859	0.00719	68.2	105.4	94.4 ± 1.0
C/U-432	0.00708	37.1	191.0	150.8 ± 1.5

The agreement between calculation and measurement of the ratio β_{eff}/Λ, is generally quite good. The discrepancy for the two cores with the lowest C/U-atom ratios probably exists because the neutron generation time in those assemblies is very close to the slowing-down time in a graphite system. Any contriubtion to the generation time from neutrons slowing down or thermalizing outside the assembly would result in a sizable effect on the generation time even though it may be insignificant with respect to the effective multiplication. In all of the calculations of the effective delayed neutron fraction and the neutron generation time, the effect of the unfilled honeycomb and other adjacent materials outside the core-reflector region was ignored. In the calculation of the generation time, a different treatment of these quantities might yield a larger value of the generation time giving closer agreement between calculation and experiment for the C/U-859 and -432 cores.

6.3. REACTIVITY WORTH OF SPECIAL MATERIALS

The experimentally determined reactivity worths for the different loadings of the special materials are summarized in Table 17. A detailed description of the calculated results for these materials in each of the five critical assemblies and the comparison of these results with experiment are given in this section.

As indicated in Section 5, the effective broad group cross sections for the special materials inserted in the central location in each of the core assemblies were obtained by averaging the fine group cross sections over the neutron energy spectrum generated by the GAM and GATHER codes using the adjacent core isotopic atom densities. Any effect from the perturbation of the averaging spectrum resulting from the insertion of the special material in the central location should be minimal because of the large number of broad groups used in the calculations. A comparison of the broad group spectrum obtained at the central location in the one-dimensional GAZE calculation with the spectrum obtained in the zero-dimensional GAM and GATHER calculations appears in Table 34. The GAZE calculation used in the comparison is made with the central location containing a fuel element having the same C/U loading as the adjacent core. The agreement between the two spectra is very good for all of the assemblies.

TABLE 34

RATIO OF BROAD GROUP FLUXES
AT CENTER CELL LOCATIONS

Broad Group	C/U-5000 GAZE Flux / GGC Flux	C/U-2500 GAZE Flux / GGC Flux	C/U-1718 GAZE Flux / GGC Flux	C/U-859 GAZE Flux / GGC Flux	C/U-432 GAZE Flux / GGC Flux
1	1.01	1.03	0.98	1.01	1.03
2	1.01	1.03	0.99	1.01	1.03
3	1.01	1.02	1.01	1.01	1.02
4	1.01	1.02	1.01	1.01	1.02
5	1.01	1.02	1.01	1.00	1.02
6	1.00	1.02	1.03	1.00	1.00
7	1.00	1.00	1.04	1.00	1.00
8	1.00	1.00	1.04	1.00	0.99
9	1.00	0.99	1.04	1.00	0.99
10	1.00	0.99	1.04	1.00	0.98
11	1.00	0.98	1.03	1.00	0.98
12	1.00	0.98	1.02	1.00	0.97
13	1.00	0.98	1.01	1.00	0.96
14	1.00	0.97	1.01	1.00	0.96
15	1.00	0.99	1.00	1.00	0.96
16	1.00	0.97	1.00	1.00	0.96
17	1.00	0.97	0.99	1.00	0.96
18	1.00	0.97	0.99	1.00	0.96
19	1.01	0.97	0.98	1.00	0.96
20	1.01	0.97	0.98	1.00	0.96
21	1.01	0.97	0.98	1.00	0.96
22	1.02	0.97	0.98	1.00	0.97
23	0.99	0.97	1.00	0.99	1.10
24	0.99	1.00	1.00	0.98	1.08
25	0.99	1.00	1.00	0.98	1.05
26	0.98	1.00	1.00	0.98	0.97
27	0.98	1.00	0.99	0.98	0.96
28	0.99	0.98	0.97	0.98	0.96
29	1.01	0.98	0.97	0.98	0.96
30	1.04	0.98	0.96	0.99	0.96

The effective broad group cross sections for the remainder of the core and reflector were obtained by averaging over the same spectrum. A comparison of the broad group flux spectrum for the core and reflector regions obtained from the GAZE calculations with the broad group flux spectrum obtained from the GAM and GATHER calculations appears in Table 35. The comparison shows the effect of the more thermal spectrum present in the low absorbing reflector region.

In some cases it was necessary to repeat the GAM and GATHER calculations using an "average" buckling from a GAZE calculation before satifactory agreement could be obtained. The neutron leakage for these assemblies is of the order of 40% which indicates that the total core buckling terms are quite large.

Thirty or more reactivity measurements were made in each of the five critical assemblies. A separate nuclear analysis was made on each of these assemblies, and in some cases the analysis was made using different sets of cross-section data and different analytical techniques. Because of the large amount of experimental and analytical data available for each of the cores, and in order to obtain a more comprehensive description of the adequacy of the cross-section data available for each nuclide, the experimental and analytical results will be presented for each nuclide separately rather than for each core assembly.

Some general comments can be made, however, about the analytical and experimental agreement for the different cores and the particular difficulties encountered in analyzing a specific core. The analytical and experimental data are quite consistent for the C/U-2500, C/U-1718, and C/U-859 core assemblies. For the C/U-5000 and C/U-432 cores, the analytical results do not agree as closely with the experimental data. For the C/U-5000 core the analytical results are generally too high by about 10% for each of nuclide loadings, and for the C/U-432 core the analytical results are about 10% too low. The difficulties in the latter case appear to be resolvable by using transport rather than diffusion theory analysis; however, the difficulties with the C/U-5000 core are yet to be resolved.

TABLE 35

RATIO OF BROAD GROUP FLUXES $\left(\frac{\text{GAZE FLUX}}{\text{GGC FLUX}}\right)$ IN CORE AND REFLECTOR

Broad Group	C/U-2500 Core Heterog. Region	C/U-2500 Core Reflector Region	C/U-1718 Core Heterog. Region	C/U-1718 Core Reflector Region	C/U-432 Core C/U-432 Region	C/U-432 Core C/U-432 Region	C/U-432 Core Reflector Region
1	1.04	I.06	0.98	0.92	1.03	0.98	1.02
2	1.04	1.03	0.99	0.95	1.03	0.98	1.01
3	1.03	0.98	1.01	0.97	1.03	0.99	1.01
4	1.02	0.96	1.01	0.98	1.02	0.99	0.97
5	1.03	0.97	1.01	0.99	1.02	0.99	0.97
6	1.00	0.95	1.05	1.00	1.01	1.00	0.96
7	0.99	0.95	1.05	1.01	1.00	1.01	1.00
8	0.98	0.95	1.05	1.01	0.99	1.01	1.00
9	0.98	0.95	1.04	1.02	0.99	1.02	1.02
10	0.98	0.95	1.04	1.02	0.98	1.02	1.03
11	0.97	0.95	1.03	1.02	0.98	1.02	1.02
12	0.97	0.96	1.03	1.01	0.97	1.01	1.06
13	0.97	0.96	1.02	1.03	0.96	1.02	1.06
14	0.97	0.97	1.01	1.03	0.96	1.02	1.07
15	0.97	0.96	1.01	1.03	0.96	1.02	1.08
16	0.97	0.96	1.00	1.03	0.96	1.03	1.09
17	0.96	0.97	1.00	1.04	0.96	1.01	1.07
18	0.96	0.97	1.00	1.03	0.96	1.01	1.07
19	0.96	0.97	1.01	1.03	0.96	1.02	1.09
20	0.96	0.97	0.99	1.02	0.96	1.02	1.08
21	0.96	0.97	0.98	1.02	0.96	1.01	1.08
22	0.96	0.97	0.99	1.01	0.97	1.01	1.04
23	0.96	0.96	1.00	1.02	1.05	1.00	1.04
24	0.95	0.97	1.00	1.02	1.03	1.00	1.03
25	0.95	0.96	1.00	1.03	1.01	0.95	1.03
26	0.95	0.96	1.00	1.03	0.97	0.94	1.04
27	0.96	0.97	0.99	1.04	1.00	0.94	1.09
28	0.98	1.07	1.02	1.18	1.02	0.93	1.18
29	1.01	1.21	1.03	1.35	1.04	0.94	1.40
30	1.08	1.46	1.04	1.64	1.08	0.98	1.84

Since insufficient C/U-432 fuel elements were available to construct a complete C/U-432 critical core, a radial driver region with C/U-859 fuel elements was used (see Fig. 42). The analysis of this core was made using effective broad group cross sections for each region averaged over their respective neutron energy spectra. Because of the significant absorption differences between the two regions, large flux gradients are present at the interface between the two radial regions. In addition, in order to meet the technical specification requirements for the critical facility, the safety devices, control and safety rods, and nuclear fuses were all located within the C/U-432 region relatively close to the central cell in which the measurements were performed. Representation of these devices in a radial model is difficult. One other factor affecting the ability to analyze the results in the C/U-432 core is the sensitivity of the results to the amount of water present in the two regions. There is significantly more water in the C/U-432 core than in any of the others.

6.3.1. Natural Boron

The seven concentrations of natural boron-loaded elements ranged in loading from 0.1 g/element to 1.9 g/element. These loadings gave a range in thermal macroscopic absorption cross section from about one half that of the lightest loaded uranium element, C/U-5000, to about one half that of the heaviest loaded uranium element, C/U-432.

The experimental and calculated reactivity worths of some of these elements in the different cores are given in Tables 17 and 36 and Fig. 9. In addition, a ratio of experimental to calculated worth is shown in Table 36. Two sets of calculated worths are given for three of the cores (C/U-2500, -1718, and -859) since a majority of the calculations for those cores were done using both sets of U^{235} cross-section data. From the comparison between analysis and experiment on these cores, it was obvious that the best agreement was obtained using the ENDF/B KAPL U^{235} (92.2352) data.

TABLE 36

COMPARISON OF CALCULATED AND
MEASURED BORON REACTIVITY WORTHS

Boron Loading (g/elem.)	Calculated Worth ($)			Ratio Measured Worth / Calculated Worth	
		C/U-5000			
0.20	-0.175			0.926	
0.55	-0.460			0.935	
1.00	-0.792		-0.808[b]	0.909	0.897[b]
1.50	-1.130			0.907	
1.90	-1.371			0.898	
		C/U-2500			
0.20					
0.55	-0.340			1.018	
1.00	-0.590	-0.596[a]		1.005	
1.50	-0.849	-0.858[a]		1.006	
1.90	-1.039	-1.051[a]	-1.070[b]	0.992	0.964[b]
		C/U-1718			
0.20		-0.099[a]			
0.55	-0.266	-0.271[a]		1.008	
1.00	-0.470	-0.478[a]		0.981	
1.50	-0.680	-0.692[a]		0.982	
1.90	-0.838	-0.853[a]	-0.842[b]	0.975	0.970[b]
		C/U-859			
0.20		-0.053[a]			
0.45	-0.123	-0.126[a]		0.976	
1.00	-0.272	-0.280[a]		1.004	
1.50	-0.398	-0.409[a]		1.003	
1.90	-0.494	-0.501[a]	-0.505[b]	1.000	0.978[b]
		C/U-432			
0.20	-0.021				
0.55	-0.070			1.114	
1.00	-0.131			1.085	
1.50	-0.192			1.099	
1.90	-0.242		-0.257[b]	1.099	1.035[b]

(a) Calculated with GA U^{235} cross-section data (92.2350) in surrounding core regions. All other calculations used ENDF/B U^{235} data throughout.

(b) These calculations were made using 30 group 1DF transport code.

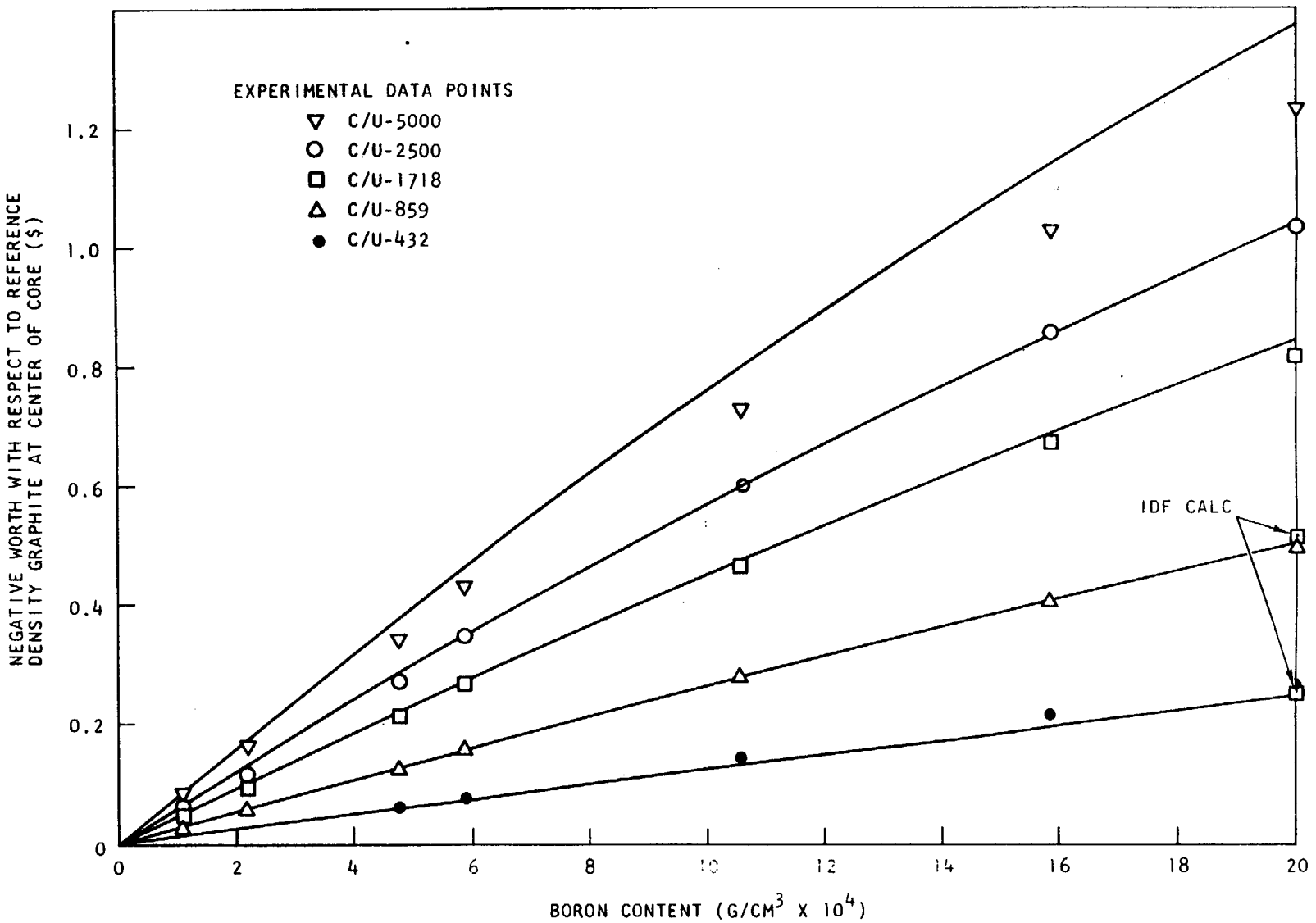

Fig.9. Calculated vs experimental reactivity worth of special boron elements in five core assemblies

Since boron has a well-known thermal cross section, it was selected as a "standard" to be used not only for confirming the validity of the analytical model used in calculating a given core but also as a measure of the reliability of the relative values of β_{eff} used in the various cores. The boron standards generated a self-consistent set of experimental/analytical results that lend credence to the conclusions drawn regarding the cross sections for the other material studies.

The results show excellent agreement in the C/U-2500,-1718, and -859 core assemblies, generally within 2%. The agreement for the C/U-432 assembly is improved by using a transport calculation in the analysis. This improvement is brought about by the ability to compute the sharp flux gradients that exist around the central cell as well as those existing at the interface between the C/U-432 and C/U-859 core regions. Transport calculations were performed for the heaviest loaded boron elements in all of the core assemblies.

The B_4C particles that were blended with the graphite flour before the compacts were pressed were sufficiently small (less than 5 microns), so that particle self-shielding could be ignored.

6.3.2. Highly Enriched Uranium Elements (U^{235})

The experimental and calculated results for the highly enriched uranium special elements are summarized in Tables 17 and 37 and Fig. 10. As in the previous discussion for boron, the calculated results are given for both sets of U^{235} cross-section data. The same cross-section data for U^{235} was used throughout the core as well as for the material in the central cell.

Comparison of the results clearly indicates that the best agreement with experiment is obtained with ENDF/B KAPL U^{235} (92.2352) cross-section data. In particular, in the case of the C/U-432 elements in the C/U-849 core, use of the ENDF/B data reduced the percentage difference between calculation and experiment from 40% to 4%. It was pointed out in Section 5 that the main difference between the U^{235} cross section sets was that the epithermal α value was lower for the ENDF/B KAPL cross-section data (see Table 21).

TABLE 37

COMPARISON OF CALCULATED AND MEASURED U^{235} REACTIVITY WORTHS

U^{235} Loading (Equiv.C/U)	U^{235} (92.2350) Data		U^{235} (92.2352) Data	
	Calculated Worth ($)	Ratio Measured / Calculated	Calculated Worth ($)	Ratio Measured / Calculated
		C/U-5000		
5000			0.090	0.911
2500			0.233	0.927
1718			0.380	0.930
859				
432				
		C/U-2500		
5000	0.038	1.237		
2500	0.074	1.081	0.076	1.053
1718	0.105	1.057	0.107	1.037
859	0.188	1.043	0.194	1.010
432	0.326	1.018	0.338	0.982
		C/U-1718		
5000	0.020	1.200		
2500	0.038	1.132	0.041	1.049
1718	0.053	1.132	0.057	1.053
859	0.094	1.106	0.102	1.020
432	0.165	1.121	0.179	1.034
		C/U-859		
5000	0.007			
2500	0.011		0.013	
1718	0.014	1.357	0.017	1.079
859	0.022	1.318	0.028	1.036
432	0.038	1.395	0.051 0.053[a]	1.039 1.000[a]
		C/U-432		
5000				
2500				
1718			0.007	
859			0.009	1.222
432			0.017 0.023[a]	1.294 0.957[a]

(a) 30 group calculations done with 1DF transport code. All others used GAZE code.

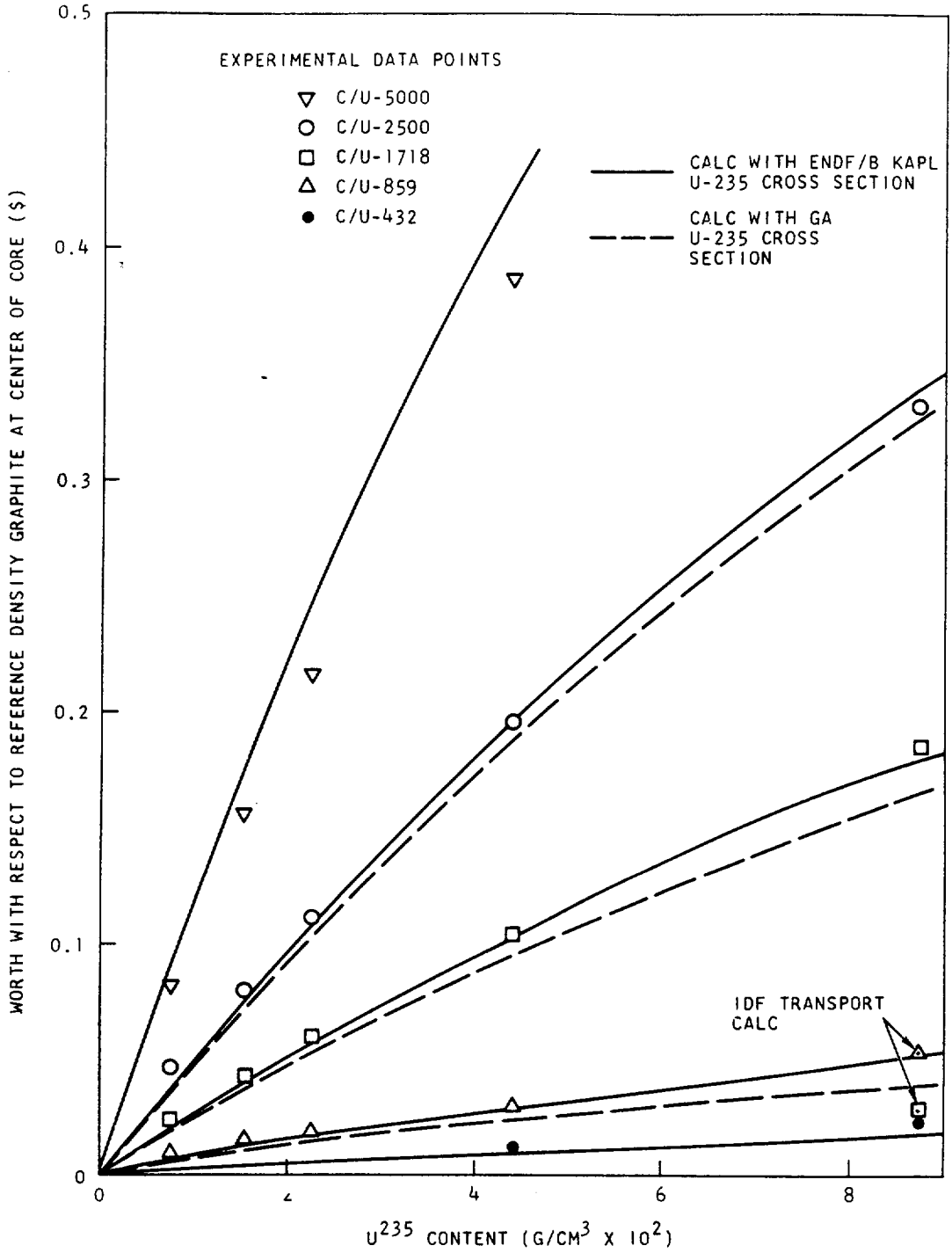

Fig.10. Calculated vs experimental reactivity worth of special U^{235} elements in five core assemblies

When the ENDF/B KAPL U^{235} cross-section data is used, the agreement between calculated and experimental results is good in the C/U-2500, -1718, and -859 cores. In the C/U-432 core, the agreement is good when the transport theory is used. Because of the low worth of uranium in that core, the reactivity change is small for even the heaviest loaded fuel element so that an uncertainty of $0.002 in measurement of the reactivity represents a 10% uncertainty on the total measured change.

6.3.3. Uranium (75 atom-% U^{235}, 15 atom-% U^{236}, 10 atom-% U^{238})

Three pairs of elements were loaded with uranium dioxide having the nominal enrichment of 75 atom-% U^{235}, 15 atom-% U^{236}, and 10 atom-% U^{238}. The U^{235} content of these elements matched that of the highly enriched uranium elements with the C/U-432, -1718, and -5000 atom ratios. As a result, the main difference between the two types of uranium elements was the presence of U^{236}. There was also a slight difference in carbon and U^{238} content, but by applying calculated or experimental corrections for the carbon and U^{238} differences, the reactivity worth of U^{236} could be obtained.

The calcuated and experimental reactivity worths of U^{236} are summarized in Table 38 and Fig. 11. The corrections for U^{238} and carbon were made utilizing the data in Tables 41 and 43 to obtain a worth/g for the U^{238} and carbon, respectively. All of the calculations summarized in Table 38 were made using ENDF/B KAPL cross-section data for U^{235}. For the heaviest-loaded element, which contained about 15 g of U^{236}, a resonance calculation using the Nordheim integral approximation in the GAM code was performed for the effective U^{236} cross sections. For the two lower loadings, resonance self-shielding was ignored. In the heavier loaded element, the calculated capture integral was 244 barns as compared to a dilute value of 321 barns.

In Fig. 11, the dotted curves are the calculated reactivity worths in the different cores for the U^{235} elements. The solid curves are for the same U^{235} loading but include the U^{236} isotope. The points shown represent the experimental measurements for the elements containing both U^{235} and U^{236}. The difference between the two curves represents the calculated reactivity worth of the U^{236} isotopes.

TABLE 38

COMPARISON OF CALCULATED AND MEASURED U^{236} REACTIVITY WORTHS

Loading Equivalent C/U	Calculated Worth($) of U^{235}	Calculated Worth($) U^{235} & U^{236}	Calculated Worth($) of U^{236}	Measured Worth($) U^{235} & U^{236}	Measured Worth($) of U^{236}	Ratio Measured / Calculated
			C/U-5000			
5000				0.071	-0.011	
1718				0.191	-0.025	
432	0.734	0.672	-0.062	0.596	-0.060	0.97
			C/U-2500			
5000	0.037(b)	0.028	-0.009	0.029	-0.018	
1718	0.107	0.078	-0.031	0.082	-0.029	0.97
432	0.338	0.267(a)	-0.071	0.263	-0.069	0.97
			C/U-1718			
5000	0.021(b)	0.008	-0.013	0.010	-0.014	
1718	0.057	0.029	-0.028	0.033	-0.027	0.96
432	0.179	0.101(a)	-0.078	0.115	-0.070	0.90
			C/U-859			
5000	0.005(b)	-0.005	-0.010	-0.004	-0.014	
1718	0.017	-0.011	-0.010	-0.005	-0.014	0.92
432	0.051	-0.022(a)	-0.073	-0.010	-0.063	0.86
			C/U-432			
5000	0.003(b)	-0.005	-0.008	-0.005	-0.008	
1718	0.007	-0.013	-0.021	-0.010	-0.017	0.81
432	0.023	-0.034(a)	-0.057	-0.026	-0.048	0.85

(a) These calculations included a resonance calculation for U^{236}.
(b) These values were obtained from Fig. 10.

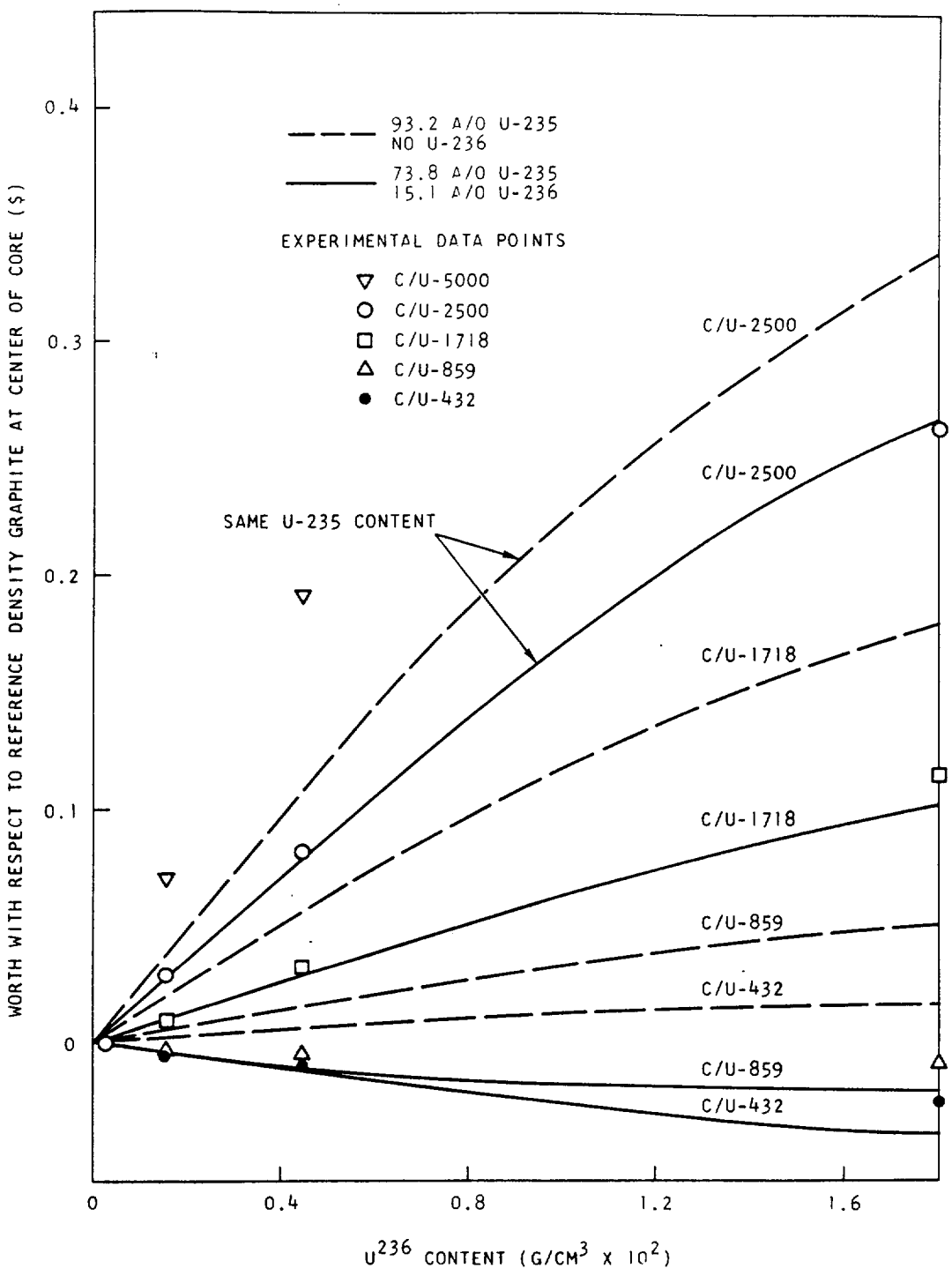

Fig.11. Calculated vs experimental reactivity worth of special U^{236} elements in five core assemblies

In regards to the data shown in Table 37, it should be noted that in the equivalent C/U-5000 element, there is so little U^{236} present (approximately 1.5 g/element) that the reactivity difference associated with its presence is of the order of the uncertainty of the measurements themselves. Therefore, the values shown for that element should be ignored. The calculated value of U^{236} for the two heavier loaded elements in all of the cores is too high, and the agreement with experiment tends to get poorer for the harder spectrum cores. This indicates that some correction is needed in the U^{236} resonance parameters.

6.3.4. Uranium (95.4 atom-% U^{233})

Three pairs of U^{233} elements were used. They were loaded so that their thermal absorption rate would match the thermal absorption rate for the enriched uranium elements with the C/U-432,-1718,and-5000 atom ratios. This was done to minimize the perturbation associated with loading these elements into the core assemblies of the same atom ratios.

The results of the analytical-experimental comparison are summarized in Tables 39 and 40 and Fig. 12. As indicated in Table 39, the analysis was performed for two sets of U^{233} cross-section data (see Tables 20 and 22). In addition, several small modifications were made to the ORNL-RPI U^{233} cross-section data, and the reactivity worth of the heaviest loaded element in the different cores was recalculated. These results are summarized in Table 40.

The initial analysis for the reactivity worth of the U^{233} elements was performed using the cross-section data for nuclide 92.2333 in the GAM and GATHER libraries. The analysis made in the first three cores (C/U-2500, C/U-1718, and C/U-859) indicated that the calculated reactivity was too high by about 10%. An improvement in the agreement with experiment was obtained when the ENDF/B KAPL U^{235} cross-section data was used in the adjacent core regions. Additional improvement was obtained when the ORNL-RPI U^{233} cross-section data was used in the analysis, but the calculated reactivity for these elements was still higher than that measured by about 3% to 5%. Table 22 summarized the primary differences between the two sets of U^{233} cross-section data.

TABLE 39

COMPARISON OF CALCULATED AND MEASURED U^{233} REACTIVITY WORTHS

U^{233} Loading Equivalent C/U	Calculated Worth($) 92.2333 Data	Calculated Worth($) 92.2333 Data With 92.2352 in Core	Calculated Worth($) 92.2334 Data With 92.2352 in Core	Measured Worth($)	Measured / Calculated 92.2334
		C/U-5000			
5000				0.110	
1718				0.284	
432			0.930	0.854	0.918
		C/U-2500			
5000			0.080	0.076	0.950
1718	0.192		0.187	0.186	0.995
432	0.601	0.593	0.584	0.565	0.967
		C/U-1718			
5000	0.064		0.061	0.054	0.885
1718	0.141		0.137	0.135	0.985
432	0.446	0.439	0.431	0.415	0.963
		C/U-859			
5000	0.034		0.031	0.025	0.806
1718	0.087		0.080	0.079	0.988
432	0.276	0.265	0.263 0.270[a]	0.243	0.924
		C/U-432			
5000			0.020		
1718			0.051	0.052	1.018
432			0.163 0.181[a]	0.164	0.906[a]

(a) Calculation was done with 1DF transport code.

TABLE 40

SUMMARY OF ANALYSIS OF U^{233} REACTIVITY WORTHS[a]

	C/U-2500	C/U-1718	C/U-859	C/U-432
Measured reactivity($)	0.565	0.415	0.243	0.164
Best calculated value($)	0.584	0.431	0.263	0.181
Discrepancy (%)	+3.4	+3.9	+8.2	+9.4
Discrepancy (%) if:[b]				
(1) ν is changed to 2.494 from 2.503 for U^{233}	+2.1		+6.6	
(2) σ_c^{233} is increased 10% for:				
(a) $2.38 \leq E \leq 14.9 \times 10^6$ eV	+2.7		+6.2	
(b) $0.1 \leq E \geq 0.414$ eV	+2.8		+7.8	
(c) $0.1 \leq E \leq 2.38$ eV	+1.9		+5.8	
(3) σ_f^{233} is decreased 10% for: 2.38 eV $\leq E \leq 14.9 \times 10^6$ eV	0.9		0.4	

(a) The calculated reactivity coefficients were made for the heaviest loaded U^{233} element (C/U-432) using ORNL-RPI U^{233} cross-section data. They were made relative to a pure graphite element and KAPL-ENDF/B U^{235} cross-section data (92.2352) was used for the adjacent core region.

(b) The following data reflects only one change at a time.

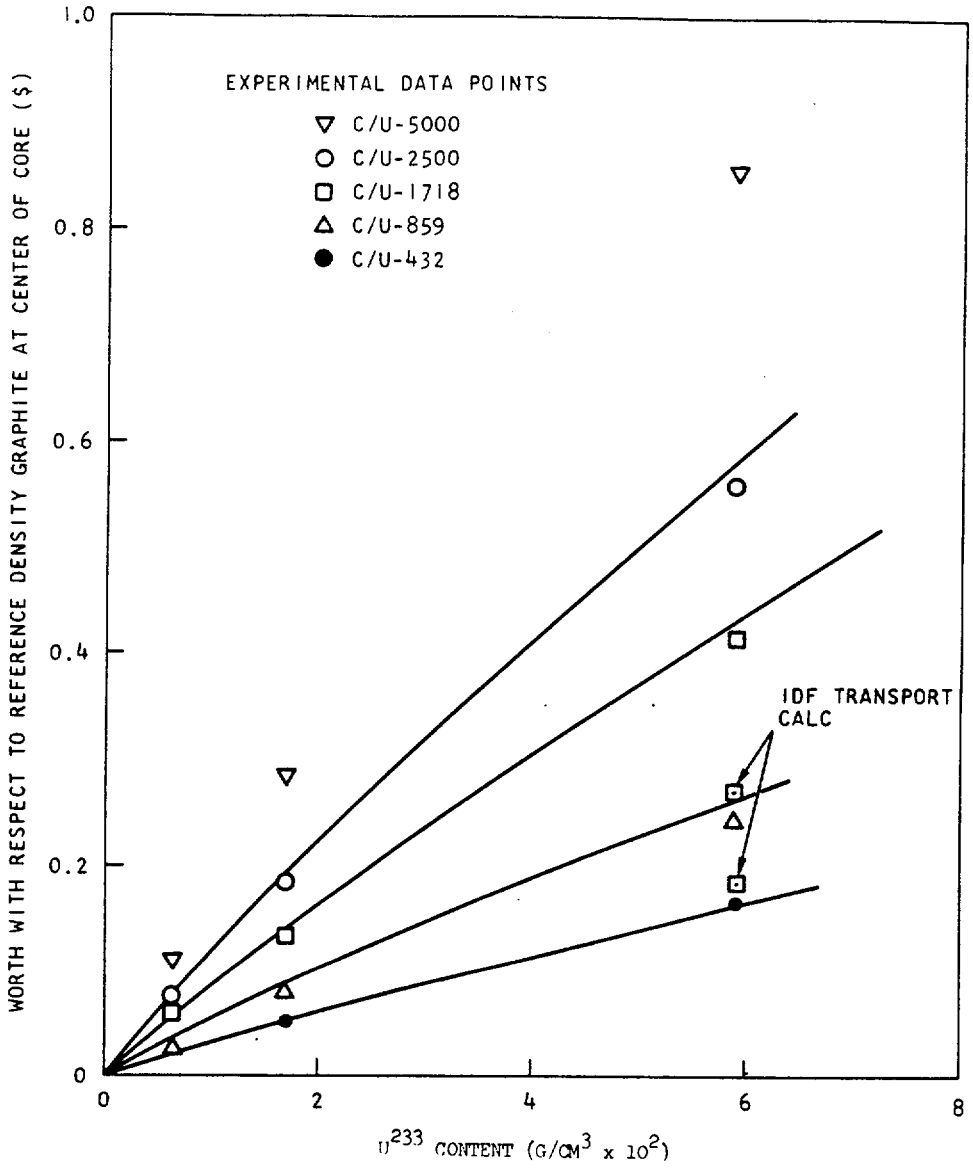

Fig.12. Calculated vs experimental reactivity worth of special U^{233} elements in five core assemblies

The experimental data indicates that the most likely source of the discrepancy between calculated and measured worth is a general underestimate of the capture cross section or an overestimate of the fission cross section over a wide energy range. Over a wide range of thermal spectra [Table 30 and Figs. 5(a) through 5(e)], the discrepancy is nearly constant at about 5%.

An investigation of the U^{233} cross-section data indicates that there are significant uncertainties in the differential data in at least three areas:[14]

(1) The value of ν of 2200 m/sec is uncertain by about ±0.4%.

(2) In the energy region below about 0.5 eV, the spectrum averaged value of η is uncertain by 1 to 2%, the most likely difficulty being with the capture cross section. A ±2% uncertainty equivalent to a 20% uncertainty in the capture cross section.

(3) In the energy region above 0.5 eV, α may be uncertain by about 5%.

These possible sources of the 5% discrepancy in the reactivity coefficient have been quantitatively investigated and the results are summarized in Table 39. A 0.4% reduction in ν of U^{233} would account for one-fourth to one-third of the discrepancy. A 20% increase in the capture cross section in the thermal range below 0.414 eV (a change in η of about 2%) could also account for one-fourth to one-third of the discrepancy, while 20% increase between 0.414 and 2.38 eV could account for 60 to 80% of the discrepancy. An adjustment in the fission cross section above 2.38 eV would also be effective.

6.3.5. Depleted Uranium (99.8 atom-% U^{238} and Thorium)

Five pairs of the depleted uranium-loaded elements ranged from 50 g/element to 500 g/element. While the boron elements provided a standard for the thermal absorbers and for absolute reactivity measurements, the depleted uranium elements provided a standard for resonance absorbing materials such as thorium. The dilute resonance integral as well as most of the resonance parameters for U^{238} are known to be within a few percent.

The five pairs of thorium-loaded elements ranged from 50 g/element to 500 g/element. The heaviest loaded thorium element had an absorber density of about 0.5 g/cm in the lump.

The experimental and calculated reactivity worths of these elements in the five separate core assemblies are summarized in Tables 41 and 42 and Figs. 13, 14, and 15. Table 41 shows the calculated reactivity worth of depleted uranium for each loading in each core as well as the ratio of measured worth to calculated worth, and Table 42 shows the same information for the thorium-loaded elements.

All of the calculated results shown in Tables 41 and 42 were performed using the model described earlier. That is, a 30-group radial GAZE calculation was performed with the specific element loaded in the center using effective broad group cross sections that were obtained from a resonance calculation in GAM. As mentioned previously, the resonance calculations were performed using the asymptotic approximation of the internal moderator to the collision density because of convergence difficulties when the Nordheim integral approximation was used. This difficulty has been corrected in GAM and the calculated result using the latter approximation is shown for the heaviest loaded element. As expected, the calculated worth for this case is reduced. These calculations were performed with ENDF/B KAPL U^{235} cross sections in the surrounding core regions.

TABLE 41

COMPARISON OF CALCULATED AND MEASURED U^{238} REACTIVITY WORTHS

Depleted U Loading (g/element)	C/U-5000		C/U-2500		C/U-1718		C/U-859		C/U-432	
	Calc. Worth($)	Calc./Meas.	Calc. Worth($)	Calc./Meas.	Calc. Worth($)	Calc./Meas.	Calc. Worth($)	Calc./Meas.	Calc. Worth($)	Calc./Meas.
50			-0.105	0.886	-0.114	0.868	-0.110	0.873	-0.085	0.918
100			-0.162	0.926	-0.177	0.859	-0.172	0.831	-0.135	0.948
200			-0.239	0.941	-0.259	0.919	-0.253	0.901	-0.200	0.950
300	-0.246[a]	0.947	-0.297	0.960	-0.321	0.935	-0.314	0.917	-0.250	0.976
500			-0.382	0.969	-0.412	0.944	-0.404	0.913	-0.323	0.985
500	-0.321[a]	0.960	-0.372[a]	0.995	-0.399[a]	0.975	-0.386[a]	0.956	-0.312[b]	1.019

(a) Resonance calculation performed with Nordheim integral approximation for both moderator and absorber contribution to collision density. All others were done with asymptotic approximation of moderator to collision density, as described in Section 4.1.

(b) This calculation was done with 1DF transport code.

TABLE 42

COMPARISON OF CALCULATED AND
MEASURED THORIUM REACTICITY WORTHS

Depleted U Loading (g/element)	C/U-5000		C/U-2500		C/U-1718		C/U-859		C/U-432	
	Calc. Worth($)	Calc./Meas.	Calc. Worth($)	Calc./Meas.	Calc. Worth($)	Calc./Meas.	Calc. Worth($)	Calc./Meas.	Calc. Worth($)	Calc./Meas.
50			-0.059	0.898	-0.061	0.902	-0.057	0.982		
100			-0.105	0.895	-0.108	0.861	-0.102	0.902	-0.085	0.941
200			-0.180	0.950	-0.182	0.934	-0.172	0.924	-0.143	0.972
300	-0.237[a]	0.920	-0.244	0.951	-0.245	0.939	-0.230	0.917	-0.191	0.969
500			-0.349	0.980	-0.347	0.954	-0.320	0.925	-0.265	0.974
500	-0.349[a]	0.946	-0.343[a]	0.997	-0.342[a]	0.968	-0.311[a]	0.952	-0.252[b]	1.024

(a) Resonance calculation performd with Nordheim integral approximation for both moderator and absorber contribution to collision density. All others were done with asymptotic approximation of moderator to collision density, as described in Section 4.1.

(b) This calculation was done with 1DF transport code.

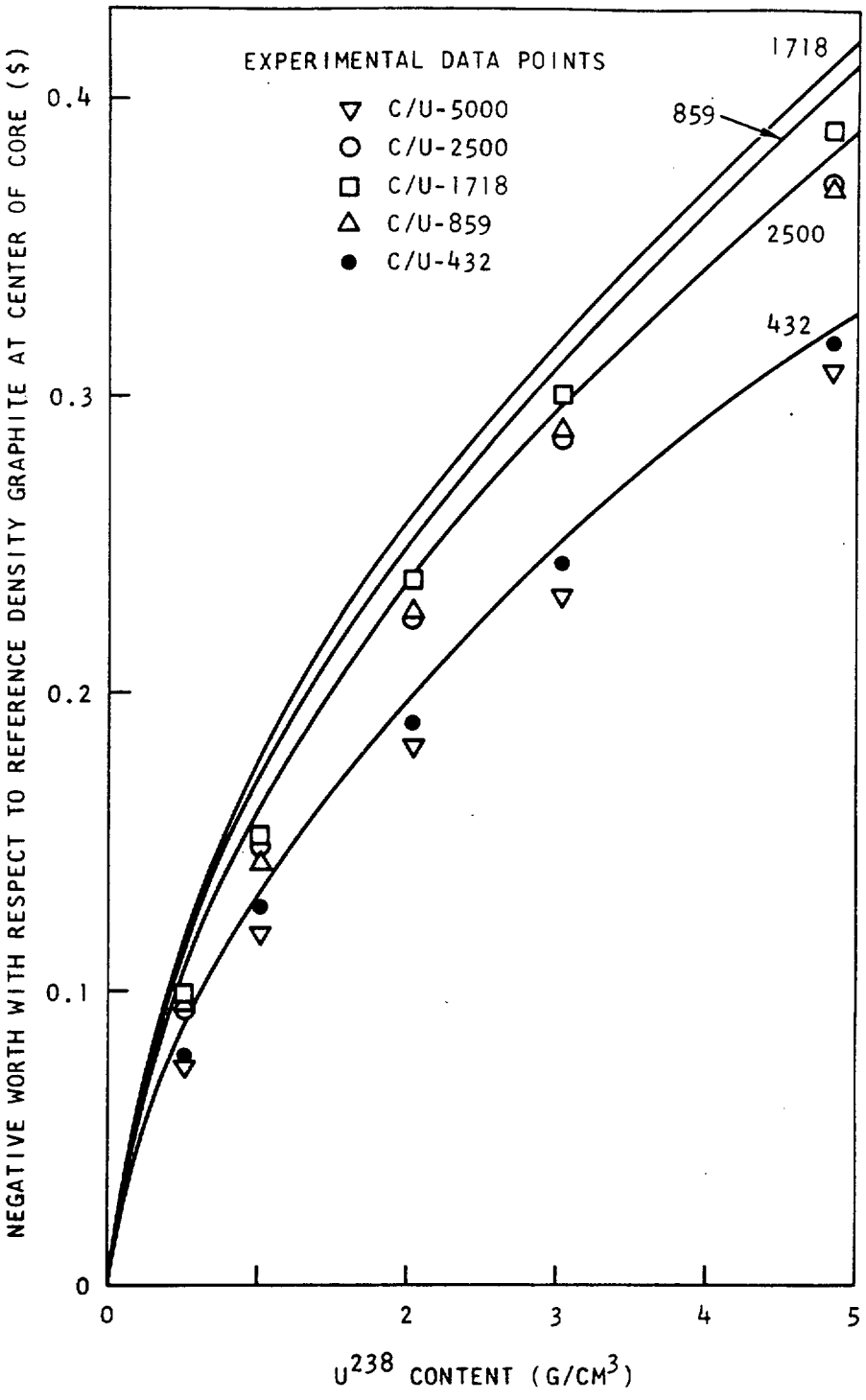

Fig.13. Calculated vs experimental reactivity worth of special depleted uranium (U^{238}) elements of five core assemblies

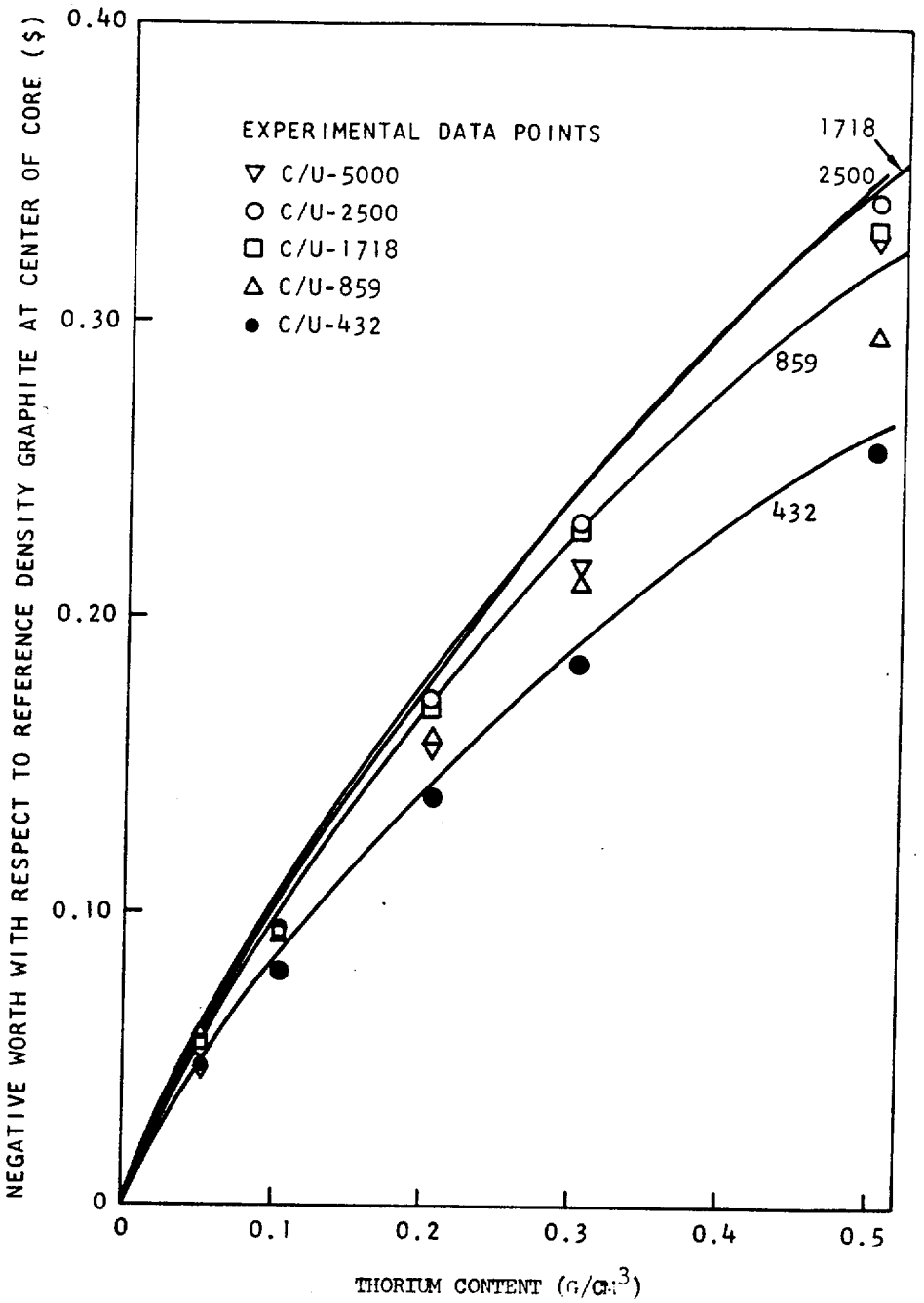

Fig.14. Calculated vs experimental reactivity worth of special thorium elements in five core assemblies

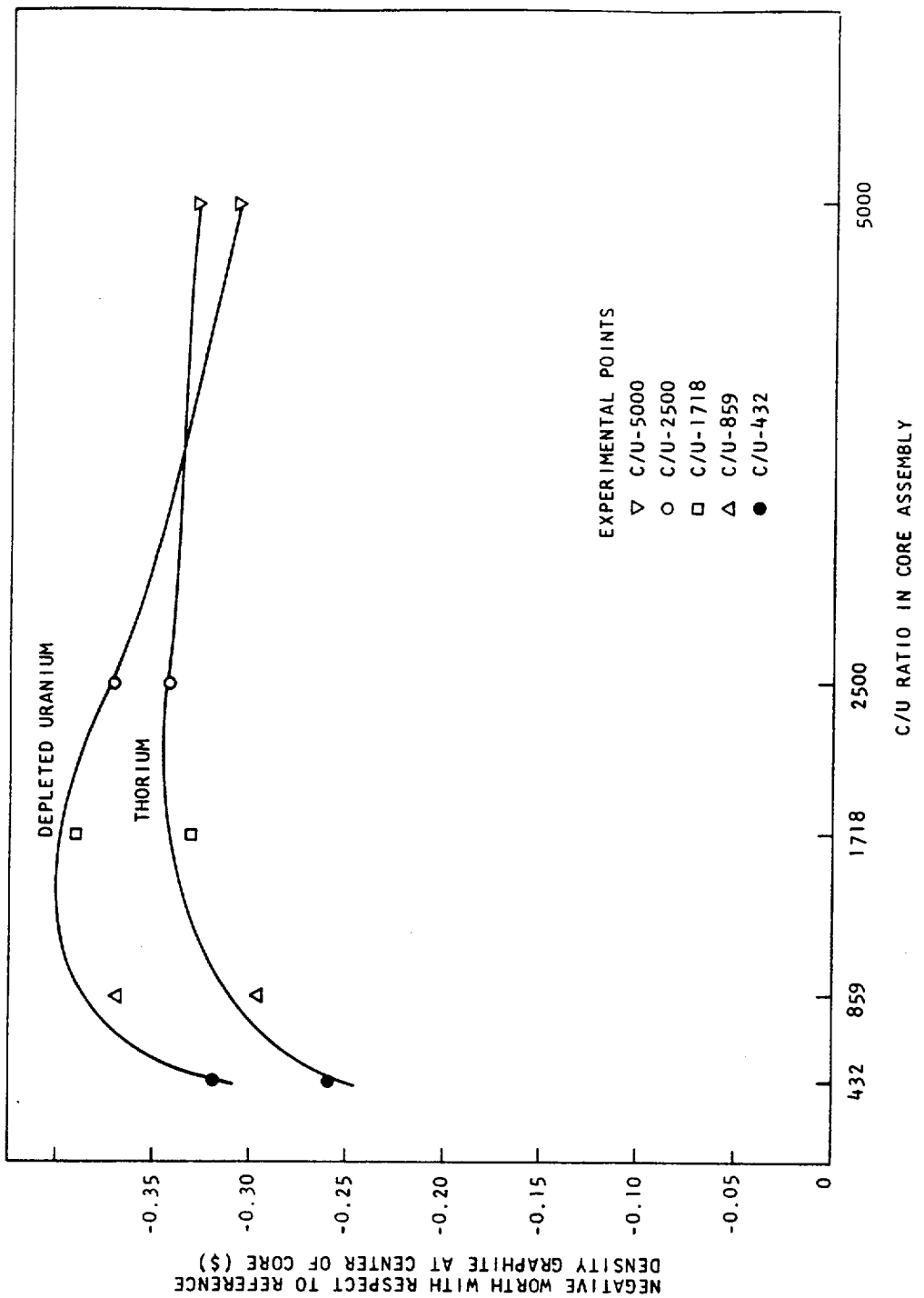

Fig. 15. Calculated vs experimental reactivity worth for heaviest loaded special thorium and depleted uranium elements in five core assemblies

Generally the agreement between the calculated and measured reactivity worth for these elements is good. For the heaviest loaded element of both thorium and U^{238}, this agreement is within 5% for all of the cores. The agreement tends to get poorer as the C/U core atom ratio is decreased and epithermal flux is increased except for the C/U-432 core where better agreement is again achieved. In light of the other difficulties in the two regions of the C/U-432 core, this change may be artificial. For the heavier loaded elements, 200, 300, and 500 g, the results are consistent for both thorium and U^{238}, but in the lighter loadings there appears to be an error in either the loading or the calculation.

The ability to predict the reactivity worth of the heaviest loaded Th and U^{238} elements in the different C/U-cores can be seen in Fig. 15.

The nuclear model used in the analysis of the resonance absorbers is not rigorously correct. The effective broad group constants obtained from the GAM resonance calculation takes into account the spatial self-shielding in the lump, at least to the extent of using a spatially constant depressed flux in the lump. It does not, however, account for any flux distribution changes in the adjacent core regions when a heavy absorber is inserted in the central core region. In using these cross sections in the "exact" GAZE calculation, the spatial self-shielding recalculated in a reduced amount yields a reaction rate in the lump somewhat reduced from what it should be. A perturbation calculation, which ignores changes in the flux distribution, using the flux and ajoint flux terms as obtained from a reference GAZE calculation, and the appropriate effective broad group cross sections from a GAM resonance calculation, yielded a calculated negative reactivity worth about 6% greater for U^{238} and 2% greater for thorium for the heaviest loaded elements. This indicates that for the case of thorium and U^{238} the nuclear model is reasonably adequate.

6.3.6. Gold

Measurements were made on three pairs of elements loaded with gold. Gold has a relatively well-known resonance integral; its resonance parameters have been extensively measured giving good agreement with the integral measurements. For these reasons, some thought was given to using gold as a "standard". The major difficulties associated with the use of gold elements as a standard are twofold. The first one concerns the uncertainty with which the elements have been loaded, and the second one involves the nuclear model used in the calculations. It is extremely difficult to obtain a uniform loading of gold in which the particles are small and uniform in size. Over two-thirds of the total resonance integral (1500 barns in the dilute integral to 0.5 eV) is contained in the single resonance at 4.906 eV. Because of this large single resonance, particle self-shielding is significant and, consequently, variations in particle size contribute to the uncertainty of the reactivity worth of the sample. As an example, for the 5-g loaded element, if the particle size were 10 μ ± 5 μ, the total reactivity worth would have an uncertainty of ± 9%. For the heaviest loaded element, 45 g, the same particle size variation would give an uncertainty in reactivity worth of ± 1%.

The two pairs of elements with the lower loadings were fabricated by mixing a gold solution with graphite flour, heating to drive off the solvent, and then pressing into compacts. Investigation of samples made in this manner showed good homogeneity and very little agglomeration of the gold. With an electron microscope it was determined that the particles in the samples analyzed were less than 5 μ. The heaviest loaded elements were made with a mixture of gold cyanide and graphite flour where the gold cyanide particles were in the range of 20 to 36 μ. In the heaviest loaded elements, the effective resonance integral is not as dependent on the particle size as in the lightly loaded cases.

Calculated and measured reactivity worths for these elements in the different assemblies are summarized in Tables 17 and 43 and Fig. 16. Also given in Table 43 is the ratio of measured to calculated worth. The nuclear model was the same as that discussed previously for thorium and depleted uranium. No particle self-shielding was included, and the calculations were done using the ENDF/B KAPL U^{235} cross sections in the adjacent core regions.

As seen in Table 43, the calculated worth for the lightest loaded element was always slightly higher than that measured. This could very easily be due to particle size, which was assumed zero in the calculation. For both of the other loadings, the calculated worth was always smaller than that measured, and inclusion of particle self-shielding would make the calculated worth even lower. However, as explained in the discussion on thorium and U^{238}, the nuclear model used in these calculations was not rigorously correct, in particular, for the gold, where the broad group capture cross section for some of the groups is very large. This is due to the duplication in the GAZE calculation of the spatial self-shielding in the absorber lump. A perturbation analysis was performed for the heaviest loading using the broad group cross sections from the GAM resonance calculation (see Table 42). The increase in calculated worth is quite sufficient and yields a value even higher than that measured. However, this method is also incorrect because it neglects the change in flux shape in the adjacent core region due to the insertion of the gold element in the central region. Using the results from the GAZE calculation with the gold element inserted explicitly at the center, the total capture rate in gold was corrected to remove the effect of the spatial self-shielding that was introduced in the different groups by the explicit calculation. This was done by multiplying the group capture rate from GAZE by the ratio of the surface flux at the cell boundary to the average flux in the cell for that particular group. The reactivity worth was then assumed to be proportional to the total capture rate in gold. The results of this modification are also shown in Table 42; the calculated worth was within 5% of that measured. The agreement between experiment and calculation is good in light of the uncertainties present in the actual loading, the particle size and distribution, and the difficulty with the nuclear model. The use of these gold elements as a standard for the reactivity measurements is therefore questionable.

TABLE 43

COMPARISON OF CALCULATED AND
MEASURED GOLD REACTIVITY WORTHS

Gold Loading (g/elem.)	C/U-5000		C/U-2500		C/U-1718		C/U-859		C/U-432	
	Calc. Worth($)	Calc./Meas.	Calc. Worth($)	Calc./Meas.	Calc. Worth($)	Calc./Meas.	Calc. Worth($)	Calc./Meas.	Calc. Worth($)	Calc./Meas.
5			-0.106	0.981	-0.108	0.954	-0.094	0.936	-0.062	1.016
15			-0.249	1.068	-0.252	1.016	-0.218	1.005	-0.148	1.115
45	-0.528	1.010	-9.508	1.098	-0.488	1.078	-0.401	1.090	-0.265	1.219
45			-0.585[a]	0.954	-0.578[a]	0.910	-0.483[a]	0.905		
45			-0.528[b]	1.057	-0.508[b]	1.035	-0.419[b]	1.043		

(a) Perturbation calculation using effective broad group cross sections from GAM resonance calculation.

(b) Total capture rate for gold corrected in exact calculation by ratio of surface flux/average flux for each of the broad groups at central cell.

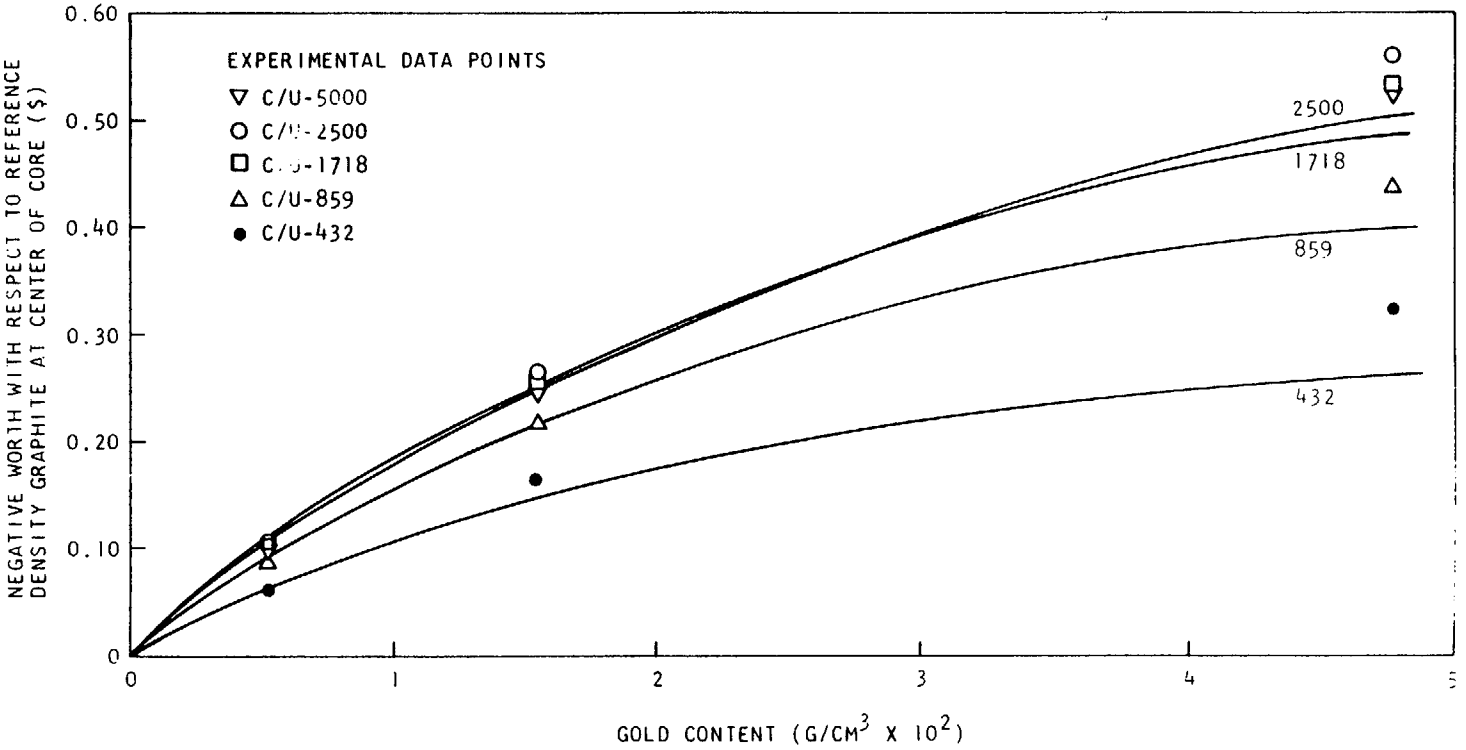

Fig.16. Calculated vs expeimental reactivity Worth of special gold elements in five core assemblies

6.3.7. Neptunium

Three pairs of elements were loaded with samples of Np^{237} dioxide on which reactivity measurements were made. Their loading was similar to that of the gold elements, ranging from 5 to 55 g per element.

The results of the analysis and experimental measurements are summarized in Tables 17 and 44 and Fig. 17. A ratio of measured to calculated reactivity worth is also given in Table 44. A nuclear model was similar to that used in the analysis of the gold elements except that resonance calculations in the GAM code were performed only for the heaviest loaded element. The effect of doing a separate resonance calculation, even for the heaviest loading, was small because of the particular resonance structure in Np^{237}. The total dilute resonance integral for Np^{237} is high, 738.2 barns; however, the majority of this integral is due to a single resonance at 0.489 eV. Because of the thermal cutoff value of 2.38 eV, the GAM resonance calculation covers only the resonances above this energy. This problem is also peculiar to plutonium and is discussed in more detail in Section 5.

The comparison between calculated and measured worth shown in Table 44 is fairly consistent for all of the elements in all of the cores. The calculated worth is about 10% lower than that measured in all cases. Particle self-shielding, which was neglected, would make the calculated value even lower if it was not negligible (particle size less than 37 μ). A resonance calculation on the lower energy resonance would have that same effect.

TABLE 44

COMPARISON OF CALCULATED AND
MEASURED Np^{237} REACTIVITY WORTHS

Np^{237} Loading (g/elem.)	C/U-5000		C/U-2500		C/U-1718		C/U-859		C/U-432	
	Calc. Worth($)	Calc./Meas.	Calc. Worth($)	Calc./Meas.	Calc. Worth($)	Calc./Meas.	Calc. Worth($)	Calc./Meas.	Calc. Worth($)	Calc./Meas.
5			-0.076	1.105	-0.072	1.069	-0.060	1.067	-0.041	1.098
15			-0.221	1.100	-0.210	1.081	-0.175	1.057	-0.120	1.133
55	-0.808(a)	0.978	-0.707(a)	1.119	-0.679(a)	1.084	-0.558(a)	1.056	-0.374(a)	1.142

(a) Resonance calculations were made for these loadings down to 2.38 eV.

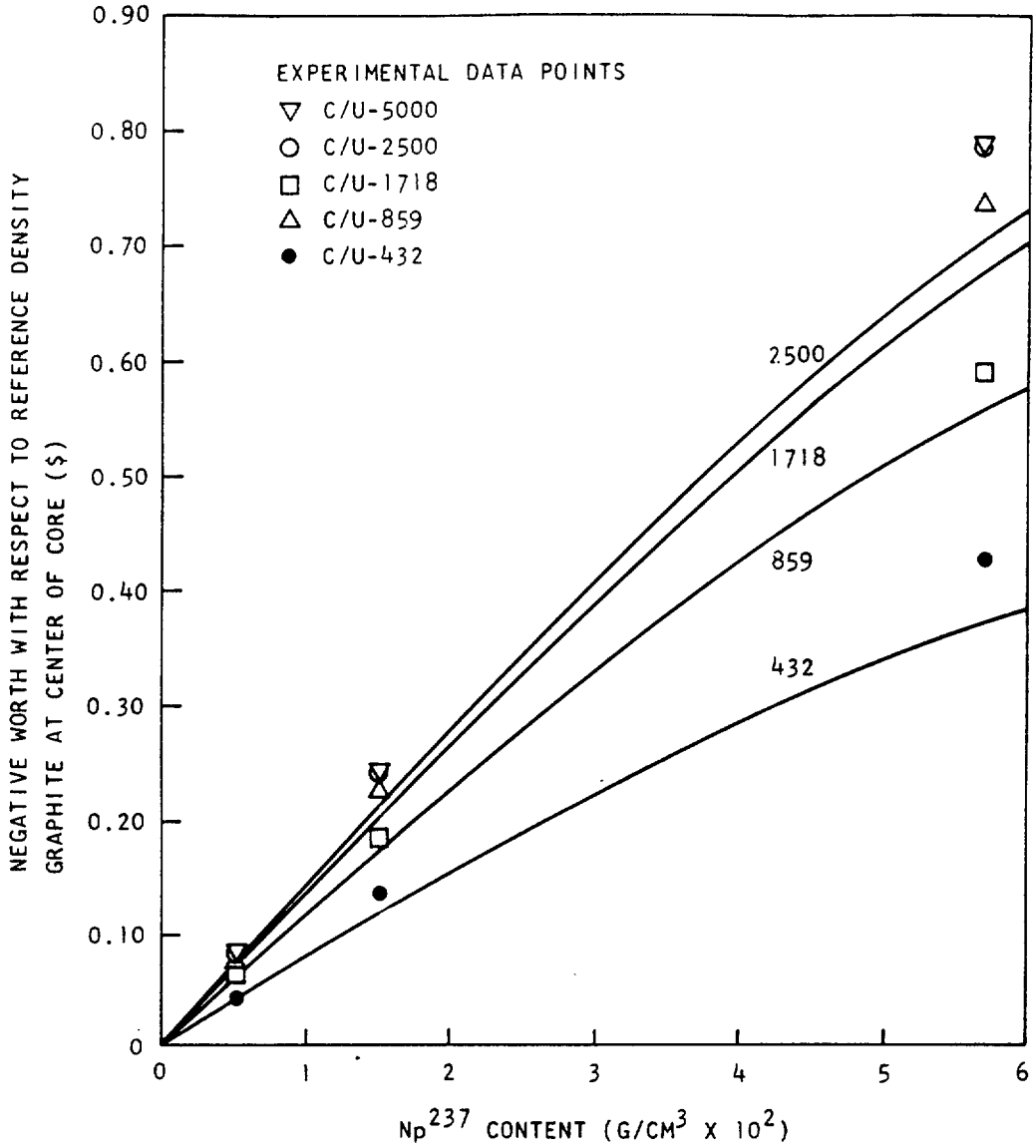

Fig.17. Calculated vs experimental reactivity worth of special Np^{237} elements in five core assemblies

6.3.8. Carbon and Aluminum

Measurements and calculations were also performed on carbon and aluminum. The results are summarized in Table 45. All of the measurements for the special materials were made relative to an all-carbon element that had essentially the came carbon density as the lighter loaded special elements. Another pair of all-carbon elements was fabricated in which the carbon compacts were pressed to a lower density, approximately 1.67 g/cm^3 as opposed to the 1.80 g/cm^3 for the reference density carbon. These elements were identical to the other special elements so that the reactivity difference could be attributed to the difference in the total mass of carbon. The comparison between calculated and measured worth of carbon was very good except in the C/U-2500 core; the small discrepancy there could be due to a number of things, including an error in the measured value.

The comparison between the experimental and calculated worths of aluminum was good, generally within a few percent.

6.3.9. Plutonium

Six pairs of fuel elements were loaded with plutonium dioxide containing two different enrichments of Pu^{240}. Three pairs contained plutonium with 95.6 atom-% Pu^{239} and 4.1 atom-% Pu^{240} and three pairs contained plutonium with 72.3 atom-% Pu^{239} and 22.2 atom-% Pu^{240}. They were loaded according to the following criteria:

1. There were three different loadings of each enrichment. The most lightly loaded elements of each enrichment had the same Pu^{239} content; similarly for the middle and most heavily loaded elements of each enrichment.

2. The lightest loading for the plutonium with the high isotopic enrichment of Pu^{240} had the same Pu^{240} content as the heaviest loading of plutonium with the low isotopic enrichment of Pu^{240}. Therefore, these two pairs of elements had identical Pu^{240} content but different amounts of Pu^{239}.

3. The thermal macroscopic absorption of Pu^{239} for the heaviest loaded elements was approximately the same as the heaviest loaded uranium elements. This was to minimize thermal flux perturbations when these elements were inserted.

TABLE 45

COMPARISON OF CALCULATED AND MEASURED
CARBON AND ALUMINUM REACTIVITY WORTHS

Material Loading	Calculated Worth ($)	Measured Worth($)	Measured / Calculated
C/U-5000			
0.9 density graphite	-0.008	-0.008	1.000
Void		-0.171	
Aluminum rod		-0.360	
C/U-2500			
0.9 density graphite	-0.013	-0.009	
Void	-0.234	-0.248	1.060
Aluminum rod	-0.370	-0.360	0.973
C/U-1718			
0.9 density graphite	-0.016	-0.015	1.067
Void	-0.292		
Aluminum rod	-0.362	-0.361	1.000
C/U-859			
0.9 density graphite	-0.018	-0.018	1.000
Void	-0.310	-0.318	1.026
Aluminum rod	-0.319	-0.301	1.060
C/U-432			
0.9 density graphite	-0.017	-0.017	1.000
Void	-0.325	-0.343	1.055
Aluminum rod	-0.247	-0.256	0.965

The measured reactivity worth for these fuel elements in the five critical assemblies is shown in Table 17 and Figs. 18 and 19. As for all of the other measurements, these results are shown relative to an all-carbon element of nearly the same carbon density. The importance of Pu^{240} as a neutron poison is shown distinctly in the figures. Even in the low enriched Pu^{240} elements, as the thermal neutron distribution is shifted toward the large 1.057-eV resonance of Pu^{240} by reducing the C/U atom ratio in the critical assembly, the negative worth of the Pu^{240} overrides the positive worth of the fissile isotope Pu^{239}. For the higher enriched Pu^{240} elements, this is true in all of the critical assemblies except the C/U-5000 core.

Analysis of these results is complicated by the presence of the lower energy resonances in the plutonium isotopes. This is discussed in detail in Section 6.1. The thermal cutoff of 2.38 eV was chosen because of the up-scattering from carbon to this energy; consequently, lumped re-resonance calculations for effective broad group constants in the GAM code could not be used. Therefore, calculations for the reactivity worth of plutonium were restricted to exact calculations using many thermal groups (8, 16, 22) in both diffusion theory (GAZE) or transport theory. Table 46 shows the thermal group structures that were used to provide finer energy detail around the Pu^{240} 1.057-eV resonances.

As can be seen from Table 47, which summarizes the results for the C/U-2500 core, the major experimental-analytical discrepancies exist in the high Pu^{240} content samples. As the number of thermal groups increases from 8 to 16 in the diffusion theory, a large improvement in agreement was achieved. However, little improvement resulted from using $P1\text{-}S_4$ transport theory. Changing the transport theory approximation from S_4 to S_8 (which increases the number of segments in the unit sphere from 8 to 24) gave a significant improvement. An important cause of the discrepancy in the high Pu^{240} samples may be the self-shielding in the individual plutonium dioxide grains. The grains were specified to be less than 44 μ in diameter, but

the exact grain size distribution is not known. However, 44 μ grains could give a significant self-shielding effect, enough to account for the discrepancy between experiment and the 16 thermal group, P1-S8 transport analytical results. Based on the results shown in Table 47, higher order approximations of the exact reatment did not appear fruitful and were not pursued, especially since the grain size distribution was not known.

In view of the results shown in Table 47 for the C/U-2500 core, calculations were made for the C/U-1718 and -859 cores using the 38 broad group set and the GAZE diffusion code. These results are summarized in Table 48 and Fig. 20. The same degree of agreement between analytical and experimental results was obtained for those two cores. In Fig. 20, only the results for the C/U-2500 and C/U-859 cores are plotted; the dash lines represent the experimental results and the solid lines the calculated results.

No calculations have been performed on the plutonium elements in either the C/U-432 core or the C/U-5000 core.

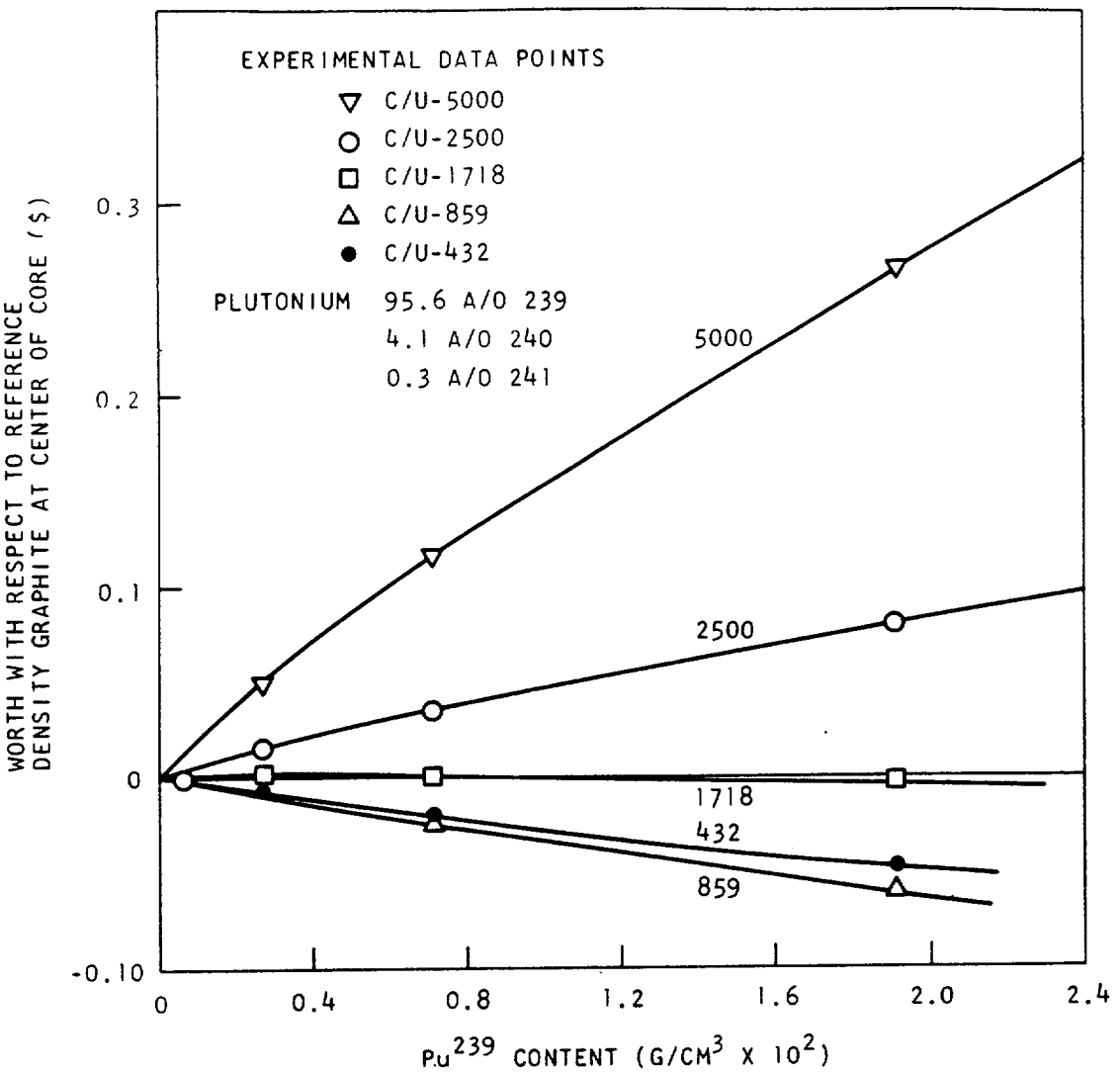

Fig.18. Experimental reactivity worth of special plutonium (low Pu^{240}) elements in five core assemblies

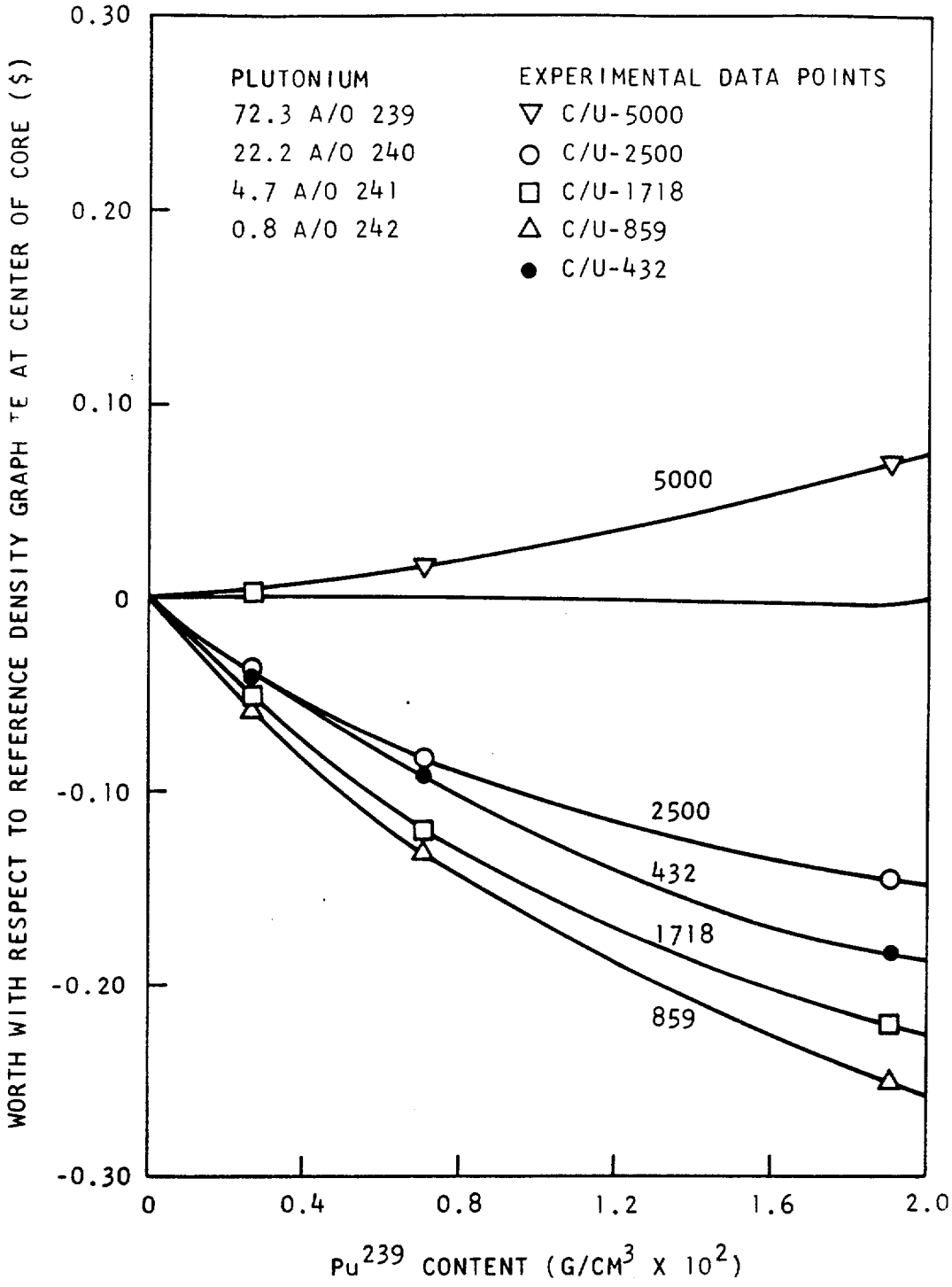

Fig.19. Experimental reactivity worth of special plutonium (high Pu^{240}) elements in five core assemblies

TABLE 46

THERMAL GROUP STRUCTURE FOR
PLUTONIUM ANALYSIS
(UPPER ENERGY POINTS)

Group Number	8-Group Set (22 Total)	16-Group Set (38 Total)	22-Group Set (44 Total)
1	2.38 eV	2.38 eV	2.38 eV
2	1.60 eV	2.20 eV	2.20 eV
3	1.30 eV	1.90 eV	1.90 eV
4	0.95 eV	1.60 eV	1.60 eV
5	0.625 eV	1.30 eV	1.30 eV
6	0.414 eV	1.11 eV	1.15 eV
7	0.100 eV	1.07 eV	1.11 eV
8	0.040 eV	1.025 eV	1.09 eV
9		0.95 eV	1.07 eV
10		0.75 eV	1.05 eV
11		0.625 eV	1.025 eV
12		0.414 eV	1.000 eV
13		0.350 eV	0.97 eV
14		0.250 eV	0.95 eV
15		0.100 eV	0.89 eV
16		0.040 eV	0.75 eV
17			0.625 eV
18			0.414 eV
19			0.350 eV
20			0.250 eV
21			0.100 eV
22			0.040 eV

TABLE 47

MEASURED AND CALCULATED PLUTONIUM REACTIVITY
WORTH IN THE C/U-2500 ASSEMBLY

Element Description	Measured Worth ($)	Calculated Worth ($)				
		Diffusion Theory 30 Groups 8 Thermal	Diffusion Theory 38 Groups 16 Thermal	Transport Theory 38 Groups P_1S_4	Transport Theory 38 Groups P_1S_8	Transport Theory 44 Groups 22 Thermal P_1S_4
PuL-240 A[(a)] (18.85 g Pu/element)	0.079	0.069	0.069	0.071		
PuL-240 B[(a)] (7.59 g Pu/element)	0.035		0.032			
PuL-240 C[(a)] (3.11 g Pu/element)	0.016	0.015	0.014			
PuH-240 A[(b)] (23 g Pu/element)	-0.145	-0.278	-0.196	-0.190	-0.175	-0.188
PuH-240 B[(b)] (9.25 g Pu/element)	-0.083	-0.138	-0.112	-0.109	-0.092	
PuH-240 C[(b)] (3.86 g Pu/element)	-0.038		-0.053			

(a) Samples contain 95.62% Pu^{239}, 4.10% Pu^{240}, 0.27% Pu^{241}, and 0.01% Pu^{242}.

(b) Samples contain 72.34% Pu^{239}, 22.19% Pu^{240}, 4.69% Pu^{241}, and 0.78% Pu^{242}.

TABLE 48

COMPARISON OF CALCULATED[(a)] AND
MEASURED PLUTONIUM REACTIVITY WORTHS

Plutonium Loading (g/elem.)	C/U-2500 Core		C/U-1718 Core		C/U-859 Core	
	Calculated Worth ($)	Measured Worth($)	Calculated Worth ($)	Measured Worth($)	Calculated Worth ($)	Measured Worth($)
PuL 240 18.85	0.069	0.079	-0.024	-0.003	-0.056	-0.061
PuL 240 7.59	0.032	0.035	-0.001	+0.001	-0.015	-0.025
PuL 240 3.11	0.014	0.016	-0.007	+0.002	+0.002	-0.009
PuH 240 23.00	-0.196	-0.145	-0.301	-0.222	-0.268	-0.251
PuH 240 9.25	-0.112	-0.083	-0.158	-0.121	-0.146	-0.131
PuH 240 3.86	-0.053	-0.038	-0.072	-0.052	-0.065	-0.058

(a) All calculations were made using 38-broad groups in the GAZE diffusion code.

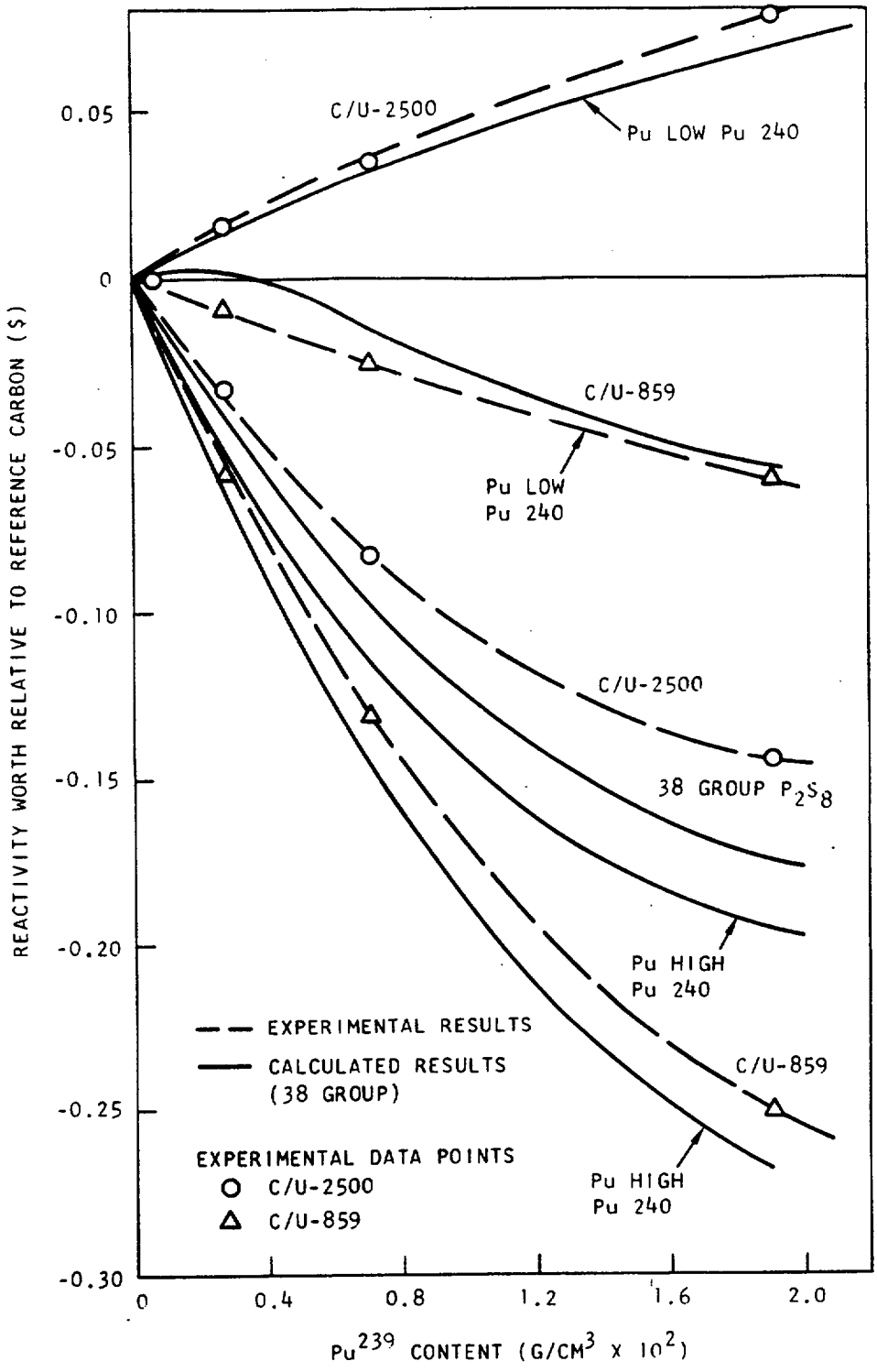

Fig.20. Calculated to experimental reactivity worth of special plutonium elements for C/U-2500 and C/U-859 core assemblies

REFERENCES

1. Pound, D. C. J. E. Larson, D. F. Nichols, and R. J. Nirschl, "Hazards Report for Modified HTGR Critical Facility," General Dynamics, General Atomic Division Report GA-6452 (Rev.2), February 8, 1966.
2. Joanou, G. D., and J. S. Dudek, "GAM II-A B_3 for the Calculation of Fast Neutron Spectra and Associated Multigroup Constants," General Dynamics, General Atomic Division GA-4265, 1963.
3. Joanou, G. D., C. V. Smith, and H. A. Vieweg, "GATHER II - An IBM 7090 Fortran II Program for the Computation of Thermal Neutron Spectra and Associated Multigroup Cross-Sections," General Dynamics, General Atomic Division Report GA-4132, 1963.
4. Smith, C. V., and M. K. Drake, "GAVER, A Neutron Cross-Section Averaging Program," USAEC Report GAMD-6692, General Dynamics, General Atomic Division, 1962.
5. Drake, M. K., "A Complilation of Resonance Integrals, Nucleonics, Vol. 48, #8, 108, August 1966.
6. Bell, J., "SUMMIT, An IBM 7090 Program for the Computation of Crystalline Scattering Kernels," General Dynamics, General Atomic Division Report GA-2492, 1962.
7. Koppel, J. U., J. R. Triplett, and Y. D. Naliboff, "GASKET, A Unified Code for Thermal Neutron Scattering," USAEC Report GA-7417, General Dynamics, General Atomic Division Report, 1966.
8. Nordheim, L. W., "A Program of Research and Calculation of Resonance Absorption," USAEC Report GA-2527, General Dynamics, General Atomic Division, August 1961.
9. Carlson, B., "Numerical Solution of Neutron Transport Problems," Proceeding of Symposium in Applied Mathematics, Vol. 11, American Mathematical Society, 1961.
10. Lathrop, K. D., "DTF-IV, A Fortran IV Program for Solving the Multigroup Transport Equation with Anisotropic Scattering," LA-3372, July 1965.
11. Lenihan, S. R., "GAZE-2, A One-Dimensional Multigroup, Neutron Diffusion Theory Code for IBM-7090," General Dyanamics, General Atomic Division Report GA-3152, 1962.
12. Bardes, R. G. et.al., "Tungsten Nuclear Rocket Phase I Final Report," NASA CR-54909 and GA-6890, General Dynamics, General Atomic Division, April 22, 1966.

REFERENCES (continued)

13. Keepin, G. R., "Physics of Nuclear Kinetics," Addision-Wesley Publishing Co., Inc., Massachusetts, 1965, p. 77.

14. Drake, M. K., "Neutron Cross-Section for U^{233}," General Dynamics, General Atomic Division Report GA-7076, September 1966.

15. Sher, R., and J. Felberbaum, "Least Squares Analysis of the 2200 m/sec parameters of U^{233}, U^{235}, and Pu^{239}," BNL-7222, June 1962.